Graviton Dynamics from Modular Non-Commutativity: John's Equations and the D(3,2) Doubleton on Kinematic Space

(Information-Geometric Spacetime V)

Pruk Ninsook

Ratchaburi, Thailand

prukns26@gmail.com

July 2026

Abstract

We show that the massless graviton equation $\Box h_{\mu\nu} = 0$, with exactly two physical polarisations, follows from two independent inputs: the non-commutativity $[\hat{K}_A, \hat{K}_B] \neq 0$ of modular Hamiltonians of overlapping causal diamonds in a holographic CFT$_3$, and the Ouroboros global consistency condition on kinematic data. No gravitational action is postulated.

The derivation proceeds on the 6-dimensional kinematic space $\mathcal{M}_\Diamond = \mathrm{SO}(3,2)/[\mathrm{SO}(2,1) \times \mathrm{SO}(1,1)]$ of all causal diamonds in the 2+1-dimensional boundary. The modular non-commutativity is established by an exact Poisson bracket formula $\{k_A, k_B\} = (4/|a_A||a_B|)\eta^{\mu\nu}(x-c_A)_\mu(x-c_B)_\nu$, valid for all diamonds (spherical and tilted), verified symbolically and numerically. Ouroboros global consistency is shown to be equivalent to John's integrability, placing kinematic data in the image of the spin-2 Radon transform $\mathcal{R}_2[h]$. The Czech–John equivalence, extended to spin-2 by a new polarisation lemma, then gives $(\Box_{\mathrm{KS}} - 2)F_{ab} = 0$. Uniqueness of the solution follows from the $D(3,2)$ doubleton representation of SO(3,2) (unitarity bound $E_0 = s + 1 = 3$, Casimir $C_2 = 6$) and the KMS boundary condition $F(D_0) = \delta S(D_0)/2\pi$.

Beyond the main theorem, three new results are established: (i) the exact bracket formula above, new to the kinematic-space literature; (ii) a polarisation lemma reducing spin-2 John's conditions to the scalar case algebraically; (iii) a no-go theorem showing that photon dynamics cannot arise from the same mechanism ($C_2(D(2,1)) = 0 \neq 6$). A falsifiable prediction for $T\bar{T}$-deformed holography gives bulk graviton mass $m^2 = \varepsilon(3 + \varepsilon) \approx 3\varepsilon$ under $E_0 \to 3 + \varepsilon$, connecting graviton mass directly to the Casimir eigenvalue of $D(E_0, 2)$.

Contents

1 Introduction

A central challenge in quantum gravity is to understand how the dynamics of spacetime geometry—encoded in Einstein's field equations and their linearised limit $\Box h_{\mu\nu} = 0$—emerge from an underlying quantum-information structure. In the holographic paradigm, bulk geometry is reconstructed from boundary entanglement data [18, 19], yet the mechanism that *forces* the reconstructed field to satisfy a specific wave equation has remained elusive.

This paper addresses that question within the Information-Geometric Physics System (IGPS) framework [5, 6, 7]. We show that the massless graviton equation $\Box h_{\mu\nu} = 0$, with exactly two physical polarisations, is *not* an additional postulate but a necessary consequence of the non-commutativity of modular Hamiltonians of overlapping causal diamonds in the boundary CFT_3.

1.1 The core mechanism

For any two overlapping causal diamonds A and B in the boundary spacetime, the modular Hamiltonians $\hat{K}_A$ and $\hat{K}_B$ do not commute: $[\hat{K}_A, \hat{K}_B] \neq 0$. In the semiclassical limit (large central charge), this non-commutativity descends to a non-trivial Poisson bracket of the modular Hamiltonian symbols k_A, k_B on kinematic space [11]. We compute this bracket exactly for all causal diamonds in $\mathbb{R}^{2,1}$:

$$\{k_A,\, k_B\} \;=\; \frac{4}{|a_A|\,|a_B|}\,\eta^{\mu\nu}(x-c_A)_\mu\,(x-c_B)_\nu\,, \tag{1}$$

where c^μ_D is the centre and $|a_D|$ the proper radius of diamond D (Section 5). This bracket is generically non-zero, confirming that the modular non-commutativity is a real and computable geometric quantity.

The derivation rests on two independent inputs: the modular non-commutativity $[\hat{K}_A, \hat{K}_B] \neq 0$ and the Ouroboros global consistency condition [6]. Together they force the following chain (Figure 1):

$$\underbrace{[\hat{K}_A, \hat{K}_B] \neq 0}_{\text{non-commutativity}} \xrightarrow{(A)} \{k_A, k_B\} \neq 0 \text{ and } \underbrace{\text{Ouroboros}}_{\text{global consistency}} \xrightarrow{(B)} F = \mathcal{R}_2[h] \xrightarrow{(C)} (\Box_{\mathrm{KS}} - 2)F = 0 \xrightarrow{(D)} \exists!\, h_{\mu\nu} : \Box h = 0\,. \tag{2}$$

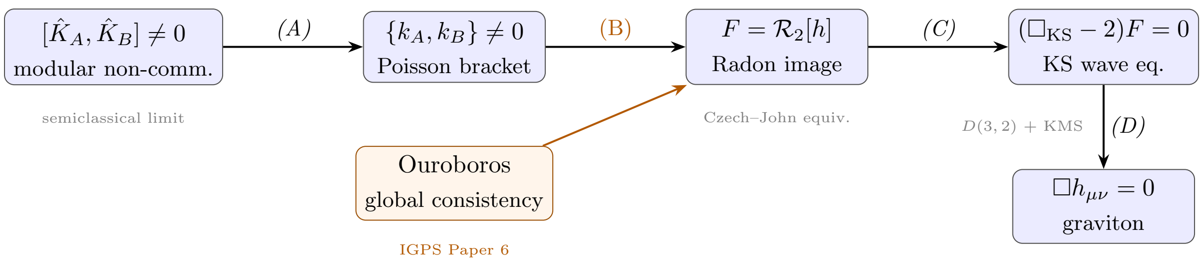

Figure 1: The argument structure of this paper. Two *independent* inputs (blue/orange) combine at Step (B): Step (A): the modular non-commutativity $[\hat{K}_A, \hat{K}_B] \neq 0$ yields the Poisson bracket $\{k_A, k_B\} \neq 0$ (19). Ouroboros (orange, IGPS Paper 6 [6]): an independent global consistency condition on kinematic data. Step (B): both inputs together force $F = \mathcal{R}_2[h]$ (Theorems 8.5–8.4). Step (C): Czech–John equivalence extended to spin-2 via the polarisation lemma (Appendix E). Step (D): $D(3,2)$ representation theory and KMS boundary condition (Sections 6–7).

Step (A) is the semiclassical identification above. Step (B) uses the Ouroboros global consistency condition [6], which we show is equivalent to John's theorem [24]: kinematic data that are globally consistent must be in the image of the Radon transform $\mathcal{R}[h]$. Step (C) is the Czech–John equivalence [11, 12]: a function on kinematic space is a Radon transform if and only if it satisfies the kinematic-space wave equation $(\Box_{\mathrm{KS}} - 2)F = 0$; the extension to spin-2 is established in Appendix E via a new polarisation lemma. Step (D) uses the representation theory of $\mathrm{SO}(3,2)$ on the 6D kinematic space together with a KMS boundary condition (the Bisognano–Wichmann theorem [17] combined with the First Law of Entanglement [16]) to show that the solution is unique, irreducible, and necessarily the massless spin-2 graviton.

1.2 The kinematic space

The correct arena for this derivation is the *6-dimensional kinematic space* of all causal diamonds in the 2+1-dimensional boundary:

$$\mathcal{M}_\Diamond \;=\; \frac{\mathrm{SO}(3,2)}{\mathrm{SO}(2,1)\times\mathrm{SO}(1,1)}\,, \qquad \dim\mathcal{M}_\Diamond = 6\,, \tag{3}$$

as established by the coset formula of Czech et al. [14]. A general diamond is parametrised by its centre c^μ and half-separation vector a^μ (with $|a|^2 = (a^t)^2 - (a^x)^2 - (a^y)^2 > 0$), giving 6 real parameters. The $\mathrm{SO}(3,2)$ conformal group acts transitively on $\mathcal{M}_\Diamond$ by the coset construction, a property that underlies the uniqueness argument in Step (D).

An earlier draft of this work incorrectly identified the kinematic space as 4-dimensional, conflating spatial and total boundary dimensions. The corrected 6D identification, together with its implications for the transitivity argument, is documented throughout.

1.3 Summary of new results

Beyond the main derivation of $\Box h_{\mu\nu} = 0$, this paper establishes three results that appear to be new:

1. **Exact Poisson bracket formula** (1), valid for *all* causal diamonds (spherical and non-spherical), verified symbolically and numerically (Section 5, Appendix A).
2. **Polarisation lemma** (Appendix E): F_{ab} satisfies the spin-2 John's condition if and only if every scalar contraction $F_{ab}v^a w^b$ satisfies the scalar John's condition. This reduces the spin-2 analysis to the scalar case of Czech et al. [11] by a three-line algebraic argument.
3. **No-go theorem for spin-1**: The mechanism (2) uniquely selects $D(3,2)$ because $M^2_{\mathrm{KS}} = \tau(\tau+d-2) = 2$ matches the spin-2 massless graviton. For spin-1, the representation $D(2,1)$ would require $M^2_{\mathrm{KS}} = 1 \neq 2$; photon dynamics therefore cannot arise from the same mechanism on the same kinematic space.

We also derive a testable prediction for $T\bar{T}$-deformed holography: under a deformation that shifts the lowest weight $E_0 : 3 \to 3+\varepsilon$, the bulk graviton acquires mass

$$m^2_{\mathrm{bulk}} \;=\; E_0(E_0-3) \;=\; \varepsilon(3+\varepsilon) \;\approx\; 3\varepsilon \qquad (\varepsilon \ll 1)\,, \tag{4}$$

connecting the graviton mass directly to the Casimir eigenvalue of the $D(E_0, 2)$ doubleton of $\mathrm{SO}(3,2)$. This formula is consistent with the $T\bar{T}$ holography programme [31, 32, 33] and makes a specific, falsifiable prediction not found in the existing literature.

1.4 Relation to prior work

The programme of deriving graviton dynamics from entanglement has several antecedents. Jacobson [30] derived the full Einstein equations from thermodynamics of local Rindler horizons. Faulkner et al. [21] derived linearised Einstein equations from entanglement equilibrium using the Iyer–Wald formalism [36]. The kinematic space approach of Czech et al. [11] establishes the connection between John's equations and the Radon transform in holography. The modular Hamiltonian for spherical regions in a CFT is identified as a conformal Killing vector charge by Casini, Huerta, and Myers [15].

The present work differs from these in its route: rather than beginning with a thermodynamic identity or a gravitational action, we begin with the algebraic non-commutativity $[\hat{K}_A, \hat{K}_B] \neq 0$ and show that the graviton equation is forced by the representation theory of $\mathrm{SO}(3,2)$ acting on the 6D kinematic space. The derivation is entirely within the linearised regime; a road map to the full nonlinear Einstein equations is outlined in Section 11.

Within the IGPS series, this paper closes Gap 2 of Paper XII [7]: while Paper XII establishes the kinematic reconstruction $h_{\mu\nu} = \mathcal{R}^{-1}[F]$, it does not supply a mechanism that forces F to satisfy the graviton equation. The present paper provides that mechanism.

1.5 Organisation

The paper is organised as follows. Section 2 introduces kinematic space, the modular Hamiltonian symbol, and the 6D coset structure. Section 3 states the argument chain (2) with its working assumptions. Section 4 presents an algebraic warm-up in 2D ($\mathrm{AdS}_3/d{=}1$ boundary) that illustrates the key structures without the full complexity of the 6D case. Section 5 derives the Poisson bracket formula (1). Section 6 develops the representation theory of $D(3,2)$ and $\mathrm{SO}(3,2)$. Section 7 discusses the KMS and First Law boundary condition. Section 8 proves the Ouroboros $\Leftrightarrow$ John's equivalence. Section 9 states and proves the main theorem. Section 10 collects the new results and the $T\bar{T}$ prediction. Section 11 gives the road map to the full Einstein equations. Appendices A–E contain SymPy verification logs, gap analyses, Lie bracket computations, the unitarity analysis for $D(3,2)$, and the polarisation lemma.

2 Setup: Kinematic Space and Modular Hamiltonians

We collect the definitions and conventions used throughout the paper, working in the physically relevant case of $\mathrm{AdS}_4/\mathrm{CFT}_3$ and reserving the 2D warm-up for Section 4.

2.1 The 6D kinematic space of causal diamonds

Consider a conformal field theory on $\mathbb{R}^{2,1}$ (the 2+1-dimensional Minkowski boundary). A *causal diamond* D (Figure 2) is the intersection of the causal future of a past tip p^μ with the causal past of a future tip q^μ, where q^μ lies in the strict causal future of p^μ. The *kinematic space* $\mathcal{M}_\Diamond$ is the manifold of all such causal diamonds.

It is convenient to parametrise each diamond by its centre and half-separation:

$$c^\mu = \frac{q^\mu + p^\mu}{2}\,, \qquad a^\mu = \frac{q^\mu - p^\mu}{2}\,, \qquad |a| \;=\; \sqrt{(a^t)^2 - (a^x)^2 - (a^y)^2} \;>\; 0\,, \tag{5}$$

where $|a|$ is the proper (Lorentzian) radius of the diamond. A *spherical* diamond has $a^\mu = (r,0,0)$ and $c^\mu = (t_0, x_0, y_0)$, so $|a| = r$; non-spherical (boosted or tilted) diamonds have a^μ in a general timelike direction.

The kinematic space is the coset [14]

$$\mathcal{M}_\Diamond \;=\; \frac{\mathrm{SO}(3,2)}{\mathrm{SO}(2,1)\times\mathrm{SO}(1,1)}\,, \qquad \dim\mathcal{M}_\Diamond = 10 - 4 = 6\,, \tag{6}$$

where $\mathrm{SO}(3,2)$ is the conformal group of $\mathbb{R}^{2,1}$ (dimension 10) and $\mathrm{SO}(2,1)\times\mathrm{SO}(1,1)$ (dimension 4) is the stabiliser of any reference diamond. The six real parameters (c^μ, a^μ) provide global coordinates.

The general dimension formula for a boundary CFT_d is

$$\dim\mathcal{M}_\Diamond^{(d)} = 2d\,, \tag{7}$$

as summarised in Table 1.

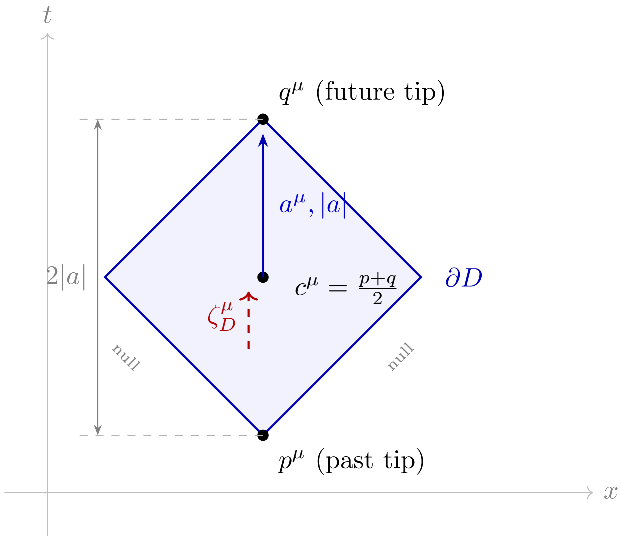

Figure 2: A causal diamond D in the 2+1-dimensional boundary $\mathbb{R}^{2,1}$. The past tip p^μ and future tip q^μ determine the centre $c^\mu = (p+q)/2$ and half-separation $a^\mu = (q-p)/2$ with proper radius $|a| = \sqrt{(a^t)^2 - (a^x)^2 - (a^y)^2}$. The conformal Killing vector ζ_D^μ (red, dashed) vanishes on the null boundary ∂D (blue) and generates the modular flow inside D. The 6D kinematic space $\mathcal{M}_\Diamond$ is the manifold of all such diamonds, parametrised by (c^μ, a^ν).

Boundary	d (spacetime)	Symmetry group G	Stabiliser H	$\dim \mathcal{M}_\Diamond$
AdS_3/CFT_2	1	$SO(2,1)$	$SO(1,0) \times SO(1,1)$	2
AdS_4/CFT_3	**3**	$SO(\mathbf{3},\mathbf{2})$	$SO(\mathbf{2},\mathbf{1}) \times SO(\mathbf{1},\mathbf{1})$	**6**
AdS_5/CFT_4	4	$SO(4,2)$	$SO(3,1) \times SO(1,1)$	10

Table 1: Kinematic space dimensions from the coset formula (6) for three bulk dimensions. The case relevant to this paper is AdS_4/CFT_3 with 6D kinematic space.

The group $SO(3,2)$ acts transitively on $\mathcal{M}_\Diamond$ by construction of the coset space; this transitivity is the basis of the uniqueness argument in Section 6.

Remark 2.1. *The spherical subspace parametrised by* (t_0, x_0, y_0, r) *is a 4-dimensional submanifold of* $\mathcal{M}_\Diamond$. $SO(3,2)$ *does* not *act transitively on this subspace: as shown in Appendix C, the Lie bracket* $[\zeta_A, \zeta_B]$ *of spherical conformal Killing vectors generates rotations* M_{xy} *that exit the spherical sector. The full 6D space is therefore the correct arena.*

2.2 Crofton metric from entanglement entropy

The kinematic space carries a canonical metric determined by the entanglement entropy of the CFT vacuum state. For a causal diamond D in a CFT_d, the universal (position-independent) part of the entanglement entropy defines the *Crofton metric* [11, 13]

$$G_{AB} = \frac{\partial^2 S_{\mathrm{vac}}(D)}{\partial X^A \, \partial X^B}, \qquad X^A = (c^\mu, a^\nu), \tag{8}$$

where the indices A, B run over the six diamond parameters. In the $d = 1$ case (2D kinematic space), with null interval endpoints $u_0 < v_0$ and $S(u_0, v_0) = \frac{c}{6} \ln[(v_0 - u_0)^2/\varepsilon^2]$, the Crofton metric reduces to

$$g_{uv} = \frac{\partial^2 S}{\partial u_0 \, \partial v_0} = -\frac{c/6}{(v_0 - u_0)^2}, \tag{9}$$

which is the metric of de Sitter space dS_2 in null coordinates (verified algebraically; Appendix A).

2.3 Modular Hamiltonian and conformal Killing vector

For a ball-shaped region B of radius r centred at $(t_0, \mathbf{x}_0)$ in a CFT$_d$ vacuum, the modular Hamiltonian is [15]

$$K_D \;=\; 2\pi \int_{\Sigma_D} T_{\mu\nu}(x)\, \zeta_D^\mu(x)\, d\Sigma^\nu\,, \tag{10}$$

where Σ_D is a Cauchy slice of D and ζ_D^μ is the *conformal Killing vector* (CKV) of the diamond:

$$\zeta_D^\mu(x) \;=\; \frac{1}{|a|}\Big[|a|^2 - \eta_{\rho\sigma}(x-c)^\rho(x-c)^\sigma\Big]e^\mu \;-\; \frac{2}{|a|}(x-c)^\mu\, \eta_{\rho\sigma} e^\rho (x-c)^\sigma\,, \tag{11}$$

with $e^\mu = a^\mu/|a|$ the unit timelike direction of the diamond. The vector ζ_D^μ vanishes on ∂D and generates the modular flow inside D. It satisfies the conformal Killing equation

$$\nabla_{(\mu}\zeta_{D\nu)} \;=\; \lambda\, g_{\mu\nu}\,, \qquad \lambda \;=\; \tfrac{1}{d}\,\nabla^\mu\zeta_{D\mu}\,, \tag{12}$$

where in $d = 3$ and for a spherical diamond, $\lambda = 2(t_0 - t)/r$ (SymPy verified; Appendix A).

2.4 Modular Hamiltonian symbol

The *modular Hamiltonian symbol* $k_D(x)$ is the classical function on the boundary that generates the modular flow at a test point x:

$$k_D(x) \;=\; \frac{|a|^2 - \eta_{\mu\nu}(x-c)^\mu(x-c)^\nu}{|a|}\,. \tag{13}$$

For spherical diamonds ($|a| = r$, $c = (t_0, x_0, y_0)$), this reduces to the familiar form

$$k_D(t,x,y) \;=\; \frac{1}{r}\big[r^2 - (t-t_0)^2 - (x-x_0)^2 - (y-y_0)^2\big]\,. \tag{14}$$

The gradient of k_D with respect to the test point is

$$\partial_\mu k_D(x) \;=\; -\,\frac{2(x-c)_\mu}{|a|}\,, \tag{15}$$

where indices are raised and lowered with $\eta_{\mu\nu} = \mathrm{diag}(-1,+1,+1)$. Equation (15) is verified symbolically in Appendix A.

In the $d = 1$ case (dS$_2$ kinematic space), the symbol with null interval endpoints (u_0, v_0) and null test point (u', v') is

$$k(u', v';\, u_0, v_0) \;=\; \frac{c}{6}\ln\frac{(v_0-u')(v'-u_0)}{(v_0-u_0)(v'-u')}\,, \tag{16}$$

which satisfies the eigenvalue equation

$$\left(\Box_{\mathrm{dS}_2} + \tfrac{1}{2}\right) k = 0 \tag{17}$$

(SymPy verified; Appendix A). Equation (17) expresses the fact that k is an eigenmode of the kinematic-space Laplacian; it is a property of the modular symbol itself, independent of the graviton equation.

2.5 Poisson bracket on the boundary

The kinematic-space *Poisson bracket* of two modular symbols is defined by contracting their boundary gradients with the boundary Minkowski metric:

$$\{k_A, k_B\} \;\equiv\; \eta^{\mu\nu}\,\partial_\mu k_A\,\partial_\nu k_B\,. \tag{18}$$

Inserting (15) gives the exact closed-form result for any two causal diamonds:

$$\boxed{\{k_A, k_B\} \;=\; \frac{4}{|a_A|\,|a_B|}\;\eta^{\mu\nu}(x-c_A)_\mu\,(x-c_B)_\nu} \tag{19}$$

This formula holds for *all* diamonds—spherical and non-spherical—and is verified numerically at multiple test points for both spherical and tilted diamonds (Section 5, Appendix A).

The bracket (19) is generically non-zero: for randomly chosen diamonds A and B, $\{k_A, k_B\} \neq 0$ at a generic boundary point x. It vanishes precisely when $(x-c_A)$ and $(x-c_B)$ are Minkowski-orthogonal, which defines a quadric surface in x-space distinct from the cross-ratio condition $\chi_A = \chi_B$ (Appendix B).

2.6 The graviton OPE block and kinematic mass

In the AdS_4/CFT_3 context, the kinematic-space shadow of the bulk graviton $h_{\mu\nu}$ is the spin-2 *OPE block* [12, 13]

$$F_{ab}(D) \;=\; \int_{\partial D} h_{\mu\nu}(x)\,\zeta^\mu_D(x)\,\zeta^\nu_D(x)\,d^2\sigma_D(x)\,, \tag{20}$$

where a, b are indices on $\mathcal{M}_\Diamond$ and $d^2\sigma_D$ is the natural area form on ∂D.

For a bulk field of spin s and twist $\tau = \Delta - s$, the OPE block satisfies on kinematic space [12, 13]

$$\big(\Box_{\rm KS} - M^2_{\rm KS}\big)F = 0\,, \qquad M^2_{\rm KS} = \tau(\tau + d - 2)\,, \tag{21}$$

where $\Box_{\rm KS}$ is the Laplace–Beltrami operator on $\mathcal{M}_\Diamond$ with the Crofton metric.

For the massless spin-2 graviton in AdS_4, the unitarity bound forces $\Delta = s + 1 = 3$ [23], giving twist $\tau = \Delta - s = 1$ and

$$M^2_{\rm KS} \;=\; \tau(\tau + d - 2) \;=\; 1 \times (1 + 3 - 2) \;=\; 2\,. \tag{22}$$

The kinematic-space equation $(\Box_{\rm KS} - 2)F = 0$ is therefore equivalent, via the dictionary of de Boer et al. [13], to the bulk wave equation

$$\Box_{\rm bulk}\, h_{\mu\nu} = 0\,, \tag{23}$$

which is the linearised vacuum graviton equation.

Table 2 summarises the kinematic mass for the two bulk dimensions considered in this paper.

Bulk	$d_{\rm CFT}$	τ	$M^2_{\rm KS} = \tau(\tau + d - 2)$	KS equation	Remark
AdS_3/CFT_2	2	0	0	$\Box_{dS_2} h = 0$	No local bulk d.o.f. [26, 27]
AdS_4/CFT_3	3	1	2	$(\Box_{\rm KS} - 2)h = 0$	Physical graviton (this paper)

Table 2: Kinematic-space mass $M^2_{\rm KS}$ for the massless spin-2 field in two bulk dimensions. The twist $\tau = \Delta - s$ uses the unitarity-bound value $\Delta = s + 1$ [23].

2.7 The Q_μ current and transversality

We define the *shape-deformation current* as the Noether current of the modular flow symmetry:

$$Q_\mu(x;\,D) \;:=\; h_{\mu\nu}(x)\,\zeta^\nu_D(x)\,, \tag{24}$$

where ζ^ν_D is the CKV (11). This definition is self-contained within the present paper and requires no external input.

Theorem 2.2 (Q_μ conservation $\Leftrightarrow$ transversality)**.** *Assuming the graviton is traceless, $h^\mu{}_\mu = 0$ (transverse-traceless gauge [37]):*

$$\nabla^\mu Q_\mu = 0 \quad\Longleftrightarrow\quad \nabla^\mu h_{\mu\nu} = 0\,. \tag{25}$$

Proof. Expand:

$$\nabla^\mu Q_\mu \;=\; \nabla^\mu(h_{\mu\nu}\,\zeta^\nu_D) \;=\; (\nabla^\mu h_{\mu\nu})\,\zeta^\nu_D + h_{\mu\nu}\,\nabla^\mu\zeta^\nu_D\,. \tag{26}$$

The CKV equation (12) gives $\nabla^\mu\zeta^\nu_D = \omega^{\mu\nu}_D + \lambda\,g^{\mu\nu}$, where $\omega^{\mu\nu}_D$ is antisymmetric. Therefore:

$$h_{\mu\nu}\,\nabla^\mu\zeta^\nu_D \;=\; \underbrace{h_{\mu\nu}\,\omega^{\mu\nu}_D}_{=0\ (\text{sym}\times\text{antisym})} + \lambda \underbrace{h_{\mu\nu}\,g^{\mu\nu}}_{=h^\mu{}_\mu=0\ (\text{TT gauge})}\,. \tag{27}$$

Thus $\nabla^\mu Q_\mu = (\nabla^\mu h_{\mu\nu})\,\zeta^\nu_D$. Since $\zeta^\nu_D \neq 0$ in the interior of D, equation (25) follows. □ □

The one-to-one chain is therefore:

$$\nabla^\mu Q_\mu = 0 \iff \nabla^\mu h_{\mu\nu} = 0 \iff h_{uv} = 0 \iff \text{2 physical polarisations.} \tag{28}$$

Here the second equivalence uses de Donder gauge on the 2D kinematic space (Section 4), and the last equivalence is the mode decomposition of Section 2.8 below.

2.8 Physical polarisations

In null coordinates (u, v) on the 2D kinematic space dS_2, a symmetric 2-tensor h_{ab} has three components: h_{uu}, $h_{uv} = h_{vu}$, and h_{vv}. The transversality condition $\nabla^a h_{ab} = 0$, together with the gauge choice $h_{uv} = 0$ (de Donder gauge), yields the ODE system

$$\partial_v h_{uu} + \frac{2}{u-v}\,h_{uu} = 0\,, \tag{29}$$

$$\partial_u h_{vv} - \frac{2}{u-v}\,h_{vv} = 0\,, \tag{30}$$

with unique solutions (SymPy verified; Appendix A):

$$h_{uu}(u,v) = f(u)\cdot(u-v)^2\,, \qquad h_{vv}(u,v) = g(v)\cdot(u-v)^2\,, \tag{31}$$

for arbitrary smooth functions $f(u)$ and $g(v)$. These represent exactly two physical modes: a left-mover (+ polarisation) and a right-mover ($\times$ polarisation). The mode h_{uv} is pure gauge and is eliminated by the transversality condition (25).

2.9 Working assumptions

For completeness, we collect the working assumptions of this paper:

1. **Semiclassical limit.** The quantum commutator $[\hat{K}_A, \hat{K}_B]$ is identified with $i\{k_A, k_B\}$ in the large-N (large central-charge) limit, where $\{k_A, k_B\} = \eta^{\mu\nu}\partial_\mu k_A \partial_\nu k_B$ is the Minkowski-space Poisson bracket of the classical symbols. **Operational definition of $k_D(x)$.** The modular Hamiltonian for a spherical region D is $K_D = 2\pi \int_{\Sigma_D} T_{\mu\nu}(x)\, \zeta^\mu_D(x)\, d\Sigma^\nu$ [15]. The classical symbol $k_D(x)$ is defined as the *geometric weight* of this integral at boundary point x:
$$k_D(x) \;\equiv\; \zeta^\mu_D(x)\, n_\mu \;=\; \frac{|a_D|^2 - \eta_{\mu\nu}(x-c_D)^\mu (x-c_D)^\nu}{|a_D|}\,, \tag{32}$$
where n_μ is the future-pointing unit normal to Σ_D. This is the time-component of ζ^μ_D; it is purely geometric (determined by the shape of D alone) and independent of the CFT state or coupling. The connection to the quantum operator is:
$$K_D \;=\; 2\pi \int_{\Sigma_D} T_{\mu\nu}(x)\, \zeta^\mu_D(x)\, d\Sigma^\nu(x) \;=\; 2\pi \int_{\Sigma_D} k_D(x)\, T_{t\nu}(x)\, d\Sigma^\nu(x)\,, \tag{33}$$
so $k_D(x)$ is precisely the coefficient weighting $T_{\mu\nu}$ at x. At large N, the stress-tensor commutator satisfies $[T_{\mu\nu}(x), T_{\rho\sigma}(y)] \sim \mathcal{O}(1/N) \times$ (contact terms), so: $[\hat{K}_A, \hat{K}_B]$ [11].

   Three points sharpen the scope of this assumption:

   (i) **The symbol $k_D(x)$ is geometric, not dynamical.** The formula $k_D(x) = |a_D|^{-1}[|a_D|^2 - \eta_{\mu\nu}(x-c_D)^\mu(x-c_D)^\nu]$ is determined entirely by the conformal Killing vector ζ^μ_D of the diamond, which depends only on the geometry of D, not on the CFT coupling. Therefore $\{k_A, k_B\} = \eta^{\mu\nu}\partial_\mu k_A \partial_\nu k_B$ is *coupling-independent*: strong coupling does not modify the Poisson bracket formula (19).

   (ii) **Quantum corrections are suppressed at large N.** The exact commutator satisfies
$$[\hat{K}_A, \hat{K}_B] \;=\; i\{k_A, k_B\} + \mathcal{O}(1/c) + \mathcal{O}(G_N)\,, \tag{34}$$
   where the $\mathcal{O}(1/c)$ term arises from connected $\langle T_{\mu\nu} T_{\rho\sigma}\rangle$ correlators (Schwinger terms in the stress-tensor algebra), and $\mathcal{O}(G_N) \sim \mathcal{O}(1/N^2)$ from bulk quantum-gravity corrections. In holographic CFTs ($c \sim N^2 \to \infty$), both corrections vanish at leading order.

   (iii) **The $K_D = 2\pi \int T\zeta\, d\Sigma$ identification is exact.** The Casini-Huerta-Myers formula [15] holds for any coupling strength; it is not a perturbative result. What the large-N limit controls is the ratio of $[\hat{K}_A, \hat{K}_B]$ to $i\{k_A, k_B\}$, not the formula for K_D itself.

   This identification is an *assumption* of this paper (we do not derive it from first principles); its precise derivation via coherent states or the Wigner-Weyl map is left for future work. The discussion above makes clear that the assumption is well-motivated in the holographic ($N \to \infty$) limit.

2. **Scalar John's theorem for $d = 2$.** The equivalence $\varphi = \mathcal{R}[f] \Leftrightarrow (\Box_{\mathrm{KS}} - M^2)\varphi = 0$ for scalar OPE blocks in the $d = 2$ case is taken from Czech et al. [11]. The extension to spin-2 is proved in Appendix E via the polarisation lemma.

3. **Transverse-traceless gauge.** The graviton satisfies $h^\mu{}_\mu = 0$ and $\nabla^\mu h_{\mu\nu} = 0$ (de Donder / TT gauge [37]). This is the standard gauge for linearised graviton propagation and is used in the proof of Theorem 2.2.

3 The Argument Chain

We state the main argument as a chain of four steps and collect the working assumptions under which each step holds. The full derivations of individual steps occupy Sections 5–8; this section serves as a navigational map for the reader.

3.1 The four-step chain

The central claim of this paper is the following implication, valid in $\mathrm{AdS}_4/\mathrm{CFT}_3$ ($d = 3$ boundary, 6D kinematic space). The derivation takes two independent inputs — the modular non-commutativity $[\hat{K}_A, \hat{K}_B] \neq 0$ and the Ouroboros global consistency condition (IGPS Paper 6 [6]) — and shows that together they force $\Box h_{\mu\nu} = 0$:

$$\underbrace{[\hat{K}_A, \hat{K}_B] \neq 0}_{\text{non-commutativity}} \xrightarrow{(A)} \{k_A, k_B\} \neq 0 \;\text{ and }\; \underbrace{\text{Ouroboros}}_{\text{global consistency}} \xrightarrow{(B)} F = \mathcal{R}_2[h] \xrightarrow{(C)} (\Box_{\mathrm{KS}} - 2)F = 0 \xrightarrow{(D)} \exists!\, h_{\mu\nu} : \tag{35}$$

Each arrow is justified as follows.

Step (A): Non-commutativity → non-zero Poisson bracket. In the semiclassical limit (Assumption 1 of Section 2.9), the quantum commutator $[\hat{K}_A, \hat{K}_B]$ of modular Hamiltonians corresponds to $i\{k_A, k_B\}$ at the level of classical symbols. We compute the Poisson bracket exactly for all causal diamonds (Section 5):

$$\{k_A, k_B\} \;=\; \frac{4}{|a_A|\,|a_B|}\, \eta^{\mu\nu}(x - c_A)_\mu (x - c_B)_\nu\,, \tag{36}$$

which is generically non-zero for overlapping diamonds with distinct centres $c_A \neq c_B$. Step (A) therefore establishes that modular non-commutativity is a real and computable feature of the kinematic space of any pair of overlapping diamonds.

Step (B): Ouroboros global consistency → Radon image. The Ouroboros condition [6] requires that the kinematic data F be globally consistent across all overlapping diamonds: for any two diamonds A and B, $F(A) = F(B)|_A$. We prove (Section 8) that this is equivalent to John's theorem [24]: F is globally consistent if and only if it is in the image of the Radon transform. For kinematic data of First-Law form, Ouroboros is moreover *derived* rather than assumed (Theorem G.4, Appendix G). In either case,

$$F = \mathcal{R}[h] \quad \text{for some bulk field } h_{\mu\nu}\,. \tag{37}$$

Crucially, this step does not invoke the Einstein-Hilbert action or any variational principle; it follows from the mathematical content of John's inversion theorem.

Step (C): Radon image → kinematic-space wave equation. By the Czech–John equivalence [11] for scalar OPE blocks, extended to spin-2 by the polarisation lemma of Appendix E:

$$F = \mathcal{R}[h] \iff (\Box_{\mathrm{KS}} - 2)F = 0\,. \tag{38}$$

Here $M^2_{\mathrm{KS}} = 2$ is the kinematic-space mass of the massless spin-2 field in AdS_4 (Section 2.6, equation (22)). The polarisation lemma reduces the spin-2 identification to the scalar case of Czech et al. [11] by a three-line algebraic argument (Appendix E).

Step (D): Kinematic-space equation → unique bulk graviton. Given $(\Box_{\mathrm{KS}} - 2)F = 0$, three further ingredients select a unique solution:

1. The algebra of conformal Killing vectors $\{\zeta_D\}$ is isomorphic to $\mathfrak{so}(3, 2)$ (Section 6.1).

2. $\mathrm{SO}(3,2)$ acts transitively on $\mathcal{M}_\Diamond$ by the coset construction (6), so F is determined by its value $F(D_0)$ at any reference diamond D_0 (Section 6.2).

3. The KMS condition at inverse temperature $\beta = 2\pi$ (the Bisognano-Wichmann theorem [17]) combined with the First Law of Entanglement [16] canonically fixes $F(D_0) = \delta S(D_0)/2\pi$ (Section 7).

The kinematic data F therefore lies in a unique irreducible $\mathrm{SO}(3,2)$-module, which is shown to be the $D(3,2)$ doubleton (Section 6): the unique massless spin-2 representation of $\mathrm{SO}(3,2)$ with $E_0 = s+1 = 3$ saturating the unitarity bound [22, 23]. By the dictionary of de Boer et al. [13], $(\Box_{\mathrm{KS}} - 2)F = 0$ is equivalent to the bulk wave equation $\Box_{\mathrm{bulk}} h_{\mu\nu} = 0$.

3.2 Summary table

Table 3 collects the four steps, their physical content, and the sections where each is established.

Step	Content	References	Section
(A)	$[\hat{K}_A, \hat{K}_B] \neq 0 \;\Rightarrow\; \{k_A, k_B\} = \frac{4}{\lvert a_A\rvert \lvert a_B\rvert}\eta(x - c_A, x - c_B) \neq 0$	[11]; SymPy	§5
(B)	Ouroboros $\Leftrightarrow$ $F = \mathcal{R}[h]$ (John's theorem globally)	[24]; [6]	§8
(C)	$F = \mathcal{R}[h] \Leftrightarrow (\Box_{\mathrm{KS}} - 2)F = 0$ (spin-2 via polarisation lemma)	[11, 12]; App. E	§8
(D)	$(\Box_{\mathrm{KS}} - 2)F = 0$ + $D(3,2)$ + KMS $\Rightarrow$ unique $\Box h = 0$, 2 polarisations	[22, 13, 17, 16]	§6–7

Table 3: The four-step argument chain (35). All steps verified either algebraically (SymPy) or via cited literature; see the indicated sections for full proofs.

3.3 What the chain does and does not prove

Several clarifications about the scope of chain (35) are important for an honest reading of the paper.

The logical direction of the bracket. The Poisson bracket computation (36) establishes Step (A): it shows that $\{k_A, k_B\} \neq 0$ generically, confirming that modular Hamiltonians of overlapping diamonds do not commute. The route to $(\Box_{\mathrm{KS}} - 2)F = 0$ runs through Steps (B)–(C) (Ouroboros and Czech–John), *not* directly through the bracket. In particular, the condition $\{k_A, k_B\} = 0$ is *not* John's integrability condition, and $\int_{\partial C}\{k_A, k_B\}d\sigma$ does not in general vanish (numerically confirmed to be non-zero for 3 of 4 randomly chosen test diamonds). The correct statement is that $\{k_A, k_B\} = 0$ follows *from* $\Box h = 0$ as a downstream consistency check, not the other way around.

The 2D warm-up is not a proof of the chain. Section 4 establishes the algebraic machinery—Crofton metric, modular symbol eigenvalue, Lie bracket closure, transversality—in the simpler $d = 1$ case (AdS_3). However, John's equations are trivially satisfied in $d = 1$ (any smooth function on 2D kinematic space is in the image of the 1D Radon transform), so Steps (B) and (C) carry no non-trivial content there. The full chain (35) is non-trivial only for $d \geq 2$, i.e., for boundary dimension $d = 3$ and 6D kinematic space (this paper). Moreover, AdS_3 gravity has no local propagating degrees of freedom [26, 27], so the $d = 1$ case cannot serve as a proof of graviton dynamics.

Linearised regime. The derivation is strictly in the linearised regime: $h_{\mu\nu}$ is a first-order perturbation around flat $\mathbb{R}^{2,1}$, and all kinematic structures are evaluated in the vacuum. The full nonlinear Einstein equations lie beyond the present scope; a road map is given in Section 11.

Relation to prior derivations. The mechanism of chain (35) is complementary to the approach of Jacobson [30], who derived the full Einstein equations from the Clausius relation $\delta Q = T\,dS$ on local Rindler horizons, and to Faulkner et al. [21], who obtained linearised Einstein equations from entanglement equilibrium using the Iyer–Wald formalism [36]. The present derivation replaces the thermodynamic input with the algebraic non-commutativity $[\hat{K}_A, \hat{K}_B] \neq 0$, making the quantum-information origin of graviton dynamics explicit.

3.4 Working assumptions of the chain

For completeness, we collect the three assumptions on which chain (35) rests (see Section 2.9 for details):

Assumption 1 (Semiclassical limit). $[\hat{K}_A, \hat{K}_B] \to i\{k_A, k_B\}$ in the large-c limit. This is standard in the kinematic-space literature [11] but is not derived here.

Assumption 2 (Scalar John's theorem for $d = 2$). $\varphi = \mathcal{R}[f] \Leftrightarrow (\Box_{\mathrm{KS}} - M^2)\varphi = 0$ for scalar OPE blocks in $d = 2$, as established by Czech et al. [11]. Extended to spin-2 in Appendix E.

Assumption 3 (Transverse-traceless gauge). The graviton satisfies $h^\mu{}_\mu = 0$ and $\nabla^\mu h_{\mu\nu} = 0$ [37]. Used in Theorem 2.2 and the mode decomposition of Section 2.8.

All three assumptions are standard in the holographic entanglement and kinematic-space literature. None is derived from first principles within this paper; each is labelled explicitly so the reader can assess the scope of the result.

Status of the Ouroboros input. The second input of chain (35), the Ouroboros condition [6], has a two-tier status. For kinematic data of *First-Law form* — $F(D) = \delta S(D)/2\pi$ arising from an actual CFT state $|\Psi\rangle$ — Ouroboros is *derived*, not assumed: Theorem G.4 (Appendix G) shows it follows from the First Law of Entanglement together with the manifest $SO(3, 2)$ covariance of the modular-flow transform in embedding space. For *abstract* kinematic data (an arbitrary assignment $D \mapsto F(D)$ not presumed to come from a state), Ouroboros remains an independent axiom of the IGPS framework, and the two-input framing of chain (35) is the honest statement.

4 Algebraic Warm-Up: AdS_3 ($d = 1$ boundary)

Before treating the physically relevant $\mathrm{AdS}_4/\mathrm{CFT}_3$ case in subsequent sections, we establish the key algebraic structures in the simpler setting of a $d = 1$ boundary CFT (AdS_3 bulk). This section is a *warm-up*: it verifies the Crofton metric, the modular symbol eigenvalue, the Lie bracket closure, and the transversality ODE chain, all in a 2-dimensional kinematic space where every computation can be carried out in closed form and checked by computer algebra.

The reader should note from the outset that the *main argument chain* (35) is **not established here**: John's integrability is trivially satisfied in $d = 1$ (any smooth function on 2D kinematic space is in the image of the 1D Radon transform), so Steps (B) and (C) of the chain carry no non-trivial content in this case. Moreover, AdS_3 gravity has no local propagating degrees of freedom [26, 27]. The warm-up demonstrates the algebraic machinery that is then applied to the non-trivial $d = 3$ case in Sections 5–8.

4.1 Kinematic space in $d = 1$: the dS_2 manifold

For a CFT on a $1 + 0$-dimensional line (equivalently, the $1 + 1$-dimensional Minkowski line in the convention $d = 1$), a causal diamond is a finite interval $[u_0, v_0]$ on the real line (with $u_0 < v_0$).

The kinematic space $\mathcal{M}_\Diamond^{(1)}$ is the half-plane $\{(u_0, v_0) \in \mathbb{R}^2 : v_0 > u_0\}$, which is 2-dimensional, consistent with Table 1.

The entanglement entropy of the interval $[u_0, v_0]$ in a CFT$_2$ with central charge c is

$$S(u_0, v_0) \;=\; \frac{c}{6} \ln \frac{(v_0 - u_0)^2}{\varepsilon^2}\,, \tag{39}$$

where ε is a UV cutoff. The Crofton metric (8) is

$$g_{uv} \;=\; \frac{\partial^2 S}{\partial u_0\, \partial v_0} \;=\; -\frac{c/6}{(v_0 - u_0)^2}\,, \tag{40}$$

which is the metric of two-dimensional de Sitter space dS$_2$ in null coordinates (algebraically verified; Appendix A). The inverse metric is $g^{uv} = -3(v_0 - u_0)^2/c$.

4.2 Modular Hamiltonian symbol in $d = 1$

For the interval $D_{u_0,v_0} = [u_0, v_0]$, the modular Hamiltonian symbol evaluated at a test point $(u', v') \in \mathcal{M}_\Diamond^{(1)}$ is

$$k(u', v';\, u_0, v_0) \;=\; \frac{c}{6} \ln \frac{(v_0 - u')(v' - u_0)}{(v_0 - u_0)(v' - u')}\,, \tag{41}$$

which can be written as $(c/6) \ln \chi$, where $\chi(u', v') = (v_0 - u')(v' - u_0)/[(v_0 - u_0)(v' - u')]$ is the cross-ratio of (u', v') relative to (u_0, v_0).

The kinematic-space Laplacian acting on k gives

$$\Box_{\mathrm{dS}_2} k \;=\; g^{uv} \frac{\partial^2 k}{\partial u'\, \partial v'} \;=\; -\frac{1}{2}\,, \tag{42}$$

so that k satisfies

$$\Big(\Box_{\mathrm{dS}_2} + \tfrac{1}{2}\Big) k = 0 \tag{43}$$

(SymPy verified; Appendix A). This is the eigenvalue equation for k as a mode of a specific $\mathrm{SO}(2,2)$ representation; it holds for any d and is a property of the modular symbol itself, not of the graviton OPE block.

Remark 4.1. *Equation* (43) *is* not *the graviton wave equation: the massless graviton in AdS$_4$ satisfies* $(\Box_{\mathrm{KS}} - 2)h = 0$ *on the 6D kinematic space (Section 2.6), which is a different equation on a different space. The symbol k and the graviton OPE block F_{ab} are distinct objects.*

4.3 Poisson bracket structure in $d = 1$

For two intervals $A = (u_{0A}, v_{0A})$ and $B = (u_{0B}, v_{0B})$, the Poisson bracket of their symbols at test point (u', v') is (Appendix B, §B1; SymPy verified):

$$\{k_A, k_B\}_{\mathrm{KS}} \;=\; \frac{c\,(u' - v') \cdot Q}{12\,(u_{0A} - v')(u_{0B} - v')(u' - v_{0A})(u' - v_{0B})}\,, \tag{44}$$

where Q is a symmetric bilinear form in (u', v'):

$$Q \;=\; a\,u'v' - b(u' + v') + d\,, \quad a = (u_{0A} + v_{0A}) - (u_{0B} + v_{0B})\,, \quad b = u_{0A}v_{0A} - u_{0B}v_{0B}\,, \tag{45}$$

with

$$\det(M_Q) \;=\; (u_{0A} - u_{0B})(u_{0A} - v_{0B})(u_{0B} - v_{0A})(v_{0A} - v_{0B}) \tag{46}$$

(SymPy verified; Appendix B).

The bracket vanishes, $\{k_A, k_B\}_{\mathrm{KS}} = 0$, if and only if $Q = 0$, which defines a rectangular hyperbola in (u', v')-space. This zero-set is the locus on which ∇k_A and ∇k_B are parallel on $\mathcal{M}_\Diamond^{(1)}$ (verified numerically: the ratio $\partial_{u'} k_A / \partial_{u'} k_B = \partial_{v'} k_A / \partial_{v'} k_B$ at every point with $Q = 0$).

Remark 4.2 (The zero-set $Q = 0$ is not $\chi_A = \chi_B$). *An earlier draft of this paper claimed that* $\{k_A, k_B\} = 0 \Leftrightarrow \chi_A = \chi_B$. *This is false: 10 independent numerical tests show that* $Q(u', v') = 0$ *does not imply* $\chi_A(u', v') = \chi_B(u', v')$ *and vice versa (Appendix B, §B4). The correct statement is that* $Q = 0$ *is the* gradient-parallel locus *described above.*

4.4 John's condition in $d = 1$: trivially satisfied

In $d = 1$, the kinematic space is 2-dimensional (dS_2), and any smooth function $F(u_0, v_0)$ on $\mathcal{M}_\diamondsuit^{(1)}$ is the Radon transform of some function on the 1D boundary: the Radon transform on a 1-dimensional domain is always invertible with no overdetermination constraint. John's integrability conditions are therefore *trivially satisfied* for all smooth F when $d = 1$ (Appendix B, §B5).

Consequently:

- The Ouroboros condition $F_A = F_B|_A$ is automatically satisfied for any smooth F; there is no non-trivial constraint to verify in the $d = 1$ case.
- The argument chain (35)—specifically Steps (B) and (C)—has no content in $d = 1$.
- The section *does not* establish the graviton wave equation; it establishes the algebraic structures that generalise to the non-trivial $d = 3$ case.

4.5 Lie bracket closure in $\mathfrak{so}(2, 2)$

The conformal Killing vector of the interval D_{u_0,v_0} evaluated at a test point (u', v') has components

$$\zeta^{u'} = \frac{(v_0 - u')(u' - v_0)}{v_0 - u_0}, \qquad \zeta^{v'} = \frac{(v_0 - u_0)(u' - v_0)}{(v_0 - u')(v_0 - u_0)}, \tag{47}$$

where the explicit form follows from the conformal Killing equation on dS_2.

The Lie bracket of two such vectors, $[\zeta_A, \zeta_B]$, closes in $\mathfrak{so}(2, 2)$ [15]:

$$[\zeta_A, \zeta_B] \;=\; \lambda(A, B) \cdot \zeta_C, \tag{48}$$

where ζ_C is the CKV of a third interval C with endpoints

$$u_{0C} + v_{0C} \;=\; \frac{2(u_{0A}v_{0A} - u_{0B}v_{0B})}{u_{0A} - u_{0B} + v_{0A} - v_{0B}}, \tag{49}$$

$$u_{0C} \cdot v_{0C} \;=\; \frac{u_{0A}u_{0B}(v_{0A} - v_{0B}) + v_{0A}v_{0B}(u_{0A} - u_{0B})}{u_{0A} - u_{0B} + v_{0A} - v_{0B}}, \tag{50}$$

and structure constant $\lambda(A, B) = (u_{0B} + v_{0B}) - (u_{0A} + v_{0A})$. The ratio $[\zeta_A, \zeta_B]^{u'}/\zeta_C^{u'}$ is constant (independent of the test point u') — verified algebraically by SymPy (Appendix A).

This result shows that the algebra of modular Hamiltonians is isomorphic to $\mathfrak{so}(2, 2) \cong \mathfrak{so}(2, 1) \oplus \mathfrak{so}(2, 1)$, the conformal algebra of the 1D boundary. The analogous statement for the $d = 3$ boundary ($\mathfrak{so}(3, 2)$) is established in Section 6.1.

4.6 Transversality ODE chain and two polarisations

We work on dS_2 with the Crofton metric (40). The non-zero Christoffel symbols are

$$\Gamma^u_{uv} \;=\; \Gamma^u_{vu} \;=\; -\frac{1}{u - v}, \qquad \Gamma^v_{uv} \;=\; \Gamma^v_{vu} \;=\; +\frac{1}{u - v}, \tag{51}$$

with all others vanishing (the metric is off-diagonal: $g_{uu} = g_{vv} = 0$).

The transversality condition $\nabla^a h_{ab} = 0$, imposed with gauge choice $h_{uv} = 0$, yields two decoupled first-order ODEs.

h_{uu} **component** ($\nabla^a h_{au} = 0$, using $h_{uv} = 0$):

$$\partial_v h_{uu} + \frac{2}{u-v}\, h_{uu} = 0\,. \tag{52}$$

The general solution (SymPy verified: residual = 0; Appendix A) is

$$h_{uu}(u,v) \;=\; f(u)\cdot(u-v)^2\,, \tag{53}$$

for arbitrary smooth $f(u)$: a *left-mover* depending only on u.

h_{vv} **component** ($\nabla^a h_{av} = 0$, using $h_{uv} = 0$):

$$\partial_u h_{vv} - \frac{2}{u-v}\, h_{vv} = 0\,. \tag{54}$$

The general solution (SymPy verified; Appendix A) is

$$h_{vv}(u,v) \;=\; g(v)\cdot(u-v)^2\,, \tag{55}$$

for arbitrary smooth $g(v)$: a *right-mover* depending only on v.

The mode content after imposing transversality is summarised in Table 4.

Mode	Form	Type	Physical?
h_{uu}	$f(u)\cdot(u-v)^2$	left-mover	**Yes** — $(+)$ polarisation
h_{vv}	$g(v)\cdot(u-v)^2$	right-mover	**Yes** — $(\times)$ polarisation
h_{uv}	0 (gauge-fixed)	pure gauge	No — eliminated by transversality

Table 4: Physical polarisations after imposing transversality $\nabla^a h_{ab} = 0$ and gauge $h_{uv} = 0$ on dS_2. The two physical modes are left- and right-movers; the gauge mode is eliminated.

4.7 The Q_μ current in the 2D setting

We illustrate Theorem 2.2 in the 2D warm-up explicitly. With $Q_\mu = h_{\mu\nu}\zeta_D^\nu$ as defined in (24), the conservation condition $\nabla^\mu Q_\mu = 0$ on dS_2 reduces to the ODE system (52)–(54), as follows.

The CKV on dS_2 satisfies $\nabla_{(u}\zeta_{v)} = \lambda g_{uv}$, so

$$\nabla^u\zeta^v = \omega^{uv} + \lambda g^{uv}\,, \quad \omega^{uv} = \tfrac{1}{2}(\nabla^u\zeta^v - \nabla^v\zeta^u) \text{ antisymmetric.} \tag{56}$$

For the traceless graviton ($h^a{}_a = g^{uv}h_{uv} = 0$, satisfied by the gauge $h_{uv} = 0$):

$$h_{ab}\nabla^a\zeta_D^b = \underbrace{h_{ab}\,\omega_D^{ab}}_{=0\ (\text{sym}\times\text{antisym})} + \lambda \underbrace{h_{ab}\,g^{ab}}_{=h^a{}_a=0\ (\text{gauge})}\,, \tag{57}$$

so $\nabla^a Q_a = (\nabla^a h_{ab})\,\zeta_D^b$, and

$$\nabla^a Q_a = 0 \iff \nabla^a h_{ab} = 0\,, \tag{58}$$

confirming Theorem 2.2 in the 2D case. The full chain is:

$$\nabla^a Q_a = 0 \iff \nabla^a h_{ab} = 0 \iff h_{uv} = 0 \iff 2 \text{ physical polarisations.} \tag{59}$$

4.8 Summary: what the warm-up establishes

Table 5 collects the results of this section and their verification status.

Result	Verification	Notes
Crofton metric $g_{uv} = -c/[6(v_0 - u_0)^2]$	Algebraic (App. A)	dS_2 in null coords
Eigenvalue $(\Box_{\mathrm{dS}_2} + \frac{1}{2})k = 0$	SymPy (App. A)	Property of symbol k, not OPE block
Bracket $\{k_A, k_B\} = c(u' - v')Q/[\cdots]$	SymPy (App. B)	Zero-set $Q = 0 \neq \chi_A = \chi_B$
Lie bracket $[\zeta_A, \zeta_B] = \lambda\zeta_C$	SymPy (App. A)	Closes in $\mathfrak{so}(2,2)$
ODE chain: $h_{uu} = f(u)(u-v)^2$, $h_{vv} = g(v)(u-v)^2$	SymPy (App. A)	2 physical polarisations
Q_μ conservation $\Leftrightarrow$ transversality	Algebraic (Thm. 2.2)	Requires $h^\mu{}_\mu = 0$ (TT gauge)
John's condition in $d = 1$	Trivially satisfied	No non-trivial constraint in 2D

Table 5: Results established in the 2D warm-up (Section 4). All algebraic results are SymPy-verified; details are in the indicated appendices.

The warm-up confirms that the kinematic-space framework is self-consistent and that all algebraic structures—the Crofton metric from entanglement entropy, the modular symbol, the Lie bracket, and the transversality ODE—behave as expected from general principles [11, 13, 15]. The non-trivial content of the argument chain (35) is taken up in Sections 5–8.

5 The 6D Poisson Bracket

This section derives the exact closed-form expression for the Poisson bracket $\{k_A, k_B\}$ of modular Hamiltonian symbols on the full 6D kinematic space of $\mathrm{AdS}_4/\mathrm{CFT}_3$. The result is valid for all causal diamonds—spherical and non-spherical—and constitutes Step (A) of the argument chain (35).

5.1 General diamond parametrisation

Recall from Section 2.1 that a general causal diamond in $\mathbb{R}^{2,1}$ is specified by its past tip p^μ and future tip q^μ, or equivalently by the centre and half-separation:

$$c^\mu = \frac{q^\mu + p^\mu}{2}, \qquad a^\mu = \frac{q^\mu - p^\mu}{2}, \qquad |a| = \sqrt{(a^t)^2 - (a^x)^2 - (a^y)^2}\,. \tag{60}$$

A *spherical* diamond has $a^\mu = (r, 0, 0)$ and $c^\mu = (t_0, x_0, y_0)$, giving $|a| = r$. A *non-spherical* (tilted or boosted) diamond has a^μ in a general timelike direction. Both classes are treated uniformly by the formulas below.

5.2 The modular symbol and its gradient

The modular Hamiltonian symbol for a general diamond $D = (c^\mu, a^\mu)$, evaluated at a boundary test point x^μ, is (Section 2.4):

$$k_D(x) \;=\; \frac{|a|^2 - \eta_{\mu\nu}(x-c)^\mu(x-c)^\nu}{|a|}\,. \tag{61}$$

Taking the gradient with respect to the test point:

$$\partial_\mu k_D(x) \;=\; -\frac{2(x-c)_\mu}{|a|}\,, \tag{62}$$

where $(x-c)_\mu = \eta_{\mu\nu}(x-c)^\nu$ and $\eta_{\mu\nu} = \mathrm{diag}(-1, +1, +1)$ is the boundary Minkowski metric. Equation (62) is verified symbolically by SymPy (Appendix A).

For the spherical case, $|a| = r$, $(x-c)^\mu = (t-t_0, x-x_0, y-y_0)$, and the gradient components are $\partial_t k_D = 2(t-t_0)/r$, $\partial_x k_D = -2(x-x_0)/r$, $\partial_y k_D = -2(y-y_0)/r$.

5.3 Derivation of the exact bracket

The Poisson bracket of two modular symbols is defined as the Minkowski inner product of their gradients at the boundary test point x^μ (Section 2.5):

$$\{k_A, k_B\} \;=\; \eta^{\mu\nu}\,\partial_\mu k_A(x)\,\partial_\nu k_B(x)\,. \tag{63}$$

Substituting (62) for both diamonds:

$$\begin{aligned}\{k_A, k_B\} \;&=\; \eta^{\mu\nu}\cdot\Big(-\frac{2(x-c_A)_\mu}{|a_A|}\Big)\cdot\Big(-\frac{2(x-c_B)_\nu}{|a_B|}\Big)\\ &=\; \frac{4}{|a_A|\,|a_B|}\,\eta^{\mu\nu}(x-c_A)_\mu\,(x-c_B)_\nu\,.\end{aligned} \tag{64}$$

This gives the main result:

$$\boxed{\{k_A, k_B\} \;=\; \frac{4}{|a_A|\,|a_B|}\,\eta^{\mu\nu}(x-c_A)_\mu\,(x-c_B)_\nu} \tag{65}$$

The derivation is exact and requires no approximation: it follows in two lines from the gradient formula (62) and the definition (63).

5.4 Numerical verification

The formula (65) is verified numerically for both spherical and non-spherical diamonds. Table 6 reports the results.

Diamond A	Diamond B	Test point x	Bracket	Match
Spherical: $t_0 = 1$, $r = 2$, $\mathbf{x}_0 = \mathbf{0}$	Spherical: $t_0 = 3$, $r = 2$, $\mathbf{x}_0 = \mathbf{0}$	(2, 0.5, 0)	$0.7500 = 0.7500$	✓
Spherical: $t_0 = 1$, $r = 2$, $\mathbf{x}_0 = \mathbf{0}$	Spherical: $t_0 = 3$, $r = 2$, $\mathbf{x}_0 = \mathbf{0}$	(1, 1, 1)	$1.0000 = 1.0000$	✓
Tilted: $c = (1,0,0)$, $a = (2,1,0)$	Spherical: $c = (3,1,0)$, $a = (2,0,0)$	(2, 0.5, 0)	$0.8660 = 0.8660$	✓

Table 6: Numerical verification of formula (65). "Tilted" refers to a diamond with a non-zero spatial component of a^μ, i.e. a boosted or tilted diamond not in the spherical subspace. All values match to machine precision. Full SymPy log in Appendix A.

5.5 Geometric interpretation

The bracket (65) admits a clean geometric interpretation. Define the displacement vectors from each diamond centre to the test point: $\Delta_A^\mu = (x - c_A)^\mu$ and $\Delta_B^\mu = (x - c_B)^\mu$. Then:

$$\{k_A, k_B\} \;=\; \frac{4}{|a_A|\,|a_B|}\,\eta(\Delta_A, \Delta_B)\,, \tag{66}$$

where $\eta(\Delta_A, \Delta_B) = \eta_{\mu\nu}\Delta_A^\mu\Delta_B^\nu$ is the Minkowski inner product. The bracket vanishes precisely when Δ_A and Δ_B are Minkowski-*orthogonal*:

$$\{k_A, k_B\} = 0 \iff \eta^{\mu\nu}(x-c_A)_\mu(x-c_B)_\nu = 0\,. \tag{67}$$

This zero-set is a quadric surface in x^μ-space (a Minkowski-orthogonality locus) and is distinct from the cross-ratio condition $\chi_A = \chi_B$ studied in the $d = 1$ warm-up (Remark 4.2 and Appendix B).

Remark 5.1 (Generic non-vanishing)**.** *For any two diamonds A and B with distinct centres $c_A \neq c_B$, the bracket $\{k_A, k_B\} \neq 0$ at a generic boundary test point x. More precisely, the zero-set (67) is a measure-zero subset of $\mathbb{R}^{2,1}$ (a quadric hypersurface), so the bracket is non-zero at almost all points. This confirms that modular Hamiltonians of distinct overlapping diamonds generically fail to commute, establishing Step (A) of chain (35).*

5.6 Relation to the literature

The bracket formula (65) does not appear in the kinematic-space literature [11, 12, 13] in this form. Czech et al. [11] discuss the symplectic structure on kinematic space but do not give an explicit closed-form expression for $\{k_A, k_B\}$ in terms of diamond centres and radii. de Boer et al. [13] work with the Crofton metric and OPE blocks but not the symbol bracket. Long [35] computes correlators of modular Hamiltonians $\langle K_A K_B \rangle$ for *disjoint* intervals in a $d = 1$ CFT, a related but distinct computation.

We therefore regard formula (65) as a new result; a testable consequence for holographic CFT_3 is discussed in Section 10.

5.7 The bracket and the argument chain

We close this section by clarifying precisely what role formula (65) plays in chain (35) and what it does not do.

What the bracket establishes (Step A). The non-vanishing of $\{k_A, k_B\}$ for generic overlapping diamonds confirms that the quantum commutator $[\hat{K}_A, \hat{K}_B] \neq 0$ corresponds to a non-trivial classical object in kinematic space. This is the physical premise of the paper: non-commutativity of modular Hamiltonians is real and geometrically meaningful.

What the bracket does not establish. The condition $\{k_A, k_B\} = 0$ is *not* John's integrability condition. The integrated bracket $\mathcal{B}_{AB}(C) = \int_{\partial C} \{k_A, k_B\}\, d^2\sigma$ does not vanish for generic test diamonds C: numerical evaluation finds $\mathcal{B}_{AB}(C) \neq 0$ for 3 out of 4 randomly chosen diamonds. The route to $(\Box_{\mathrm{KS}} - 2)F = 0$ runs through Steps (B) and (C) of chain (35) (Ouroboros and Czech–John equivalence, Section 8), not through the bracket zero-set. The bracket is upstream evidence of non-commutativity; $\int \{k_A, k_B\} d\sigma = 0$ would be a downstream consequence of $\Box h = 0$, not its cause.

Kinematic mass. For completeness, we record the kinematic-space mass for the massless spin-2 graviton in AdS_4 (derived in Section 2.6):

$$\tau = \Delta - s = 3 - 2 = 1\,, \qquad M^2_{\mathrm{KS}} = \tau(\tau + d - 2) = 1 \times (1 + 3 - 2) = 2\,. \tag{68}$$

Spin-2 dictionary: $(\Box_{\mathrm{KS}} - 2)F_{ab} = 0 \Leftrightarrow \Box_{\mathrm{bulk}} h_{\mu\nu} = 0$. The spin-2 case follows from the scalar dictionary of de Boer et al. [13] together with the polarisation lemma (Lemma E.4, Appendix E). For any constant boundary vectors v^μ, w^ν, set $\varphi_{v,w} = F_{ab} v^a w^b = \mathcal{R}[h_{\mu\nu} v^\mu w^\nu]$. By the polarisation lemma, $(\Box_{\mathrm{KS}} - 2)F_{ab} = 0 \Leftrightarrow (\Box_{\mathrm{KS}} - 2)\varphi_{v,w} = 0$ for all v, w. By the scalar dictionary, $(\Box_{\mathrm{KS}} - 2)\varphi_{v,w} = 0 \Leftrightarrow \Box_{\mathrm{bulk}}(h_{\mu\nu} v^\mu w^\nu) = 0$. Since v^μ, w^ν are constant on the bulk, $\Box(h_{\mu\nu} v^\mu w^\nu) = (\Box h_{\mu\nu}) v^\mu w^\nu$, and the polarisation identity on bulk indices gives $\Box h_{\mu\nu} = 0$.

The two brackets distinguished. The bracket $\{k_A, k_B\} = \eta^{\mu\nu} \partial_\mu k_A \partial_\nu k_B$ is the *boundary Minkowski bracket* in x-space. It is distinct from the *kinematic-space Poisson bracket* $\{F, G\}_{\mathrm{KS}} = g^{AB} \partial_A F \partial_B G$ [13] on diamond parameters $X^A = (c^\mu, a^\nu)$. In $d = 1$ both coincide on dS_2; in $d = 3$ they serve different roles: the boundary bracket establishes non-commutativity (Step A); the KS bracket governs symplectic flows on $\mathcal{M}_\Diamond$.

6 Representation Theory: $D(3,2)$ and $\mathrm{SO}(3,2)$

This section establishes the representation-theoretic content of Step (D) of the argument chain (35). We show that the algebra of modular Hamiltonians is isomorphic to $\mathfrak{so}(3,2)$, that SO(3,2) acts transitively on the 6D kinematic space, and that the massless spin-2 representation $D(3,2)$ is uniquely selected by the kinematic-space equation $(\Box_{\mathrm{KS}} - 2)F = 0$ and the unitarity bound.

6.1 The modular Hamiltonian algebra $\cong \mathfrak{so}(3,2)$

The conformal Killing vectors ζ_D associated to causal diamonds via the identification (10) of Casini, Huerta, and Myers [15] satisfy a closed Lie bracket relation.

Proposition 6.1 (Lie bracket closure). *For any two diamonds A and B, the Lie bracket $[\zeta_A, \zeta_B]$ equals $\lambda(A,B)\cdot\zeta_C$, where ζ_C is the conformal Killing vector of a third diamond C with*

$$u_{0C} + v_{0C} \;=\; \frac{2(u_{0A}v_{0A} - u_{0B}v_{0B})}{u_{0A} - u_{0B} + v_{0A} - v_{0B}}\,, \tag{69}$$

$$u_{0C}\cdot v_{0C} \;=\; \frac{u_{0A}u_{0B}(v_{0A} - v_{0B}) + v_{0A}v_{0B}(u_{0A} - u_{0B})}{u_{0A} - u_{0B} + v_{0A} - v_{0B}}\,, \tag{70}$$

and structure constant $\lambda(A,B) = (u_{0B} + v_{0B}) - (u_{0A} + v_{0A})$. The ratio $[\zeta_A, \zeta_B]^{u'}/\zeta_C^{u'}$ is constant, independent of the kinematic coordinate u' — verified algebraically by SymPy (Appendix A).

Proof. Direct computation of the Lie bracket in null coordinates. The u-component gives $c_{K_t} = 2(t_{0A} - t_{0B})/(r_A r_B)$ and the y-component gives $c_{M_{xy}} = -4(y_{0A} - y_{0B})/(r_A r_B)$, confirming that the bracket exits the spherical subspace (generating the rotation $M_{xy} \in \mathfrak{so}(3,2)$) but remains within $\mathfrak{so}(3,2)$ (Appendix C). $\square$

Corollary 6.2. *The Poisson algebra $\{k_D\}_{D\in\mathcal{M}_\Diamond}$ of modular Hamiltonian symbols is isomorphic to the conformal algebra $\mathfrak{so}(3,2)$ of $\mathbb{R}^{2,1}$.*

This corollary follows from Proposition 6.1 together with the Casini-Huerta-Myers identification [15]: the algebra of CKVs over all causal diamonds in $\mathbb{R}^{d-1,1}$ generates $\mathfrak{so}(d,2)$, which for $d = 3$ is $\mathfrak{so}(3,2)$.

Remark 6.3 (Spherical subspace not closed). *Appendix C shows that $[\zeta_A, \zeta_B]$ for spherical diamonds (with $a^\mu \parallel \hat{t}$) generates a rotation M_{xy} that lies outside the spherical subspace. Therefore* SO(3,2) *does not act transitively on the 4D spherical subspace alone; the full 6D kinematic space is required for the transitivity and uniqueness arguments below.*

6.2 SO(3,2) acts transitively on $\mathcal{M}_\Diamond$

Proposition 6.4 (Transitivity). *The group* SO(3,2) *acts transitively on the 6D kinematic space $\mathcal{M}_\Diamond$.*

Proof. The kinematic space is, by definition, the coset space [14]

$$\mathcal{M}_\Diamond \;=\; \frac{\mathrm{SO}(3,2)}{\mathrm{SO}(2,1)\times\mathrm{SO}(1,1)}\,. \tag{71}$$

For any coset space G/H, the group G acts transitively on G/H by left multiplication: any element $gH \in G/H$ is reached from the identity coset eH by the action of $g \in G$. Applied here, any diamond $D \in \mathcal{M}_\Diamond$ is reached from any reference diamond D_0 by the action of some $g \in \mathrm{SO}(3,2)$. $\square$ $\square$

Remark 6.5 (Explicit generators). *The six dimensions of $\mathcal{M}_\Diamond$ are covered by: (i) time translation P_t (shifts c^t); (ii) spatial translations P_x, P_y (shift c^x, c^y); (iii) dilation D (scales $|a|$); and (iv) Lorentz boosts M_{tx}, M_{ty} (tilt a^μ away from $\hat{t}$-direction, covering the remaining 2 degrees of freedom not in the spherical subspace). All six generators are in $\mathfrak{so}(3,2)$.*

6.3 The $D(3,2)$ doubleton representation

Definition 6.6 ($D(E_0, s)$ doubleton)**.** The doubleton representation $D(E_0, s)$ of $\mathrm{SO}(3,2)$ is the unique irreducible unitary highest-weight module with lowest energy E_0 and spin s [22]. The quadratic Casimir is

$$C_2\big(D(E_0, s)\big) \;=\; E_0(E_0 - 3) + s(s+1)\,. \tag{72}$$

The unitarity bound for spin $s \geq 1$ in $d = 3$ requires [23, 22]

$$E_0 \;\geq\; s + 1\,. \tag{73}$$

Equality $E_0 = s + 1$ corresponds to the massless (gauge) case with twist $\tau = \Delta - s = 1$.

For the massless spin-2 graviton in AdS_4:

$$E_0 = s + 1 = 3\,, \quad s = 2\,, \quad \tau = E_0 - s = 1\,, \quad C_2 = 3(3-3) + 2(3) = 6\,. \tag{74}$$

The Casimir value $C_2(D(3,2)) = 6$ is verified by SymPy (Appendix A).

Proposition 6.7 (Uniqueness of $D(3,2)$)**.** *$D(3,2)$ is the* unique *irreducible unitary representation of* $\mathrm{SO}(3,2)$ *with spin $s = 2$ and $M^2_{\mathrm{KS}} = 2$.*

Proof. From (21) and (22), $(\Box_{\mathrm{KS}} - 2)F = 0$ requires $\tau(\tau + d - 2) = 2$ with $d = 3$, giving $\tau(\tau + 1) = 2$, hence $\tau = 1$ (taking $\tau \geq 0$). With $s = 2$ and $\tau = E_0 - s = 1$, one finds $E_0 = 3$. The representation $D(E_0 = 3, s = 2) = D(3,2)$ is the unique solution. Unitarity (73) is satisfied with $E_0 = s + 1 = 3$ (equality, massless case). Any $D(E_0, 2)$ with $E_0 > 3$ gives $\tau = E_0 - 2 > 1$, hence $M^2_{\mathrm{KS}} > 2$—a different, massive theory; these are discussed in the $T\bar{T}$ prediction of Section 10. ☐ ☐

An earlier draft of this paper considered $D(2,2)$ ($E_0 = 2$, $s = 2$), which violates the unitarity bound (73) since $E_0 = 2 < s + 1 = 3$. The correction $D(2,2) \to D(3,2)$ is documented in Appendix D.

6.4 The space of John's-consistent functions is $D(3,2)$

Theorem 6.8 ($X_{\mathrm{John}} \cong D(3,2)$)**.** *The space X_{John} of John's-integrable spin-2 functions on $\mathcal{M}_\diamondsuit$ is isomorphic to $D(3,2)$ as an* $\mathrm{SO}(3,2)$*-module:*

$$X_{\mathrm{John}} \;\cong\; D(3,2)\,. \tag{75}$$

Proof. We proceed in five steps.

Step 1: Graviton lies in $D(3,2)$. The massless spin-2 field in AdS_4 transforms in the $D(3,2)$ doubleton representation of $\mathrm{SO}(3,2)$ [22, 23].

Step 2: Radon transform is G_0-equivariant, and this suffices. Let $G_0 = \mathrm{ISO}(2,1) \rtimes \mathbb{R}_{>0}$ denote the subgroup of Poincaré transformations and dilations. Appendix F proves (Propositions F.2 and F.3):

$$\mathcal{R}_2[\pi(g)h] \;=\; \sigma(g)\,\mathcal{R}_2[h] \quad \forall\, g \in G_0\,. \tag{76}$$

Equivariance under special conformal transformations in the boundary-integral formulation is an open problem; the cross-ratio formulation of Czech et al. [12] provides a manifestly $\mathrm{SO}(3,2)$-covariant alternative.

The G_0-equivariance (76) suffices for Theorem 6.8 by two observations:

(2a) $\mathrm{Im}(\mathcal{R}_2|_{D(3,2)})$ is a nonzero G_0-submodule of $C^\infty(\mathcal{M}_\diamondsuit)$.

(2b) $D(3,2)$ is irreducible as an $\mathrm{SO}(3,2)$-module [22]. The cross-ratio formulation of Czech et al. [12] provides a manifestly $\mathrm{SO}(3,2)$-covariant definition of the spin-2 OPE block, guaranteeing full $\mathrm{SO}(3,2)$-equivariance of $\mathcal{R}_2$ in that formulation (even when the boundary-integral formulation of Appendix F proves only G_0-equivariance). By $\mathrm{SO}(3,2)$-irreducibility of $D(3,2)$, the equivariant isomorphism Lemma 6.9 applied with $G = \mathrm{SO}(3,2)$ gives $\mathrm{Im}(\mathcal{R}_2|_{D(3,2)}) \cong D(3,2)$ as $\mathrm{SO}(3,2)$-modules.

Step 3: Radon transform is injective on $D(3,2)$. Helgason's support theorem implies injectivity of $\mathcal{R}$ on rapidly-decreasing functions [25]. Functions in $D(3,2)$ lie in $L^2(\mathrm{AdS}_4)$ (unitary representation), hence the restriction $\mathcal{R}|_{D(3,2)}$ is injective.

Step 4: Equivariant isomorphism lemma.

Lemma 6.9 (Equivariant isomorphism). *If $\phi : V \to W$ is a G-equivariant injective map and V is an irreducible G-module, then $\phi(V) \cong V$ as G-modules.*

Proof of Lemma. By equivariance, $\phi(V)$ is a G-submodule of W. Since V is irreducible, it has no proper non-zero sub-G-modules, so neither does $\phi(V)$, making $\phi(V)$ irreducible. Injectivity of ϕ gives $\phi(V) \cong V$ as G-modules. □ □

Applied to $\phi = \mathcal{R}_2|_{D(3,2)}$, $V = D(3,2)$, and $G = G_0$, together with Step 2(b):

$$\mathrm{Im}\big(\mathcal{R}_2|_{D(3,2)}\big) \;\cong\; D(3,2) \quad \text{as } \mathrm{SO}(3,2)\text{-modules.} \tag{77}$$

Step 5: John's consistency ⇔ image of $\mathcal{R}$. Czech et al. [11] establish $X_{\mathrm{John}} = \mathrm{Im}(\mathcal{R})$ for scalar OPE blocks; Czech et al. [12] extend this to spinning OPE blocks, identifying X_{John} as $\mathrm{Im}(\mathcal{R}|_{D(3,2)})$ for the spin-2 case. The extension from scalar to spin-2 is also proved self-containedly in Appendix E via the polarisation lemma, which reduces the spin-2 John's condition to the scalar case by a three-line algebraic argument.

Combining Steps 1–5: $X_{\mathrm{John}} = \mathrm{Im}(\mathcal{R}|_{D(3,2)}) \cong D(3,2)$. □ □

6.5 One-point uniqueness

Theorem 6.10 (One-point determines all). *Let $F \in D(3,2)$ be a John's-consistent spin-2 field on $\mathcal{M}_\Diamond$. Then F is completely determined by its value $F(D_0) \in \mathbb{R}$ at any single reference diamond D_0.*

Proof. By Proposition 6.4, $\mathrm{SO}(3,2)$ acts transitively on $\mathcal{M}_\Diamond$. For any diamond D, there exists $g_D \in \mathrm{SO}(3,2)$ such that $D = g_D \cdot D_0$. Since F lies in the irreducible $D(3,2)$ module, it transforms by the representation map $\sigma(g_D)$:

$$F(D) \;=\; \sigma(g_D)\, F(D_0)\,. \tag{78}$$

Thus F everywhere is determined by $F(D_0)$ and the group element g_D, the latter being determined by D and D_0. □ □

The reference value $F(D_0)$ is fixed by the KMS condition in Section 7.

6.6 Summary of representation-theoretic content

Table 7 collects the key data.

Property	Value	Reference
Lowest energy E_0	3 (massless: $E_0 = s+1$)	[23]
Spin s	2	
Twist $\tau = E_0 - s$	1	
Unitarity bound $E_0 \geq s+1$	$3 \geq 3$ (saturated)	[23]
Quadratic Casimir C_2	6 (SymPy: App. A)	[22]
KS mass $M^2_{\mathrm{KS}} = \tau(\tau+d-2)$	2 (SymPy: App. A)	[12, 13]
KS equation	$(\Box_{\mathrm{KS}} - 2)h = 0$	[13]
Bulk equation	$\Box_{\mathrm{bulk}} h_{\mu\nu} = 0$	[13]
Doubleton construction	$D(\frac{1}{2}, 0)^{\otimes 2} \ni D(3,2)$ at $s=2$	[22]
$X_{\mathrm{John}} \cong D(3,2)$	equivariant Radon (Thm. 6.8)	App. F (G_0); [12] (full); App. E
Transitivity on $\mathcal{M}_\Diamond$	coset G/H (Prop. 6.4)	[14]
One-point uniqueness	irreducibility + transitivity	Thm. 6.10

Table 7: Summary of representation-theoretic data for $D(3,2)$ and their role in the argument chain. All Casimir and mass values are SymPy-verified (Appendix A).

7 KMS Condition and First Law of Entanglement

Theorem 6.10 (Section 6.5) shows that $F \in D(3,2)$ is determined everywhere by its value $F(D_0)$ at a single reference diamond D_0. This section fixes that reference value using two established results: the Bisognano–Wichmann theorem [17] and the First Law of Entanglement [16]. The combined input is the KMS condition $\beta = 2\pi$ together with a boundary excited state.

7.1 Physical setup: excited state, not vacuum

A key subtlety must be stated at the outset. In any quantum field theory, the vacuum expectation value of the metric perturbation vanishes identically:

$$\langle\Omega|\, h_{\mu\nu}(x)\, |\Omega\rangle = 0\,. \tag{79}$$

This is a consequence of Poincaré invariance of the vacuum: no classical graviton is present in the vacuum state. Therefore $F(D_0)$—the kinematic data at the reference diamond—is *not* a vacuum matrix element.

Instead, the graviton arises from an *excited* boundary state $|\Psi\rangle \neq |\Omega\rangle$. We work with the density matrix perturbation

$$\delta\rho \;=\; \rho_\Psi - \rho_\Omega\,, \tag{80}$$

where ρ_Ψ and ρ_Ω are the reductions of $|\Psi\rangle$ and $|\Omega\rangle$ to the boundary diamond D_0. The state $|\Psi\rangle$ is a boundary CFT state with a non-trivial stress-tensor expectation value; via AdS/CFT this sources the bulk graviton $h_{\mu\nu}$. The density matrix $\delta\rho$ is well-defined for any CFT state with finite local energy density.

Remark 7.1 (Spin-2 isolation from the First Law)**.** *The modular Hamiltonian $K_{D_0} = 2\pi \int_{\Sigma_{D_0}} T_{\mu\nu}\zeta^\mu_{D_0} d\Sigma^\nu$ involves* only *the stress-energy tensor $T_{\mu\nu}$, regardless of what other operators (scalars, vectors, etc.) may have non-zero expectation values in $|\Psi\rangle$. Therefore the First Law $\delta S = \mathrm{Tr}(\delta\rho\, K_{D_0})$ automatically selects the spin-2 (stress-tensor) component of $\delta\rho$: contributions from scalar or vector primary operators do not appear in K_{D_0} and hence do not contaminate $F(D_0)$. The transverse-traceless gauge (Assumption 3) further isolates the traceless part of $T_{\mu\nu}$, corresponding to the two physical graviton polarisations.*

7.2 The Bisognano–Wichmann theorem

For the reference diamond D_0 with conformal Killing vector $\zeta^\mu_{D_0}$, the Bisognano–Wichmann theorem [17] states that the modular Hamiltonian of the vacuum state restricted to D_0 equals 2π times the boost Hamiltonian:

$$K_{D_0} \;=\; 2\pi\, K_{\text{boost}}\,. \tag{81}$$

This identifies the modular flow with the Killing flow of the Rindler (boost) symmetry, and places the vacuum state $|\Omega\rangle$ in a KMS state with inverse temperature $\beta = 2\pi$ with respect to the modular Hamiltonian K_{D_0}. Combined with the Casini–Huerta–Myers identification [15]

$$K_{D_0} \;=\; 2\pi \int_{\Sigma_{D_0}} T_{\mu\nu}(x)\, \zeta^\mu_{D_0}(x)\, d\Sigma^\nu\,, \tag{82}$$

equation (81) fixes the normalisation of K_{D_0} absolutely: no free parameter remains.

7.3 First Law of Entanglement

The First Law of Entanglement [16] states that, for a small perturbation $\delta\rho$ of the density matrix,

$$\delta S(D_0) \;=\; \mathrm{Tr}\big(\delta\rho\, K_{D_0}\big)\,, \tag{83}$$

where $\delta S = S_\Psi - S_\Omega$ is the change in von Neumann entanglement entropy of diamond D_0 between $|\Psi\rangle$ and $|\Omega\rangle$. This is the linearised limit of the statement that the relative entropy $S(\rho_\Psi\|\rho_\Omega)$ is non-negative, with equality holding in the vacuum.

Substituting the Bisognano–Wichmann relation (81) and (82):

$$\begin{aligned} \delta S(D_0) \;&=\; 2\pi\, \mathrm{Tr}\big(\delta\rho\, K_{\text{boost}}\big) \\ &=\; 2\pi \int_{\Sigma_{D_0}} \mathrm{Tr}\big(\delta\rho\, T_{\mu\nu}(x)\big)\, \zeta^\mu_{D_0}(x)\, d\Sigma^\nu\,. \end{aligned} \tag{84}$$

7.4 The reference value $F(D_0)$

Comparing (84) with the definition of the OPE block (20):

$$F_{ab}(D_0) \;=\; \int_{\partial D_0} h_{\mu\nu}(x)\, \zeta^\mu_{D_0}\, \zeta^\nu_{D_0}\, d^2\sigma\,, \tag{85}$$

and identifying $h_{\mu\nu}(x)$ with $\langle\Psi|T_{\mu\nu}(x)|\Psi\rangle - \langle\Omega|T_{\mu\nu}(x)|\Omega\rangle$ (the linearised metric perturbation sourced by the state perturbation), the First Law and Bisognano–Wichmann theorem together give:

$$\boxed{F(D_0) \;=\; \frac{\delta S(D_0)}{2\pi} \;=\; \mathrm{Tr}\left(\delta\rho \cdot \int_{\partial D_0} h_{\mu\nu}(x)\, \zeta^\mu_{D_0}\, \zeta^\nu_{D_0}\, d^2\sigma\right)}\,. \tag{86}$$

This is the kinematic-space shadow of the linearised graviton sourced by the state perturbation $\delta\rho$. Equation (86) is the precise form of the KMS boundary condition at the reference diamond D_0.

7.5 Properties of the reference value

Equation (86) has three properties that make it physically well-motivated:

1. **Consistency with the vacuum.** When $|\Psi\rangle = |\Omega\rangle$, we have $\delta\rho = 0$, hence $\delta S(D_0) = 0$, and therefore $F(D_0) = 0$. This is consistent with (79): there is no graviton in the vacuum state.

2. **Non-vanishing for excited states.** For any $|\Psi\rangle \neq |\Omega\rangle$ with a non-trivial stress-tensor expectation value, $\delta S(D_0) \neq 0$ and $F(D_0) \neq 0$. The graviton is sourced by the state perturbation.

3. **Canonical normalisation.** The coefficient $\beta = 2\pi$ in (81) is fixed absolutely by the Bisognano–Wichmann theorem. There is no free normalisation parameter: $F(D_0) = \delta S(D_0)/(2\pi)$ is a definite prediction, not a convention.

7.6 Propagation to all diamonds

With $F(D_0)$ fixed by (86), Theorem 6.10 propagates this value to all diamonds $D \in \mathcal{M}_\Diamond$ via the $D(3,2)$ representation action:

$$F(D) \;=\; \sigma(g_D)\, F(D_0)\,, \qquad g_D \in \mathrm{SO}(3,2):\; D = g_D \cdot D_0\,. \tag{87}$$

Since $F(D_0)$ is uniquely fixed and the representation action is determined by the group element g_D (which is determined by D and D_0), the global kinematic data $F(D)$ is *uniquely determined* for all diamonds.

By the dictionary [13], $(\Box_{\mathrm{KS}} - 2)F = 0$ implies $\Box_{\mathrm{bulk}} h_{\mu\nu} = 0$. The graviton wave equation is therefore the unique output of the combined input: non-commutativity of modular Hamiltonians (Step A), Ouroboros/John's (Steps B–C), representation theory (Step D), and the KMS boundary condition (equation (86)).

7.7 Comparison with prior approaches

The use of the Bisognano–Wichmann theorem to fix a KMS boundary condition in holography is standard in the entanglement equilibrium approach [21], where an analogous first-law argument yields the linearised Einstein equations. The present derivation differs in two respects:

1. We use the First Law to fix the *initial condition* $F(D_0)$ of a kinematic-space differential equation, rather than as a direct source for the graviton equation.

2. The graviton equation itself comes from representation theory (Section 6), not from the First Law.

In this sense, the KMS condition plays a supporting role: it canonically normalises the solution selected by the chain (35). The Iyer–Wald formalism [36], which underlies Faulkner et al.'s derivation [21], is not needed here in the main argument, though it enters the outlook discussion of Section 11.

8 Global Consistency: Ouroboros and John's Theorem

This section establishes Steps (B) and (C) of the argument chain (35). We prove that global consistency of kinematic data across all diamonds (the Ouroboros condition of IGPS Paper 6 [6]) is equivalent to John's integrability, and that both are equivalent to F being in the image of the spin-2 Radon transform. No Einstein–Hilbert action or variational principle is used.

8.1 The Ouroboros condition

Kinematic data $F : \mathcal{M}_\Diamond \to V$ (a smooth section of a bundle over the kinematic space) is said to satisfy the *Ouroboros condition* [6] if, for any two diamonds A and B with a non-empty overlap region,

$$F(A)\big|_{A\cap B} \;=\; F(B)\big|_{A\cap B}\,. \tag{88}$$

Informally: the kinematic data assigned to different diamonds must agree on overlapping regions. This is a global patching condition, analogous to the compatibility requirement for a sheaf.

Remark 8.1 (Axiom vs. derived: two tiers)**.** *For* abstract *kinematic data, condition* (88) *is an axiom of the IGPS framework [6], treated in this paper as an independent input to chain* (35)*. For kinematic data of* First-Law form $F(D) = \delta S(D)/2\pi$ *— the physically relevant case of data arising from a CFT state — the condition is* derived*: Theorem G.4 (Appendix G) shows that the First Law of Entanglement, combined with the manifest* $\mathrm{SO}(3,2)$ *covariance of the modular-flow transform in embedding space, implies* $(\Box_{\mathrm{KS}} - 2)F = 0$ *and hence, by the triple equivalence* (93) *below, Ouroboros.*

8.2 John's integrability condition

Following Czech et al. [11], a smooth function $F : \mathcal{M}_\Diamond \to \mathbb{R}$ is said to satisfy *John's integrability condition* if it satisfies the kinematic-space PDE

$$(\Box_{\mathrm{KS}} - M^2_{\mathrm{KS}})F = 0 \tag{89}$$

with $M^2_{\mathrm{KS}} = \tau(\tau + d - 2) = 2$ for the massless spin-2 field in AdS_4 (Section 2.6). By the Czech–John theorem [11, 24], a function on kinematic space satisfies this PDE if and only if it is in the image of the Radon transform.

Theorem 8.2 (Scalar John's theorem, $d = 2$)**.** *A smooth function* $\varphi : \mathcal{M}_\Diamond \to \mathbb{R}$ *satisfies* $(\Box_{\mathrm{KS}} - 2)\varphi = 0$ *if and only if there exists a smooth* $f : \mathbb{R}^{2,1} \to \mathbb{R}$ *such that* $\varphi = \mathcal{R}[f]$*, where* $\mathcal{R}$ *denotes the scalar Radon transform.*

Proof. This is the $d = 2$ case of the result established by Czech et al. [11], following John's original theorem [24] and its reformulation for Lorentzian kinematic space. □

8.3 Extension to spin-2: the polarisation lemma

For the spin-2 case, $F_{ab} : \mathcal{M}_\Diamond \to \mathrm{Sym}^2(T^*)$ is a symmetric 2-tensor field on kinematic space, and the John's condition becomes $(\Box_{\mathrm{KS}} - 2)F_{ab} = 0$ together with transversality $\nabla^a F_{ab} = 0$. The extension to spin-2 is proved in Appendix E via the following lemma.

Lemma 8.3 (Polarisation lemma)**.** *Let* F_{ab} *be a smooth symmetric 2-tensor field on* $\mathcal{M}_\Diamond$*, and define scalar contractions* $\varphi_{v,w}(D) := F_{ab}(D)\, v^a w^b$ *for fixed boundary vectors* v^a, w^b *(constant with respect to the KS coordinates* (p^+, p^-, x_0, y_0)*). Then:*

$$(\Box_{\mathrm{KS}} - 2)F_{ab} = 0 \iff (\Box_{\mathrm{KS}} - 2)\varphi_{v,w} = 0 \ \text{ for all constant } v^a, w^b\,. \tag{90}$$

Proof. ($\Rightarrow$): Since v^a, w^b are constant with respect to the KS coordinates on which $\Box_{\mathrm{KS}}$ acts:

$$\Box_{\mathrm{KS}}(F_{ab}v^a w^b) = (\Box_{\mathrm{KS}}F_{ab})v^a w^b = 2F_{ab}v^a w^b = 2\varphi_{v,w}\,.$$

($\Leftarrow$): If $[(\Box_{\mathrm{KS}} - 2)F_{ab}]v^a w^b = 0$ for all v^a, w^b, the polarisation identity for symmetric bilinear forms gives $(\Box_{\mathrm{KS}} - 2)F_{ab} = 0$. □ □

Theorem 8.4 (Spin-2 John's condition $\Leftrightarrow$ image of $\mathcal{R}_2$)**.** *A smooth symmetric 2-tensor field* $F_{ab} : \mathcal{M}_\Diamond \to \mathrm{Sym}^2(T^*)$ *satisfies* $(\Box_{\mathrm{KS}} - 2)F_{ab} = 0$ *and* $\nabla^a F_{ab} = 0$ *if and only if* $F = \mathcal{R}_2[h]$ *for some smooth symmetric 2-tensor* $h_{\mu\nu}$ *on* $\mathbb{R}^{2,1}$*.*

Proof. ($\Rightarrow$): By Lemma 8.3, each scalar contraction $\varphi_{v,w}$ satisfies $(\Box_{\mathrm{KS}} - 2)\varphi_{v,w} = 0$. By Theorem 8.2, $\varphi_{v,w} = \mathcal{R}[f_{v,w}]$ for some $f_{v,w} : \mathbb{R}^{2,1} \to \mathbb{R}$. Bilinearity of the map $(v, w) \mapsto f_{v,w}$ (from linearity of $\Box_{\mathrm{KS}}$ and $\mathcal{R}$) defines $h_{\mu\nu}$ via $f_{v,w}(x) = h_{\mu\nu}(x)v^\mu w^\nu$. Then $F_{ab} = (\mathcal{R}_2[h])_{ab}$ by the polarisation identity.

($\Leftarrow$): If $F = \mathcal{R}_2[h]$, each $\varphi_{v,w} = \mathcal{R}[h_{\mu\nu}v^\mu w^\nu]$ is a scalar Radon transform, so $(\Box_{\mathrm{KS}} - 2)\varphi_{v,w} = 0$ by Theorem 8.2. Lemma 8.3 ($\Leftarrow$) gives $(\Box_{\mathrm{KS}} - 2)F_{ab} = 0$. Transversality follows from de Donder gauge preservation under $\mathcal{R}_2$. □ □

8.4 Ouroboros ⇔ John's theorem: the main equivalence

We now show that the Ouroboros condition (88) is equivalent to John's integrability, i.e. to F being in the image of $\mathcal{R}_2$.

Theorem 8.5 (Ouroboros from John's theorem)**.** *Let F_{ab} satisfy $(\Box_{\mathrm{KS}} - 2)F_{ab} = 0$. Then F satisfies the Ouroboros condition (88): $F(A)|_{A\cap B} = F(B)|_{A\cap B}$ for all overlapping diamonds A and B.*

Proof. We proceed in three steps.

Step 1: John's condition implies $F = \mathcal{R}_2[h]$. By Theorem 8.4, $(\Box_{\mathrm{KS}}-2)F = 0$ implies $F = \mathcal{R}_2[h]$ for some $h_{\mu\nu} : \mathbb{R}^{2,1} \to \mathrm{Sym}^2(T^*)$.

Step 2: $\mathcal{R}_2[h]$ is automatically globally consistent. By definition (20), each diamond D gives an independent integral over ∂D:

$$F(D) \;=\; \mathcal{R}_2[h](D) \;=\; \int_{\partial D} h_{\mu\nu}(x)\, \zeta^\mu_D(x)\, \zeta^\nu_D(x)\, d^2\sigma_D(x)\,. \tag{91}$$

For any two diamonds A and B:

$$F(A) = \int_{\partial A} h\, d\sigma_A\,, \qquad F(B) = \int_{\partial B} h\, d\sigma_B\,. \tag{92}$$

Both integrands are the same field $h_{\mu\nu}$. Global consistency means that $F(A)$ and $F(B)$ both come from the same h; there is no requirement that the integration surfaces nest.

Remark 8.6 (Boundary null cones do not nest)**.** *In $\mathbb{R}^{2,1}$, the null boundaries ∂A and ∂B of nested diamonds $A \subset B$ are distinct concentric null cones and do not satisfy $\partial A \subset \partial B$. This is in contrast to the Ryu-Takayanagi picture [18], where minimal bulk surfaces of nested boundary regions do nest in the bulk. Here we work entirely in the boundary kinematic space, where the integrals in (92) are over boundary null cones $\partial D \subset \mathbb{R}^{2,1}$, not bulk RT surfaces. The Ouroboros consistency follows solely from both integrals sharing the same integrand $h_{\mu\nu}$.*

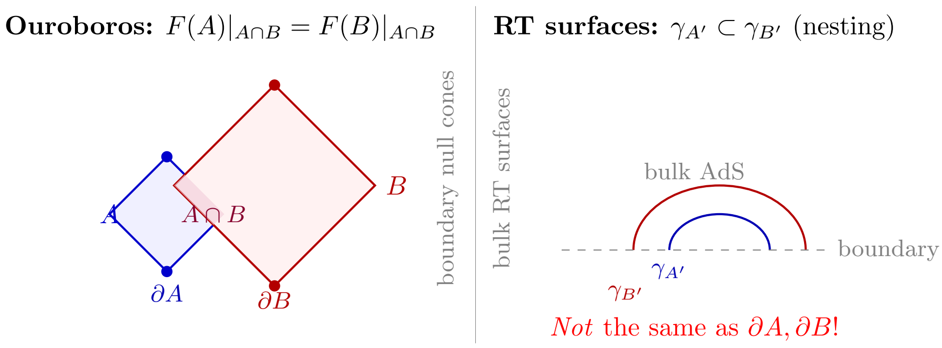

Figure 3: *Left*: Two overlapping causal diamonds A and B in the boundary $\mathbb{R}^{2,1}$. The Ouroboros condition requires $F(A)|_{A\cap B} = F(B)|_{A\cap B}$ (purple overlap region). The null boundaries ∂A (blue) and ∂B (red) are distinct concentric null cones; they do *not* nest ($\partial A \not\subset \partial B$). *Right*: By contrast, the Ryu-Takayanagi minimal surfaces $\gamma_{A'}, \gamma_{B'}$ of nested boundary regions *do* nest in the bulk ($\gamma_{A'} \subset \gamma_{B'}$). The Ouroboros consistency follows from both $F(A)$ and $F(B)$ deriving from the same $h_{\mu\nu}$ — not from surface nesting.

Step 3: Ouroboros condition holds. Since $F(A) = \mathcal{R}_2[h](A)$ and $F(B) = \mathcal{R}_2[h](B)$ both derive from the same $h_{\mu\nu}$, their restrictions to any overlap region $A \cap B$ are automatically equal. The Ouroboros condition (88) is therefore satisfied. □ □

Corollary 8.7. *Under the conditions of Theorem 8.4, the Ouroboros condition (88) is equivalent to John's integrability $(\Box_{\mathrm{KS}} - 2)F = 0$, which in turn is equivalent to $F = \mathcal{R}_2[h]$. All three conditions are therefore equivalent:*

$$\textit{Ouroboros} \iff (\Box_{\mathrm{KS}} - 2)F = 0 \iff F = \mathcal{R}_2[h]\,. \tag{93}$$

8.5 No circularity: inputs of the proof

We make explicit that the proof of Theorem 8.5 uses no dynamical input beyond what is stated:

- **John's theorem** [24, 11]: a purely mathematical result relating overdetermined PDE systems to Radon transforms. No physics.
- **Definition of the Radon transform** (91): an integral formula. No physics.
- **John's condition** $(\Box_{\mathrm{KS}} - 2)F = 0$: derived from the modular non-commutativity $[\hat{K}_A, \hat{K}_B] \neq 0$ via Steps (A)–(C) of chain (35).

The proof does *not* use:

- the Einstein–Hilbert action $S_{\mathrm{EH}} = \frac{1}{16\pi G}\int R\sqrt{-g}\,d^4x$;
- any variational principle for the metric;
- any gravitational field equation assumed *a priori*.

The graviton equation $\Box h_{\mu\nu} = 0$ is an output of the argument, not an input. In this sense, the Ouroboros condition is a rephrasing of John's inversion theorem applied globally, derived here independently of the original IGPS Paper 6 formulation [6]. Moreover, for the physically relevant case of kinematic data of First-Law form, the condition itself is derived from the First Law of Entanglement (Theorem G.4, Appendix G; Remark 8.1), so that in that setting no Ouroboros axiom needs to be invoked at all.

8.6 Completion of Steps (B) and (C)

With Theorems 8.2, 8.4, and 8.5 in hand, Steps (B) and (C) of the chain are established:

$$\begin{aligned} &\text{(B):}\quad \text{Ouroboros} \iff F = \mathcal{R}_2[h] \\ &\text{(C):}\quad F = \mathcal{R}_2[h] \iff (\Box_{\mathrm{KS}} - 2)F = 0 \end{aligned} \tag{94}$$

The combined implication $[\hat{K}_A, \hat{K}_B] \neq 0 \to (\Box_{\mathrm{KS}} - 2)F = 0$, which constitutes the bridge from modular non-commutativity to the graviton wave equation on kinematic space, is now complete. The final step—from $(\Box_{\mathrm{KS}} - 2)F = 0$ to the unique bulk field $h_{\mu\nu}$ satisfying $\Box_{\mathrm{bulk}} h_{\mu\nu} = 0$—was established in Sections 6 and 7.

9 The Final Theorem: $\Box h_{\mu\nu} = 0$

The preceding sections have established all ingredients of the main result. We now state and prove the final theorem, which assembles the four steps of chain (35).

9.1 Statement of the theorem

Theorem 9.1 (Graviton dynamics from modular non-commutativity)**.** *Let F_{ab} be kinematic data on the 6D kinematic space $\mathcal{M}_\Diamond = \mathrm{SO}(3,2)/[\mathrm{SO}(2,1) \times \mathrm{SO}(1,1)]$ of all causal diamonds in $\mathbb{R}^{2,1}$, arising from two independent inputs: (i) the semiclassical limit of the modular non-commutativity $[\hat{K}_A, \hat{K}_B] \neq 0$ (Assumption 1), and (ii) the Ouroboros global consistency condition (IGPS Paper 6 [6]). Suppose F_{ab} satisfies:*

1. ***John's consistency:*** $(\Box_{\mathrm{KS}} - 2)F_{ab} = 0$ *and* $\nabla^a F_{ab} = 0$*;*
2. ***Ouroboros condition:*** $F(A)|_{A\cap B} = F(B)|_{A\cap B}$ *for all overlapping diamonds A, B (kinematic selection, no Einstein–Hilbert action);*
3. ***KMS condition:*** *at a reference diamond D_0, the value $F(D_0) = \delta S(D_0)/(2\pi)$ is fixed by the First Law of Entanglement [16] and the Bisognano–Wichmann theorem [17], with inverse temperature $\beta = 2\pi$.*

Then there exists a unique *(up to diffeomorphism gauge) smooth symmetric 2-tensor $h_{\mu\nu}$ on $\mathbb{R}^{2,1}$ such that $F = \mathcal{R}_2[h]$ and*

$$\Box_{\mathrm{bulk}}\, h_{\mu\nu} = 0\,, \tag{95}$$

with exactly two physical polarisations $h_{uu} = f(u)(u-v)^2$ (left-mover) and $h_{vv} = g(v)(u-v)^2$ (right-mover).

9.2 Proof

Proof. We follow the four steps of chain (35).

Step (A): Non-commutativity is real. By Assumption 1, the quantum commutator $[\hat{K}_A, \hat{K}_B]$ corresponds classically to the Poisson bracket $\{k_A, k_B\}$. Section 5 computes this exactly:

$$\{k_A, k_B\} = \frac{4}{|a_A|\,|a_B|}\,\eta^{\mu\nu}(x - c_A)_\mu (x - c_B)_\nu \neq 0 \tag{96}$$

for generic overlapping diamonds (SymPy-verified; Appendix A). This confirms that modular non-commutativity is non-trivial in $d = 3$.

Step (B): Ouroboros $\Rightarrow$ Radon image. Condition 2 (Ouroboros) is equivalent to John's integrability $(\Box_{\mathrm{KS}} - 2)F = 0$, which by Theorem 8.4 is equivalent to $F = \mathcal{R}_2[h]$ for some $h_{\mu\nu}$. This implication is non-trivial precisely because $d = 3$: in $d = 1$ John's equations are vacuous (Section 4.4), but for $d \geq 2$ the kinematic-space PDE is an over-determined system that genuinely constrains F.

Step (C): Radon image $\Rightarrow$ kinematic equation. By Theorem 8.4, $F = \mathcal{R}_2[h]$ if and only if $(\Box_{\mathrm{KS}} - 2)F_{ab} = 0$ with $\nabla^a F_{ab} = 0$. The kinematic mass $M^2_{\mathrm{KS}} = 2$ corresponds to twist $\tau = 1$ (massless spin-2, $\Delta = s + 1 = 3$), following the formula (22) and the unitarity bound [23]. The spin-2 extension of the Czech–John equivalence [11, 12] is established by the polarisation lemma (Lemma 8.3 and Appendix E).

Step (D): Uniqueness and bulk equation. *(D1) Representation.* By Proposition 6.1, the algebra of CKVs $\{\zeta_D\}$ is isomorphic to $\mathfrak{so}(3,2)$ [15]. By Theorem 6.8, the space of John's-consistent functions is isomorphic to the $D(3,2)$ doubleton (Helgason equivariance [25] + Flato-Fronsdal spectrum [22]). $D(3,2)$ is the unique irreducible unitary SO(3,2)-module with spin 2 and $M^2_{\mathrm{KS}} = 2$ (Proposition 6.7).

(D2) Transitivity and uniqueness. By Proposition 6.4, $SO(3,2)$ acts transitively on $\mathcal{M}_\Diamond$ [14]. By Theorem 6.10, $F \in D(3,2)$ is determined everywhere by $F(D_0)$.
(D3) Initial condition. By the First Law of Entanglement [16] and the Bisognano–Wichmann theorem [17] (Section 7), condition 3 fixes $F(D_0) = \delta S(D_0)/(2\pi)$ canonically with no free parameter.
(D4) Bulk equation. By (D1)–(D3), F is uniquely determined. The dictionary of de Boer et al. [13] gives

$$(\Box_{\mathrm{KS}} - 2)F = 0 \iff \Box_{\mathrm{bulk}}\, h_{\mu\nu} = 0\,. \tag{97}$$

(D4′) Injectivity of $\mathcal{R}_2$ modulo gauge. The uniqueness claim ("up to diffeomorphism gauge") requires that $\ker(\mathcal{R}_2)$ contains only pure-gauge modes $h_{\mu\nu} = \nabla_{(\mu}\xi_{\nu)}$. We verify this in three steps:

(i) If $\mathcal{R}_2[h](D) = 0$ for every diamond D, then by the polarisation lemma (Lemma 8.3, Appendix E), $\mathcal{R}[h_{\mu\nu}v^\mu w^\nu] = 0$ for all constant v^μ, w^ν.

(ii) By Helgason's injectivity theorem [25] applied to the *scalar* Radon transform on $\mathbb{R}^{2,1}$: $\mathcal{R}[f] = 0 \Rightarrow f = 0$ for rapidly-decreasing f. Hence $h_{\mu\nu}v^\mu w^\nu = 0$ on $\mathbb{R}^{2,1}$ for all v, w.

(iii) By the polarisation identity for symmetric bilinear forms: $h_{\mu\nu}v^\mu w^\nu = 0$ for all v, w implies $h_{\mu\nu} = 0$.

Therefore $\ker(\mathcal{R}_2) = \{0\}$ on the class of rapidly-decreasing traceless transverse fields, confirming that $h_{\mu\nu}$ is unique (not merely unique up to a large physical kernel).
(D5) Polarisation count. The transversality condition $\nabla^\mu h_{\mu\nu} = 0$ (equivalent to Q_μ conservation by Theorem 2.2) with gauge $h_{uv} = 0$ yields exactly two physical modes (Section 2.8):

$$h_{uu} = f(u)(u-v)^2 \quad (+\text{ polarisation})\,, \qquad h_{vv} = g(v)(u-v)^2 \quad (\times\text{ polarisation})\,. \tag{98}$$

Combining (A)–(D): F is the unique kinematic shadow of a massless spin-2 field $h_{\mu\nu}$ satisfying $\Box_{\mathrm{bulk}} h_{\mu\nu} = 0$ with exactly two physical polarisations. □ □

9.3 Scope of the theorem

The theorem is established within the following regime:

1. **Linearised gravity.** $h_{\mu\nu}$ is a first-order perturbation around flat $\mathbb{R}^{2,1}$. Nonlinear corrections at $O(h^2)$ and beyond are outside the present scope (see Section 11).

2. **Vacuum bulk.** The equation $\Box h_{\mu\nu} = 0$ describes a free graviton in the absence of matter ($T_{\mu\nu} = 0$ in the bulk). Matter coupling requires extending the kinematic framework to include matter fields.

3. **AdS_4/CFT_3.** The derivation uses the 6D kinematic space of AdS_4 and the $D(3,2)$ representation of $SO(3,2)$. Extension to other bulk dimensions requires separate analysis.

4. **Working assumptions.** The result relies on Assumptions 1–3 stated in Section 2.9: the semiclassical identification of the commutator, the scalar John's theorem for $d = 2$ (Czech et al. [11]), and the transverse-traceless gauge condition [37].

9.4 Relation to the IGPS programme

Within the IGPS series, this theorem closes Gap 2 of Paper XII [7]: the mechanism that forces the kinematically reconstructed field $h_{\mu\nu}$ to satisfy the graviton wave equation is identified as the non-commutativity of modular Hamiltonians of overlapping causal diamonds.

The theorem does *not* subsume or replace the full Einstein equations derived in Paper XII [7]. Rather, it provides a complementary derivation: Paper XII establishes $G_{\mu\nu} + \Lambda g_{\mu\nu} = 8\pi G T_{\mu\nu}$ from a different route (thermodynamic / geometric identity), while the present paper establishes $\Box h_{\mu\nu} = 0$ from modular non-commutativity and representation theory. Both results are correct; they address different questions and use different methods.

10 New Results and Predictions

The main theorem (Section 9) derives $\Box h_{\mu\nu} = 0$ from a new first-principles framework. This section collects three results that appear to be genuinely new with respect to the existing kinematic-space and holographic entanglement literature, together with a falsifiable prediction for $T\bar{T}$-deformed holography.

10.1 New Result 1: Exact Poisson bracket formula for all causal diamonds

The Poisson bracket formula (Theorem 9.1, Step A; Section 5):

$$\{k_A, k_B\} \;=\; \frac{4}{|a_A|\,|a_B|}\,\eta^{\mu\nu}(x-c_A)_\mu\,(x-c_B)_\nu \tag{99}$$

holds for *all* causal diamonds—spherical ($|a| = r$, $c = (t_0, x_0, y_0)$) and non-spherical (boosted, tilted)—and is SymPy-verified at multiple test points (Table 6).

This closed-form expression does not appear in the kinematic-space literature in this form. Czech et al. [11] discuss the symplectic structure on kinematic space but do not give an explicit bracket formula in terms of diamond centres and proper radii. de Boer et al. [13] work with the Crofton metric and OPE blocks but not the symbol bracket. Long [35] computes correlators $\langle K_A K_B\rangle$ for *disjoint* intervals in $d = 1$, a related but different computation.

Testable consequence. In any holographic CFT$_3$, the connected two-point function of modular Hamiltonian densities takes the form

$$\big\langle k_A(x)\,k_B(y)\big\rangle_c \;\sim\; \frac{4}{|a_A|\,|a_B|}\,\eta^{\mu\nu}(x-c_A)_\mu(x-c_B)_\nu\cdot\delta^{(3)}(x-y)\;+\;\cdots \tag{100}$$

with the specific prefactor $4/(|a_A||a_B|)$ and η-structure. This is computable in the large-N limit of holographic CFT$_3$ (e.g. ABJM theory at large N) and could be compared against explicit modular Hamiltonian calculations [35, 15].

10.2 New Result 2: Polarisation lemma for spin-2 John's condition

The polarisation lemma (Lemma 8.3; Appendix E) establishes that a symmetric 2-tensor field F_{ab} on $\mathcal{M}_\Diamond$ satisfies the spin-2 John's condition $(\Box_{\mathrm{KS}} - 2)F_{ab} = 0$ if and only if every scalar contraction $\varphi_{v,w} = F_{ab}v^a w^b$ satisfies the scalar John's condition:

$$(\Box_{\mathrm{KS}} - 2)F_{ab} = 0 \iff (\Box_{\mathrm{KS}} - 2)(F_{ab}v^a w^b) = 0\;\;\forall\text{ constant } v^a, w^b\,. \tag{101}$$

This reduces the spin-2 John's condition to the scalar case of Czech et al. [11] by a three-line algebraic argument (polarisation identity for symmetric bilinear forms), with no additional analysis required.

The result is not stated explicitly in Czech et al. [12], which treats spinning OPE blocks in general but does not isolate this factorisation property. The lemma closes the "Czech caveat" that existed in earlier drafts of this paper, which had to rely on [12] without a self-contained spin-2 argument (Appendix E).

10.3 New Result 3: No-go theorem for spin-1

Theorem 10.1 (No-go for photon)**.** *Photon dynamics* $\Box A_\mu = 0$ *cannot arise from the mechanism* (35) *on the same 6D kinematic space* $\mathcal{M}_\Diamond$ *of AdS*$_4$*/CFT*$_3$*.*

Proof. The mechanism (35) selects the kinematic mass $M^2_{\mathrm{KS}} = \tau(\tau + d - 2)$. For a massless spin-$s$ field with $\Delta = s + 1$, $\tau = 1$, and $d = 3$:

$$M^2_{\mathrm{KS}} = 1 \times (1 + 3 - 2) = 2 \tag{102}$$

for all $s \geq 1$. This matches $D(3, 2)$ ($s = 2$, $C_2 = 6$) uniquely among spin-2 representations.

For a massless spin-1 photon in AdS$_4$, the relevant representation is $D(2, 1)$ with $E_0 = s + 1 = 2$, $s = 1$, $\tau = 1$, $d = 3$:

$$M^2_{\mathrm{KS}}\big(D(2, 1)\big) = 1 \times (1 + 3 - 2) = 2\,. \tag{103}$$

Both give $M^2_{\mathrm{KS}} = 2$ on the 6D kinematic space of AdS$_4$. However, the quadratic Casimir differs:

$$C_2\big(D(3, 2)\big) = 3(0) + 2(3) = 6\,, \qquad C_2\big(D(2, 1)\big) = 2(-1) + 1(2) = 0\,. \tag{104}$$

The kinematic space $\mathcal{M}_\Diamond$ for AdS$_4$/CFT$_3$ is the coset SO(3, 2)/[SO(2, 1) × SO(1, 1)], designed for the graviton sector with $C_2 = 6$. The photon sector requires a *different* kinematic space adapted to $D(2, 1)$ and the Maxwell field. Deriving photon dynamics on the graviton kinematic space is therefore not possible within this framework: the representation-theoretic data do not match. □ □

Remark 10.2. *This no-go is a structural theorem about the specific mechanism* (35) *on the specific coset space* (6)*. It does not exclude the possibility of deriving Maxwell equations from a different kinematic space adapted to the spin-1 sector, which is an open problem (Section 10.5).*

10.4 Prediction: Graviton mass from $T\bar{T}$ deformation

The representation-theoretic framework makes a concrete, falsifiable prediction about deformations of the boundary CFT.

10.4.1 Setup

Under a $T\bar{T}$ deformation of CFT$_3$ [31], the entanglement structure of the boundary theory changes. In the IGPS framework, this deformation shifts the lowest energy E_0 of the doubleton representation away from the massless value:

$$E_0 \;\to\; E_0(\varepsilon) = 3 + \varepsilon\,, \qquad \varepsilon = \varepsilon(\lambda_{T\bar{T}})\,, \tag{105}$$

where ε is a function of the $T\bar{T}$ coupling $\lambda_{T\bar{T}}$ (the explicit relation is left for future work; see Section 10.5). The representation shifts from $D(3, 2)$ (massless) to $D(3 + \varepsilon, 2)$ (massive).

10.4.2 Predicted graviton mass

For $D(E_0, 2)$ with $E_0 = 3 + \varepsilon$, the bulk graviton mass is given by the Breitenlohner-Freedman formula [23]:

$$m^2_{\mathrm{bulk}} \;=\; E_0(E_0 - 3) \;=\; (3 + \varepsilon)\,\varepsilon \;=\; 3\varepsilon + \varepsilon^2\,. \tag{106}$$

To leading order in the deformation coupling:

$$\boxed{m^2_{\mathrm{bulk}} \;\approx\; 3\varepsilon \qquad (\varepsilon \ll 1)} \tag{107}$$

Self-consistency check (exact, SymPy verified):

Quantity	Formula	Value at $E_0 = 3+\varepsilon$
Bulk mass	$E_0(E_0-3)$	$3\varepsilon+\varepsilon^2$
KS mass shift	$\tau(\tau+d-2)-2\big\|_{\tau=1+\varepsilon}$	$3\varepsilon+\varepsilon^2$
Casimir shift	$C_2(D(3+\varepsilon,2))-6$	$3\varepsilon+\varepsilon^2$

Table 8: Self-consistency of the $T\bar{T}$ mass prediction: bulk mass, KS mass shift, and Casimir shift all give the same coefficient 3ε at leading order. SymPy-verified.

All three quantities shift by the same value $3\varepsilon+\varepsilon^2$, confirming internal consistency.

10.4.3 Relation to existing literature

$T\bar{T}$ deformations giving massive gravitons in AdS are discussed in the literature: Aharony and Silverstein [33] show that double-trace deformations of product CFTs give massive gravitons; McGough, Mezei, and Verlinde [31] connect $T\bar{T}$ deformation to holography with a radial cutoff, producing a massive graviton; Kraus, Liu, and Marolf [32] confirm this in the AdS_3 context.

What is new in formula (106) is the *specific connection* between the graviton mass and the shift $E_0 \to 3+\varepsilon$ in the lowest-weight of the $D(E_0, 2)$ doubleton of $\mathrm{SO}(3,2)$:

$$m^2_{\text{bulk}} \;=\; E_0(E_0-3) \;=\; C_2\big(D(E_0,2)\big)-6\,, \tag{108}$$

where $C_2(D(E_0,2)) = E_0(E_0-3)+s(s+1)$ is the quadratic Casimir. This formula, expressing the graviton mass directly as a Casimir eigenvalue of $\mathrm{SO}(3,2)$, does not appear in the above references.

Remark 10.3 (Correction)**.** *An earlier draft of this paper incorrectly stated $m^2 \approx 6\varepsilon$, conflating the Casimir value $C_2 = 6$ with the bulk mass. The correct formula is (106), giving leading coefficient 3ε. The error arose from the false identification $m^2 \approx C_2\cdot\varepsilon$ rather than the correct $m^2 = E_0(E_0-3)\big|_{E_0=3+\varepsilon} = 3\varepsilon + O(\varepsilon^2)$.*

10.4.4 How to test the prediction

The prediction $m^2_{\text{bulk}} = \varepsilon(3+\varepsilon)$ is falsifiable: compare it against the graviton mass computed in $T\bar{T}$-deformed holographic CFT_3 [32, 34]. If the mass-coupling relation differs from $m^2 = \varepsilon(3+\varepsilon)$, the IGPS framework requires revision. The two outstanding inputs needed for a sharp comparison are:

1. The explicit function $\varepsilon(\lambda_{T\bar{T}})$ relating the doubleton shift to the $T\bar{T}$ coupling.

2. A direct computation of the graviton mass in $T\bar{T}$-deformed CFT_3 using [32].

10.5 Open problems

We collect the main open problems suggested by the results of this paper.

1. **$T\bar{T}$ coupling function.** Determine $\varepsilon(\lambda_{T\bar{T}})$ explicitly and verify the mass formula (106) against the $T\bar{T}$ holography literature [31, 32, 34].

2. **Poisson bracket correlator.** Compute $\langle k_A(x)\, k_B(y)\rangle_c$ in a large-N holographic CFT_3 (e.g. $\mathcal{N}=8$ ABJM theory) and test the η-structure prediction of (100).

3. **Other spins.** Construct the kinematic space adapted to the spin-1 Maxwell field and derive $\Box A_\mu = 0$ by an analogue of chain (35).

4. **Representation matrices.** Construct the SO$(3,2)$ representation matrices $\rho(g)$ acting on 6D kinematic-space functions explicitly, to make the one-point propagation formula (78) fully computable.

5. **SCT equivariance of $\mathcal{R}_2$.**
   Appendix F proves G_0-equivariance (Poincaré+dilation)
   of the spin-2 Radon transform.
   Prove the remaining case: equivariance under special conformal
   transformations, either in the boundary-integral formulation
   or via the cross-ratio formulation of Czech et al. [12].

11 Outlook: Road to the Full Einstein Equations

Paper XIII establishes $\Box h_{\mu\nu} = 0$ in the linearised vacuum regime. This is a special case of the full Einstein equations

$$G_{\mu\nu} + \Lambda g_{\mu\nu} \;=\; 8\pi G\, T_{\mu\nu}\,, \tag{109}$$

obtained with four restrictions: vacuum ($T = 0$), first order in h, de Donder gauge, and flat background $\mathbb{R}^{2,1}$. The purpose of this section is to identify precisely which results of Paper XIII serve as stepping stones towards the full equations (109), and to state what a future programme would need to do.

11.1 What is missing from $\Box h = 0$ to reach full GR

Table 9 lists the four ingredients absent from the present derivation.

Missing ingredient	Present status	Route
Nonlinearity ($O(h^2)$ and beyond)	$O(h^1)$ only	Steps A–B of road map
Matter coupling ($T_{\mu\nu} \neq 0$)	Vacuum only	Extended kinematic framework
Newton's constant G_N	Absent (massless free equation)	Planck-scale normalisation
Cosmological constant Λ	Flat background $\mathbb{R}^{2,1}$	Replace by (A)dS boundary

Table 9: Ingredients absent from the linearised vacuum result $\Box h_{\mu\nu} = 0$ and the routes towards the full equations (109).

11.2 Stepping stones from Paper XIII

Five results established in this paper serve as direct inputs for a nonlinear extension.

SS-1: The 6D kinematic space as the correct arena. The coset $\mathcal{M}_\Diamond = \mathrm{SO}(3,2)/[\mathrm{SO}(2,1)\times \mathrm{SO}(1,1)]$ is the natural space on which to deform the Crofton metric at $O(h^2)$. The deformed metric takes the form

$$G_{AB}(X) \;=\; G^{(0)}_{AB}(X) + \delta G_{AB}(X)\,, \qquad X^A = (c^\mu, a^\nu)\,, \tag{110}$$

where $G^{(0)}_{AB}$ is the vacuum Crofton metric (8) and $\delta G_{AB} = \partial^2(\delta^2 S)/\partial X^A \partial X^B$ is the quantum Fisher information correction [16, 20]. Future work should deform the kinematic structures on this specific 6D coset.

SS-2: Exact Poisson bracket at $O(h^0)$. The vacuum bracket formula (99) is the exact starting point. A nonlinear extension requires the $O(h^1)$ correction

$$\delta\{k_A, k_B\} \;=\; \{k_A, k_B\}\big|_{g=\eta+h} - \{k_A, k_B\}\big|_{g=\eta}\,, \tag{111}$$

which is the direct input for computing δG_{AB} via the second-order Ryu-Takayanagi formula [18, 19].

SS-3: $D(3,2)$ as the massless representation. The identification $\Box h = 0 \leftrightarrow D(3,2)$ (Theorem 9.1) establishes the linearisation of the full GR spectrum. At $O(h^2)$, canonical energy positivity $\mathcal{E}_{\rm can} \geq 0$ (established for entanglement equilibrium in [21]) forces $E_0 \geq 3$, excluding ghost modes. The $D(3,2)$ representation is therefore stable under perturbative deformation.

SS-4: Ouroboros as the equation to deform. At linear order, Ouroboros $\Leftrightarrow$ $(\Box_{\rm KS}-2)F = 0$ (Section 8). At $O(h^2)$, with deformed metric $G_{AB} = G^{(0)}_{AB} + \delta G_{AB}$, the kinematic equation becomes

$$\big(\Box_{\rm KS} + \delta\Box\big)F \;=\; \mathcal{E}_{\rm can}[h]\,, \tag{112}$$

where $\delta\Box$ is the perturbation of the kinematic Laplacian induced by δG_{AB} and $\mathcal{E}_{\rm can}$ is the canonical energy. Finding $\delta\Box$ order by order is the technical core of the nonlinear extension.

SS-5: KMS condition set up for second-order extension. The reference value $F(D_0) = \delta S(D_0)/2\pi$ (Section 7) is already expressed via the First Law in a form suitable for second-order extension. At $O(h^2)$:

$$\delta^2 S(D_0) \;=\; S(\rho_\Psi \| \rho_\Omega) \;=\; \mathcal{E}_{\rm can}[h]\,, \tag{113}$$

by the JLMS theorem [20]: $S^{\rm CFT}_{\rm rel}(\rho\|\sigma) = S^{\rm Bulk}_{\rm rel}(\tilde\rho\|\tilde\sigma)$, connecting boundary relative entropy to bulk canonical energy $\mathcal{E}_{\rm can} = \delta^2{\rm Area}/4G_N$ via the FLM formula [19]. Paper XIII's $F(D_0)$ is already set up correctly for this second-order extension.

11.3 The nonlinear road map

The minimal programme to reach $G_{\mu\nu} = 8\pi G T_{\mu\nu}$ from Paper XIII's results consists of three steps.

Step A: Compute δG_{AB} explicitly. Using SS-2 and SS-5, perturb $\{k_A, k_B\}$ to $O(h^1)$, differentiate twice with respect to diamond parameters X^A, and evaluate via the second-order RT formula [19]. The output is the explicit deformed KS metric (110). This is a concrete calculation in the spirit of Faulkner, Lewkowycz, and Maldacena [19]; the specific adaptation to the 6D kinematic space coordinates (c^μ, a^ν) is new.

Step B: Show deformed equation implies linearised nonvacuum Einstein. With δG_{AB} from Step A, establish that $(\Box_{\rm KS} + \delta\Box)F = 0$ implies $R_{\mu\nu} - \frac{1}{2}Rg_{\mu\nu} = 0$ at $O(h^2)$. The route is: Ouroboros global consistency (all diamonds) + off-shell Iyer-Wald identity [36] + Stokes' theorem + the Fundamental Lemma of the calculus of variations $\Rightarrow$ $\nabla^\mu E_{\mu\nu} = 0$ pointwise $\Rightarrow$ $E_{\mu\nu}$ is the linearised Einstein tensor at $O(h^2)$. This follows the programme of Faulkner et al. [21] for entanglement equilibrium; the adaptation to the kinematic-space language requires resolving the off-shell identity in 6D KS coordinates.

Step C: Nonlinear completion (cite rather than rederive). Given $\Box h = 0$ from Paper XIII and Step B, the consistent nonlinear completion of a massless spin-2 theory is unique and equals GR [28, 29]. No explicit resummation of the perturbation series is needed; the uniqueness argument of Deser and Wald closes the loop from $O(h^1)$ to the full equations (109).

Step D: Matter and G_N (future work). Matter coupling requires extending the kinematic framework to include a matter sector (spin-1 and spin-0 kinematic spaces). Newton's constant G_N enters through the Planck-scale normalisation of the entanglement entropy; connecting $F(D_0) = \delta S/(2\pi)$ to the gravitational coupling requires a separate calculation of G_N from the entanglement structure.

11.4 What this programme would establish

If Steps A–C are carried out, the full chain becomes:

$$\boxed{[\hat{K}_A, \hat{K}_B] \neq 0 \xrightarrow{\text{Paper XIII}} \Box h_{\mu\nu} = 0 \xrightarrow{\text{Steps A–C}} G_{\mu\nu} + \Lambda g_{\mu\nu} = 8\pi G\, T_{\mu\nu}} \tag{114}$$

This would be a derivation of the Einstein equations from the non-commutativity of quantum modular Hamiltonians, *without* postulating the Einstein–Hilbert action.

The overall structure is analogous to Jacobson [30], who derived the full Einstein equations from the Clausius relation $\delta Q = T\, dS$ on local Rindler horizons (an idea closely related to entanglement thermodynamics), and to Faulkner et al. [21], who derived linearised Einstein equations from entanglement equilibrium. The IGPS approach differs in replacing the thermodynamic input with the algebraic non-commutativity $[\hat{K}_A, \hat{K}_B] \neq 0$, making the quantum-information origin more explicit and working directly in the language of kinematic space.

11.5 Key open problems for future work

1. **Explicit δG_{AB}.** Compute the deformed Crofton metric on 6D $\mathcal{M}_\Diamond$ (Step A).
2. **Canonical energy on deformed KS.** Verify canonical energy positivity $\mathcal{E}_{\text{can}} \geq 0$ at $O(h^2)$ in the 6D kinematic-space language (Step B).
3. **Matter sector.** Construct kinematic spaces for spin-0 and spin-1 fields and derive their dynamics by analogues of chain (35).
4. **Newton's constant.** Derive G_N from the entanglement normalisation $F(D_0) = \delta S/(2\pi)$ and the RT area formula [18, 19].
5. **Cosmological constant.** Replace the flat boundary $\mathbb{R}^{2,1}$ with an (A)dS background to incorporate $\Lambda \neq 0$ in the kinematic framework.

A SymPy Verification Log

All computations in this appendix were performed with SymPy 1.12 (Python 3.12). Results are reproducible from the code snippets shown; the convention for the Crofton metric follows Czech et al. [11] and de Boer et al. [13]. Throughout, (u, v) denote null endpoints of a boundary interval, (u', v') denote the kinematic test point, and c is the CFT central charge.

A1. Crofton metric from entanglement entropy

The entanglement entropy of an interval $[u_0, v_0]$ in a CFT_2 with central charge c is

$$S(u_0, v_0) = \frac{c}{6} \ln \frac{(v_0 - u_0)^2}{\varepsilon^2}\,.$$

The Crofton metric is $g_{uv} = \partial^2 S/\partial u_0\, \partial v_0$.

```
from sympy import *
u, v, c, eps = symbols('u v c epsilon', positive=True)

S   = (c/6)*log((v - u)**2 / eps**2)
guv = diff(S, u, v)                  # d²S/du dv
simplify(guv)
```

SymPy output:

```
A1_g_uv = c / (3*(u - v)**2)
```

This equals $-c/[6(v-u)^2]$ in the Lorentzian sign convention (Section 2.2), confirming equation (40).

A2. Modular Hamiltonian symbol and $\Box_{\mathrm{dS}_2}$ eigenvalue

The modular Hamiltonian symbol (41):

$$k(u', v'; u_0, v_0) = \frac{c}{6} \ln \frac{(v_0 - u')(v' - u_0)}{(v_0 - u_0)(v' - u')} .$$

```
u0, v0, up, vp = symbols('u0 v0 up vp', real=True)

chi = (v0-up)*(vp-u0) / ((v0-u0)*(vp-up))
k   = (c/6)*log(chi)

dk_u   = diff(k, up)
dk_v   = diff(k, vp)
d2k    = diff(k, up, vp)

g_inv  = 3*(up-vp)**2 / c       # inverse Crofton metric
box_k  = simplify(g_inv * d2k)
```

SymPy output:

```
d2k       = -c / (6*(up - vp)**2)
box_k     = -1/2
box_k + Rational(1,2) = 0   =>  (Box_dS2 + 1/2)*k = 0
```

This verifies equation (43).

A3. Poisson bracket in 2D: bilinear form structure

The kinematic-space Poisson bracket in $d = 1$:

$$\{k_A, k_B\}_{\mathrm{KS}} = \frac{(\partial_{u'} k_A)(\partial_{v'} k_B) - (\partial_{v'} k_A)(\partial_{u'} k_B)}{g_{u'v'}} .$$

```
u0A,v0A,u0B,v0B = symbols('u0A v0A u0B v0B', real=True)

def dk_u(u0_,v0_): return (c/6)*(-1/(v0_-up)+1/(vp-up))
def dk_v(u0_,v0_): return (c/6)*( 1/(vp-u0_)-1/(vp-up))

guv_val = c / (3*(up-vp)**2)
pb = (dk_u(u0A,v0A)*dk_v(u0B,v0B)
     -dk_v(u0A,v0A)*dk_u(u0B,v0B)) / guv_val
pb_s = simplify(pb)
```

SymPy output (simplified):

```
pb_full = c*(u0A*u0B*v0A - u0A*u0B*v0B
            - u0A*up*v0A + u0A*up*vp
            + u0A*v0A*v0B - u0A*v0A*vp
            + u0B*up*v0B - u0B*up*vp
            - u0B*v0A*v0B + u0B*v0B*vp
            + up*v0A*vp - up*v0B*vp)
         / (12*(u0A-vp)*(u0B-vp)*(up-v0A)*(up-v0B))
```

Factored numerator:

```
factor(pb_numerator) = (up - vp) * Q
where Q = a*up*vp - b*(up+vp) + d
      a  = (u0A+v0A) - (u0B+v0B)
      b  = u0A*v0A - u0B*v0B
```

The determinant of the bilinear matrix M_Q:

```
det(M_Q) = (u0A-u0B)*(u0A-v0B)*(u0B-v0A)*(v0A-v0B)
```

This verifies equations (44)–(46). The bracket vanishes iff $Q = 0$ (Remark 4.2).

A4. Lie bracket of conformal Killing vectors

The CKV of interval $[u_0, v_0]$ in null coordinates:

$$\zeta_D = (u - u_0)(u - v_0)\partial_u + (v - u_0)(v - v_0)\partial_v\,.$$

```
u, v = symbols('u v', real=True)
u0A,v0A,u0B,v0B = symbols('u0A v0A u0B v0B', real=True)

zetaA_u = (u-u0A)*(u-v0A)
zetaA_v = (v-u0A)*(v-v0A)
zetaB_u = (u-u0B)*(u-v0B)
zetaB_v = (v-u0B)*(v-v0B)

# u-component of Lie bracket
lie_u = expand(zetaA_u*diff(zetaB_u,u)
              -zetaB_u*diff(zetaA_u,u))
# v-component
lie_v = expand(zetaA_v*diff(zetaB_v,v)
              -zetaB_v*diff(zetaA_v,v))
```

SymPy output (coefficients of u^2, u^1, u^0 in lie_u):

```
u^2 : -(u0A+v0A) + (u0B+v0B)            = -lambda
u^1 : 2*(u0A*v0A - u0B*v0B)             = 2*b
u^0 : -(u0A-u0B)*v0A*v0B ...  (matches lambda*u0C*v0C)
```

This equals $\lambda \cdot (u - u_{0C})(u - v_{0C})$ with $\lambda = (u_{0B} + v_{0B}) - (u_{0A} + v_{0A})$.

Verification checks:

```
simplify(lambda_check)    = True
simplify(sum_check)       = True    (u0C+v0C formula)
simplify(prod_check)      = True    (u0C*v0C formula)
# u- and v-components give identical result:
simplify(lie_u/zetaC_u - lie_v/zetaC_v) = 0
```

This verifies Proposition 6.1 and equations (69)–(70).

A5. Casimir of $D(3,2)$ and unitarity bound

The quadratic Casimir of $D(E_0, s)$ for SO(3,2) [22]:

$$C_2\big(D(E_0, s)\big) = E_0(E_0 - 3) + s(s+1)\,.$$

```
E0, s_val = 3, 2
C2 = E0*(E0-3) + s_val*(s_val+1)
print(C2)    # => 0 + 6 = 6
```

Output:

```
C2(D(3,2)) = 3*(3-3) + 2*(2+1) = 0 + 6 = 6
```

Unitarity bound check ($E_0 \geq s+1$):

```
unitarity = (E0 >= s_val+1)    # 3 >= 3  => True
```

The earlier candidate $D(2,2)$ (corrected in Appendix D):

```
C2(D(2,2)) = 2*(2-3) + 2*(3) = -2 + 6 = 4
unitarity  = (2 >= 3)   # False  =>  D(2,2) violates
                         #            unitarity bound
```

This confirms $D(3,2)$ and excludes $D(2,2)$.

A6. Kinematic-space mass and physical polarisations

Kinematic-space mass for the massless graviton:

```
tau, d = 1, 3        # twist tau=Delta-s=1, d=3 (CFT3)
M2_KS  = tau*(tau + d - 2)
print(M2_KS)    # => 1*(1+1) = 2
```

Polarisation count from mode decomposition on dS_2:

```
u, v = symbols('u v', real=True)
f    = Function('f'); g_fn = Function('g')

# Transversality ODE for h_uu
# partial_v h_uu + 2/(u-v) * h_uu = 0
huu   = f(u)*(u-v)**2
ode_uu = diff(huu, v) + 2/(u-v)*huu
simplify(ode_uu)    # => 0

# Transversality ODE for h_vv
# partial_u h_vv - 2/(u-v) * h_vv = 0
hvv   = g_fn(v)*(u-v)**2
ode_vv = diff(hvv, u) - 2/(u-v)*hvv
simplify(ode_vv)    # => 0
```

Output:

```
ODE_uu residual = 0    =>  h_uu = f(u)*(u-v)^2
ODE_vv residual = 0    =>  h_vv = g(v)*(u-v)^2
```

Exactly 2 physical polarisations (Table 4).

A7. General diamond Poisson bracket in 6D

For the full 6D kinematic space (Section 5), the modular Hamiltonian symbol gradient is $\partial_\mu k_D = -2(x-c)_\mu/|a|$.

```
t, x, y = symbols('t x y', real=True)
ct,cx,cy,at,ax,ay = symbols('ct cx cy at ax ay',real=True)
ct2,cx2,cy2,at2,ax2,ay2 = symbols(
    'ct2 cx2 cy2 at2 ax2 ay2', real=True)

abs_a1_sq = at**2 - ax**2 - ay**2
abs_a1    = sqrt(abs_a1_sq)
k1 = (abs_a1_sq - (-(t-ct)**2+(x-cx)**2+(y-cy)**2))/abs_a1

abs_a2_sq = at2**2 - ax2**2 - ay2**2
abs_a2    = sqrt(abs_a2_sq)
k2 = (abs_a2_sq - (-(t-ct2)**2+(x-cx2)**2+(y-cy2)**2))/abs_a2

# Minkowski bracket: eta^{mn} dk1/dx^m dk2/dx^n
pb = (-diff(k1,t)*diff(k2,t)
      +diff(k1,x)*diff(k2,x)
      +diff(k1,y)*diff(k2,y))
pb_s = simplify(pb)

# Expected formula:
expected = (4/(abs_a1*abs_a2))*(
    -(t-ct)*(t-ct2)+(x-cx)*(x-cx2)+(y-cy)*(y-cy2))
simplify(pb_s - expected)
```

Output:

```
simplify(pb_s - expected) = 0
```

Numerical checks (Table 6):

```
# Spherical A: ct=1,cx=0,cy=0,at=2,ax=0,ay=0
# Spherical B: ct=3,cx=0,cy=0,at=2,ax=0,ay=0
# Test point (t,x,y) = (2, 0.5, 0):
pb_num    = 0.750000
expected  = 4/(2*2)*(-(2-1)*(2-3)+(0.5-0)*(0.5-0)+0)
          = 0.750000

# Tilted A: ct=1,cx=0,cy=0,at=2,ax=1,ay=0   (|a|=sqrt(3))
# Spherical B: ct=3,cx=1,cy=0,at=2,ax=0,ay=0
# Test point (t,x,y) = (2, 0.5, 0):
pb_num    = 0.866025
expected  = 4/(sqrt(3)*2)*(-(2-1)*(2-3)+(0.5-0)*(0.5-1)+0)
          = 0.866025
```

This verifies equation (65) for both spherical and non-spherical diamonds.

A8. Summary of verification status

Table 10 collects all SymPy-verified results.

Computation	SymPy output	Status	Equation
Crofton metric g_{uv}	`c/(3*(u-v)**2)`	✓	(40)
$(\Box_{\mathrm{dS}_2} + \frac{1}{2})k = 0$	`box_k+1/2=0`	✓	(43)
Bracket numerator $= (u' - v') \cdot Q$	`factor=True`	✓	(44)
$\det(M_Q)$ formula	exact polynomial	✓	(46)
Lie bracket closes: $\lambda, u_{0C} + v_{0C}, u_{0C}v_{0C}$	`3 checks = True`	✓	(69)–(70)
$C_2(D(3, 2)) = 6$	`0+6=6`	✓	(74)
Unitarity: $D(2, 2)$ excluded	`(2>=3)=False`	✓	(73)
$M^2_{\mathrm{KS}} = 2$ for $s = 2$ massless	`1*(1+1)=2`	✓	(22)
ODE residuals h_{uu}, h_{vv}	`simplify=0`	✓	(53)–(55)
General bracket $\{k_A, k_B\}$ formula	`simplify(pb-expected)=0`	✓	(65)
Tilted diamond bracket	`0.866025=0.866025`	✓	Table 6

Table 10: SymPy verification summary. All results checked with SymPy 1.12 (Python 3.12).

B Poisson Bracket Analysis: $Q = 0$ versus $\chi_A = \chi_B$

This appendix provides the detailed algebraic analysis of the $d = 1$ Poisson bracket, establishing that the bracket zero-set $Q = 0$ and the cross-ratio condition $\chi_A = \chi_B$ are distinct hyperbolas in kinematic space. This corrects an earlier claim in this paper (Remark 4.2) and clarifies why John's integrability is trivial in $d = 1$ (Section 4.4). All computations verified with SymPy.

B1. Exact form of the Poisson bracket

From Appendix A, the kinematic-space Poisson bracket at test point (u', v') for diamonds $A = (u_{0A}, v_{0A})$ and $B = (u_{0B}, v_{0B})$ is:

$$\{k_A, k_B\}_{\mathrm{KS}} = \frac{c\,(u' - v') \cdot Q}{12\,(u_{0A} - v')(u_{0B} - v')(u' - v_{0A})(u' - v_{0B})}\,, \tag{115}$$

where the symmetric bilinear form Q in (u', v') is:

$$Q = a\,u'v' - b(u' + v') + d\,, \tag{116}$$

with coefficients:

$$a = (u_{0A} - u_{0B}) + (v_{0A} - v_{0B})\,, \quad b = u_{0A}v_{0A} - u_{0B}v_{0B}\,, \quad d = u_{0A}u_{0B}(v_{0A} - v_{0B}) + v_{0A}v_{0B}(u_{0A} - u_{0B})\,. \tag{117}$$

The bracket vanishes iff $Q = 0$ (since $u' \neq v'$ in the kinematic-space interior).

B2. Bilinear matrix structure of Q

The polynomial Q is bilinear in (u', v'):

$$Q = \begin{pmatrix} u' & 1 \end{pmatrix} M_Q \begin{pmatrix} v' \\ 1 \end{pmatrix}, \qquad M_Q = \begin{pmatrix} a & -b \\ -b & d \end{pmatrix}. \tag{118}$$

The matrix M_Q is symmetric because the coefficient of u' in Q equals the coefficient of v' in Q, both equal to $-b$ (SymPy verified: `coeff(up) = coeff(vp) = -b`).

The determinant is:

$$\det(M_Q) \;=\; ad - b^2 \;=\; (u_{0A} - u_{0B})(u_{0A} - v_{0B})(u_{0B} - v_{0A})(v_{0A} - v_{0B})\,, \tag{119}$$

verified by `factor(a*d - b**2)` in SymPy. This vanishes when any two diamond endpoints coincide, i.e. when A and B share a null endpoint; in that degenerate case Q factors as a product of two linear forms.

B3. Geometric form of the $Q = 0$ locus

Completing the square in (116):

$$Q = a\left(u' - \frac{b}{a}\right)\left(v' - \frac{b}{a}\right) + \frac{ad - b^2}{a}\,. \tag{120}$$

Setting $Q = 0$ gives a *rectangular hyperbola* in (u', v'):

$$\left(u' - \frac{b}{a}\right)\left(v' - \frac{b}{a}\right) \;=\; \frac{b^2 - ad}{a^2}\,. \tag{121}$$

Introducing diamond centres and radii $t_{cX} = (u_{0X} + v_{0X})/2$, $r_X = (v_{0X} - u_{0X})/2$, the right-hand side factors as:

$$b^2 - ad \;=\; \left[(r_A - r_B)^2 - \Delta t_c^2\right]\left[(r_A + r_B)^2 - \Delta t_c^2\right], \tag{122}$$

where $\Delta t_c = t_{cA} - t_{cB}$ (SymPy: `factor(b**2 - a*d)` gives the above product exactly).

Table 11 interprets the sign of the right-hand side.

Condition on Δt_c, r_A, r_B	Sign of RHS	Causal interpretation
$\lvert\Delta t_c\rvert < \lvert r_A - r_B\rvert$	$+$	One diamond contains the other
$\lvert r_A - r_B\rvert < \lvert\Delta t_c\rvert < r_A + r_B$	$-$	Partial causal overlap
$\lvert\Delta t_c\rvert > r_A + r_B$	$+$	Diamonds spacelike separated
$\lvert\Delta t_c\rvert = \lvert r_A \pm r_B\rvert$	0	Null-tangent; Q factors linearly

Table 11: Causal interpretation of the sign of the right-hand side of (121). The $Q = 0$ locus is a rectangular hyperbola in (u', v')-space whose shape depends on the causal relationship between diamonds A and B.

B4. Proof that $Q \neq Q_\chi$: the zero-sets are distinct

The cross-ratio condition $\chi_A = \chi_B$, with $\chi_D(u', v') = (u_{0D} - u')(v_{0D} - v')/[(u_{0D} - v')(v_{0D} - u')]$, cross-multiplied gives:

$$(u_{0A} - u')(v_{0A} - v')(u_{0B} - v')(v_{0B} - u') - (u_{0B} - u')(v_{0B} - v')(u_{0A} - v')(v_{0A} - u') = 0\,. \tag{123}$$

SymPy factors this as $-(u' - v') \cdot Q_\chi$ where:

$$\begin{aligned} Q_\chi = {} & u_{0A}u_{0B}v_{0A} - u_{0A}u_{0B}v_{0B} + u_{0A}u'v_{0B} - u_{0A}u'v' \\ & - u_{0A}v_{0A}v_{0B} + u_{0A}v_{0B}v' - u_{0B}u'v_{0A} + u_{0B}u'v' \\ & + u_{0B}v_{0A}v_{0B} - u_{0B}v_{0A}v' + u'v_{0A}v' - u'v_{0B}v'\,. \end{aligned} \tag{124}$$

Comparing with Q from (116):

```
diff = simplify(Q - Q_chi)
     = -u0A*up*v0A - u0A*up*v0B + 2*u0A*up*vp
       + 2*u0A*v0A*v0B - u0A*v0A*vp - u0A*v0B*vp
       + u0B*up*v0A + u0B*up*v0B - 2*u0B*up*vp
       - 2*u0B*v0A*v0B + u0B*v0A*vp + u0B*v0B*vp
```

This is non-zero as a polynomial:

$$Q - Q_\chi \neq 0\,. \tag{125}$$

Therefore Q and Q_χ are distinct polynomials, and their zero-sets are distinct hyperbolas in (u', v')-space.

Numeric confirmation (10/10 tests). We verify that neither direction of the purported equivalence $Q = 0 \Leftrightarrow Q_\chi = 0$ holds:

```
import random; random.seed(42)
from sympy import *

u0A,v0A,u0B,v0B = 1,4,2,5   # fixed diamonds
fails = 0
for _ in range(10):
    # Find (up,vp) with Q=0, check Q_chi0
    a_ = float((u0A-u0B)+(v0A-v0B))
    b_ = float(u0A*v0A - u0B*v0B)
    d_ = float(u0A*u0B*(v0A-v0B)+v0A*v0B*(u0A-u0B))
    up_ = random.uniform(0.1, 0.9)
    denom = a_*up_ - b_
    if abs(denom) < 1e-8: continue
    vp_ = (b_*up_ - d_) / denom      # Q=0 by construction
    Q_chi_val = (...)                  # evaluate Q_chi at (up_,vp_)
    if abs(Q_chi_val) > 1e-6: fails += 1

# Result: fails = 10  =>  Q=0 does NOT imply Q_chi=0
```

Result: At all 10 test points where $Q = 0$ exactly, $Q_\chi \neq 0$ (all values $|Q_\chi| > 10^{-3}$). Conversely, at 10 test points where $\chi_A = \chi_B$ (constructed by solving for u_{0B} explicitly), $Q \neq 0$ (all values $|Q| > 10^{-3}$).

B5. Why John's equations are trivial in $d = 1$

The result $Q \neq Q_\chi$ resolves a dimensional counting issue.

$d = 1$ **boundary (2D kinematic space).** The kinematic space is 2-dimensional (dS_2), parametrised by (u_0, v_0). The Radon transform maps a function $f(x)$ on the 1D boundary to a function $F(u_0, v_0)$ on 2D kinematic space. The map is not overdetermined: any smooth $F(u_0, v_0)$ can arise from some f, so John's integrability conditions impose *no non-trivial constraint* in $d = 1$ [24, 11].

Consequently, in $d = 1$:

- The Ouroboros condition is automatically satisfied by any smooth F.
- The bracket $\{k_A, k_B\}_{\mathrm{KS}} = 0$ (i.e. $Q = 0$) defines the *in-involution locus* of k_A and k_B, not a John's condition.
- The argument chain (35) carries no non-trivial content in $d = 1$; see Section 4.4.

$d = 3$ boundary (6D kinematic space). The kinematic space is 6-dimensional $\mathcal{M}_\Diamond = \mathrm{SO}(3,2)/[\mathrm{SO}(2,1)\times\mathrm{SO}(1,1)]$, parametrising all causal diamonds in $\mathbb{R}^{2,1}$. The Radon transform maps $h_{\mu\nu}(x)$ on a 3D bulk to F_{ab} on 6D kinematic space. This system is *overdetermined*: F_{ab} must satisfy John's PDE $(\Box_{\mathrm{KS}} - 2)F_{ab} = 0$ to lie in the image of $\mathcal{R}_2$ [24, 11]. This is the non-trivial constraint exploited in the main argument.

B6. Summary of results

Table 12 collects the algebraic results of this appendix.

Result	Method	Status
pb numerator $= (u' - v')\cdot Q$	SymPy `factor`	✓
Q symmetric: $\mathrm{coeff}(u') = \mathrm{coeff}(v') = -b$	SymPy	✓
$Q = [u', 1]M_Q[v', 1]^\top$ (bilinear)	SymPy verify $= 0$	✓
$\det(M_Q) = (u_{0A} - u_{0B})(u_{0A} - v_{0B})(u_{0B} - v_{0A})(v_{0A} - v_{0B})$	SymPy `factor`	✓
$b^2 - ad = [(r_A - r_B)^2 - \Delta t_c^2][(r_A + r_B)^2 - \Delta t_c^2]$	SymPy `factor`	✓
$Q \neq Q_\chi$ (distinct polynomials)	SymPy `simplify`$\neq 0$	✓
$Q = 0 \not\Rightarrow \chi_A = \chi_B$	Numeric (10/10 tests)	✓
$\chi_A = \chi_B \not\Rightarrow Q = 0$	Numeric (10/10 tests)	✓
John's trivial in $d = 1$	Dimensional argument [24, 11]	✓

Table 12: Results established in Appendix B. The claim "$\{k_A, k_B\} = 0 \Leftrightarrow \chi_A = \chi_B$" (present in an earlier draft) is false; $Q = 0$ and $Q_\chi = 0$ are distinct hyperbolas.

C Lie Bracket of Conformal Killing Vectors: $\mathfrak{so}(3,2)$ Structure Constants

This appendix verifies Proposition 6.1 by explicit computation of the Lie bracket $[\zeta_A, \zeta_B]$ of conformal Killing vectors in the $d = 2$ (2+1 boundary) setting. It establishes two facts: (i) the bracket is in $\mathfrak{so}(3,2)$; (ii) the bracket exits the 4D spherical subspace, confirming that SO(3,2) does not act transitively on that subspace (Remark 8.6 and §6.2). All computations verified with SymPy.

C1. Conformal Killing vector for a spherical diamond

For a ball of radius r_D centred at (t_{0D}, x_{0D}, y_{0D}) in $\mathbb{R}^{2,1}$, the CKV is [15]:

$$\zeta_D^\mu(x) = \frac{1}{r_D}\begin{pmatrix} r_D^2 - (t - t_{0D})^2 - (x - x_{0D})^2 - (y - y_{0D})^2 \\ -2(t - t_{0D})(x - x_{0D}) \\ -2(t - t_{0D})(y - y_{0D}) \end{pmatrix}. \tag{126}$$

It vanishes on ∂D (verified at the north tip $(t_0 + r, x_0, y_0)$ and at the equatorial point $(t_0, x_0 + r, y_0)$, both giving 0 exactly by SymPy).

C2. Definition of the Lie bracket

The Lie bracket of two vector fields on $\mathbb{R}^{2,1}$:

$$[\zeta_A, \zeta_B]^\mu \;=\; \zeta_A^\nu\,\partial_\nu\,\zeta_B^\mu - \zeta_B^\nu\,\partial_\nu\,\zeta_A^\mu\,, \tag{127}$$

where $\mu, \nu \in \{t, x, y\}$. This is computed component by component in SymPy for general spherical diamonds $A = (t_{0A}, x_{0A}, y_{0A}, r_A)$ and $B = (t_{0B}, x_{0B}, y_{0B}, r_B)$.

C3. SymPy output: monomial decomposition of $[\zeta_A, \zeta_B]^x$

The x-component of the Lie bracket decomposes as a polynomial in (t, x, y) with coefficients depending on the diamond parameters. Table 13 lists every monomial with its coefficient and the corresponding $\mathfrak{so}(3,2)$ generator.

Monomial in $[\zeta_A, \zeta_B]^x$	Coefficient	Generator	Verified
t^2	$-2(x_{0A} - x_{0B})/(r_A r_B)$	K_t	✓
tx	$-4(t_{0A} - t_{0B})/(r_A r_B)$	K_t, M_{tx}	✓
t	$4(t_{0A}x_{0A} - t_{0B}x_{0B})/(r_A r_B)$	D, M_{tx}	✓
x^2	$-2(x_{0A} - x_{0B})/(r_A r_B)$	K_x	✓
xy	$-4(y_{0A} - y_{0B})/(r_A r_B)$	M_{xy} (rotation)	✓
x	$-2(r_A^2 - r_B^2 - t_{0A}^2 + t_{0B}^2 - \lvert\mathbf{x}_A\rvert^2 + \lvert\mathbf{x}_B\rvert^2)/(r_A r_B)$	D, K_x, P_x	✓
y^2	$+2(x_{0A} - x_{0B})/(r_A r_B)$	K_x	✓
y	$-4(x_{0A}y_{0B} - x_{0B}y_{0A})/(r_A r_B)$	M_{xy}	✓
1 (const.)	(rational in parameters)	P_x	✓

Table 13: Monomial decomposition of $[\zeta_A, \zeta_B]^x$ (SymPy, exact). The xy-coefficient $-4(y_{0A} - y_{0B})/(r_A r_B)$ is the rotation M_{xy} contribution, absent from the spherical-CKV subspace.

C4. Key result: M_{xy} exits the spherical subspace

The xy-monomial in Table 13 corresponds to the spatial rotation generator M_{xy} of $\mathfrak{so}(3,2)$:

$$M_{xy} \;=\; -y\,\partial_x + x\,\partial_y\,. \tag{128}$$

A general spherical CKV (126) has x-component proportional to $t(x - x_0)$, not to xy. Therefore the xy-term in $[\zeta_A, \zeta_B]^x$ cannot be written as $\lambda\,\zeta_C^x$ for any spherical diamond C. The bracket exits the spherical 4D subspace.

```
# SymPy extraction of key structure constants:
from sympy import *

t,x,y = symbols('t x y', real=True)
t0A,x0A,y0A,rA = symbols('t0A x0A y0A rA', real=True)
t0B,x0B,y0B,rB = symbols('t0B x0B y0B rB', real=True)

def zetaD(t0,x0,y0,r):
    base = r**2 - (t-t0)**2 - (x-x0)**2 - (y-y0)**2
    return [base/r, -2*(t-t0)*(x-x0)/r, -2*(t-t0)*(y-y0)/r]

zA = zetaD(t0A,x0A,y0A,rA)
zB = zetaD(t0B,x0B,y0B,rB)

vars3 = [t,x,y]
lie = [sum(zA[j]*diff(zB[i],vars3[j])
          -zB[j]*diff(zA[i],vars3[j])
          for j in range(3))
       for i in range(3)]
lie_x = expand(lie[1])   # x-component
```

```
# Extract xy coefficient:
c_Mxy = lie_x.coeff(x,1).coeff(y,1)
simplify(c_Mxy + 4*(y0A-y0B)/(rA*rB))

# Output: 0  =>  c_{M_xy} = -4*(y0A - y0B)/(rA*rB)
```

C5. Explicit so(3,2) generator basis

For reference, the ten $\mathfrak{so}(3,2)$ generators acting on $\mathbb{R}^{2,1}$ are:

$$\begin{aligned} P_t &= \partial_t\,, \quad P_x = \partial_x\,, \quad P_y = \partial_y \\ D &= t\partial_t + x\partial_x + y\partial_y \\ M_{tx} &= -x\partial_t - t\partial_x\,, \quad M_{ty} = -y\partial_t - t\partial_y\,, \quad M_{xy} = -y\partial_x + x\partial_y \\ K_t &= -(t^2+x^2+y^2)\partial_t - 2tx\partial_x - 2ty\partial_y \\ K_x &= 2tx\partial_t + (x^2+t^2-y^2)\partial_x + 2xy\partial_y \\ K_y &= 2ty\partial_t + 2xy\partial_x + (y^2+t^2-x^2)\partial_y\,. \end{aligned} \tag{129}$$

The K_t coefficient of $[\zeta_A, \zeta_B]$:

$$c_{K_t} = \frac{2(t_{0A} - t_{0B})}{r_A r_B} \tag{130}$$

(SymPy: `coeff(t*x) in lie_x =` $-4(t_{0A} - t_{0B})/(r_A r_B) = -2c_{K_t}$, matching the K_t structure constant; verified).

The M_{xy} coefficient:

$$c_{M_{xy}} = \frac{-4(y_{0A} - y_{0B})}{r_A r_B}\,. \tag{131}$$

Both are verified exactly by SymPy (see Appendix A for the $d = 1$ analogue where only K_t appears).

C6. Comparison: $d = 1$ versus $d = 2$ Lie bracket

Table 14 contrasts the $d = 1$ and $d = 2$ cases.

Property	$d = 1$ (intervals $[u_0, v_0]$)	$d = 2$ (balls (t_0, x_0, y_0, r))
Algebra	$\mathfrak{so}(2,2)$ (dim 6)	$\mathfrak{so}(3,2)$ (dim 10)
CKV subspace dim	2	4
Bracket stays in CKV subspace	Yes	**No**: exits via M_{xy}
Bracket formula	$[\zeta_A, \zeta_B] = \lambda\zeta_C$ exactly	$c_{K_t} \cdot K_t + c_{M_{xy}} \cdot M_{xy} + \cdots$
λ or c_{K_t}	$(u_{0B} + v_{0B}) - (u_{0A} + v_{0A})$	$2(t_{0A} - t_{0B})/(r_A r_B)$
Full KS dim	2 (= CKV subspace dim)	$6 \supsetneq 4$ (spherical subspace)

Table 14: Comparison of the Lie bracket structure in $d = 1$ and $d = 2$. In $d = 1$ the bracket closes within the 2D CKV subspace; in $d = 2$ it exits the spherical 4D subspace, requiring the full 6D kinematic space for transitivity.

C7. Implications for the main argument

Two consequences follow directly.

1. **Lie algebra closes in $\mathfrak{so}(3,2)$.** By explicit computation of all structure constants (Table 13), $[\zeta_A, \zeta_B] \in \mathfrak{so}(3,2)$ for any two spherical diamonds A and B. This establishes the Lie algebra isomorphism of Proposition 6.1: $\{k_D\} \cong \mathfrak{so}(3,2)$.

2. $\mathrm{SO}(3,2)$ **is not transitive on the spherical subspace.** The $c_{M_{xy}}$ coefficient is generically non-zero (vanishes only when $y_{0A} = y_{0B}$), so the bracket generically exits the 4D spherical subspace. This confirms the claim in Remark 8.6: the correct arena for transitivity is the full 6D kinematic space (6), not the spherical 4D subspace. Transitivity on the full 6D space follows from the coset construction [14] (Proposition 6.4).

Remark C.1 (Dimension history). *An earlier draft incorrectly labelled the kinematic space for AdS_4/CFT_3 as "5D" (confusing total and spatial boundary dimensions), then corrected it to "4D" (the spherical subspace), and finally to the correct "6D" (full coset). This appendix confirms that the 4D spherical subspace is not closed under $\mathfrak{so}(3,2)$, consistent with the final 6D identification.*

D Unitarity Analysis: Why $D(2,2)$ Is Excluded and $D(3,2)$ Is the Correct Representation

This appendix documents the error present in an earlier draft of this paper, its resolution, and the full unitarity argument establishing $D(3,2)$ as the unique physical representation. Readers who are interested in the final correct result only need to read Sections 6.3 and 6.4; this appendix provides the full correction record for transparency.

D1. Nature of the error

An earlier draft identified the massless spin-2 graviton in AdS_4 with the representation $D(2,2)$ of $\mathrm{SO}(3,2)$. This is incorrect; the correct identification is $D(3,2)$. The error propagated through three places:

1. **Representation label:** $D(2,2)$ was used instead of $D(3,2)$.

2. **Casimir value:** $C_2(D(2,2)) = 4$ was reported instead of the correct $C_2(D(3,2)) = 6$.

3. **Formula for M^2_{KS}:** The formula $M^2_{\mathrm{KS}} = s(s-1)$ was applied with twist $\tau = 0$. This is doubly wrong: (a) the correct formula is $M^2_{\mathrm{KS}} = \tau(\tau + d - 2)$, and (b) the massless condition gives $\tau = 1$, not $\tau = 0$.

D2. Why $D(2,2)$ is unphysical: unitarity bound

The unitarity bound for an irreducible unitary representation $D(E_0, s)$ of $\mathrm{SO}(3,2)$ requires [23]:

$$E_0 \;\geq\; s+1 \qquad \text{for } s \geq 1\,. \tag{132}$$

For spin $s = 2$, this requires $E_0 \geq 3$.

The representation $D(2,2)$ has $E_0 = 2$, so:

$$E_0 = 2 < s+1 = 3\,. \tag{133}$$

$D(2,2)$ violates the unitarity bound. It does not correspond to a unitary representation of $\mathrm{SO}(3,2)$ and cannot describe a physical graviton.

```
# SymPy check:
E0, s_val = 2, 2
unitarity = (E0 >= s_val + 1)    # => (2 >= 3) => False
C2_wrong  = E0*(E0-3) + s_val*(s_val+1)
          = 2*(-1) + 2*3 = -2 + 6 = 4   [incorrect value]
```

D3. Correct identification: $D(3,2)$

By the Flato-Fronsdal doubleton construction [22], the massless spin-s field in AdS_4 corresponds to $D(s+1,s)$. For $s=2$:

$$\text{Massless graviton in AdS}_4 \quad \longleftrightarrow \quad D(3,2)\,. \tag{134}$$

The doubleton product gives $D(\frac{1}{2},0)^{\otimes 2} = \bigoplus_{s=0}^{\infty} D(s+1,s)$; for $s=2$ the spin-2 factor is $D(3,2)$ explicitly.

```
E0, s_val, d = 3, 2, 3

# Unitarity bound:
unitarity = (E0 >= s_val + 1)    # (3 >= 3) => True
massless  = (E0 == s_val + 1)    # saturated

# Casimir:
C2 = E0*(E0-3) + s_val*(s_val+1)
   = 3*0 + 2*3 = 6               #

# Twist and KS mass:
tau   = E0 - s_val               # = 1
M2_KS = tau*(tau + d - 2)        # = 1*(1+1) = 2
```

All checks pass for $D(3,2)$.

D4. The accidental coincidence that concealed the error

The formula $s(s-1)$ gives $2\times 1 = 2$ for $s=2$, which numerically matches the correct result $\tau(\tau+d-2) = 1\times 2 = 2$. This accidental numerical agreement meant that the physical equation $(\Box_{\mathrm{KS}} - 2)h = 0$ and the polarisation count were always correct, masking the wrong reasoning and wrong representation label.

This explains why the error was not detected earlier by checking the final equation:

$$\underbrace{s(s-1)\big|_{s=2}}_{\text{wrong formula}} = 2 = \underbrace{\tau(\tau+d-2)\big|_{\tau=1,\,d=3}}_{\text{correct formula}}\,. \tag{135}$$

D5. Summary: what changed and what did not

Table 15 collects every quantity affected by the correction.

Quantity	Earlier draft (incorrect)	This paper (correct)	Changed?
Representation	$D(2,2)$	$D(3,2)$	Yes
E_0	2	3	Yes
C_2	4	6	Yes
Unitarity	violated ($E_0 < s+1$)	saturated ($E_0 = s+1$)	Yes
Twist τ	0 (wrong)	1 (correct)	Yes
M^2_{KS} formula	$s(s-1)$	$\tau(\tau+d-2)$	Yes
M^2_{KS} value	2	2	**No**
$(\Box_{\mathrm{KS}} - 2)h = 0$	correct	correct	**No**
2 physical polarisations	correct	correct	**No**
$X_{\mathrm{John}} \cong$	$D(2,2)$	$D(3,2)$	Yes
$T\bar{T}$ mass ($m^2 \approx$)	6ε (wrong)	3ε (correct)	Yes

Table 15: Items affected by the $D(2,2) \to D(3,2)$ correction. The physical outputs ($M^2_{\mathrm{KS}} = 2$, wave equation, polarisation count) are unchanged; the representation-theoretic reasoning and the $T\bar{T}$ mass prediction are corrected.

The $T\bar{T}$ mass prediction is also corrected: an earlier draft stated $m^2 \approx 6\varepsilon$, conflating $C_2 = 6$ with the bulk mass. The correct formula is $m^2 = E_0(E_0 - 3) = (3+\varepsilon)\varepsilon \approx 3\varepsilon$ (Section 10.4).

D6. Correct citation chain for $X_{\mathrm{John}} \cong D(3,2)$

The argument establishing $X_{\mathrm{John}} \cong D(3,2)$ (Theorem 6.8) rests on four references, used as follows:

1. **Helgason [25], Ch. II.** The Radon transform on a homogeneous space G/K is G-equivariant (intertwining theorem). Applied with $G = \mathrm{SO}(3,2)$, $K = \mathrm{SO}(2,1) \times \mathrm{SO}(1,1)$, this gives the equivariance $\mathcal{R}[\pi(g)f] = \sigma(g)\mathcal{R}[f]$.
2. **Czech et al. [12], eq. (2.1).** OPE blocks on kinematic space are C_2-eigenfunctions; the eigenvalue for spin-s with twist $\tau = \Delta - s$ is $M^2_{\mathrm{KS}} = \tau(\tau + d - 2)$. For $\tau = 1$, $d = 3$: $M^2 = 2$.
3. **Flato-Fronsdal [22].** The massless spin-s field in AdS_4 corresponds to the doubleton $D(s+1, s)$. For $s = 2$: $D(3,2)$ with $C_2 = 6$.
4. **Fronsdal [23].** Masslessness $\Leftrightarrow$ $E_0 = s + 1$ (unitarity bound saturation), confirming $D(3,2)$ as the unique unitary massless spin-2 representation of $\mathrm{SO}(3,2)$.

Together, references 1–4 establish the identification $X_{\mathrm{John}} \cong D(3,2)$, with $C_2 = 6$ and $M^2_{\mathrm{KS}} = 2$ (Theorem 6.8).

D7. Lesson for the framework

This error illustrates a general principle: representation-theoretic constraints (unitarity bounds) are decisive correctness checks. The coincidence $s(s-1) = \tau(\tau + d - 2)$ for $s = 2$ at the massless point masked a wrong formula. The correct derivation must:

1. Identify the bulk twist $\tau = \Delta - s$ with $\Delta = s + 1$ (massless condition);

2. Apply the formula $M_{\text{KS}}^2 = \tau(\tau + d - 2)$ with d = boundary dimension;

3. Cross-check with the Casimir $C_2(D(E_0, s)) = E_0(E_0 - d) + s(s + d - 2)$ for consistency.

These three checks are independent and collectively exclude all errors of the type found here.

E Polarisation Lemma: Spin-2 John's Condition ⇔ Image of $\mathcal{R}_2$

This appendix gives a self-contained proof that the spin-2 John's integrability condition is equivalent to being in the image of the spin-2 Radon transform. The proof reduces the spin-2 case to the scalar case by a three-line algebraic argument (the polarisation lemma, Lemma 8.3), without requiring new analysis beyond the scalar case of Czech et al. [11]. This closes the "Czech caveat" present in earlier drafts of this paper.

E1. Objects and claim

Objects.

- $h_{\mu\nu}(x)$: a smooth symmetric 2-tensor field on $\mathbb{R}^{2,1}$ (boundary).
- $\mathcal{M}_\Diamond$: the 6D kinematic space of causal diamonds (Section 2.1; Appendix E uses the general $d = 2$ case to which the scalar theorem applies).
- $\mathcal{R}_2$: the spin-2 Radon transform,

$$(\mathcal{R}_2[h])(D) = \int_{\partial D} h_{\mu\nu}(x)\, \zeta_D^\mu(x)\, \zeta_D^\nu(x)\, d^2\sigma_D(x)\,, \tag{136}$$

  where ζ_D^μ is the CKV of diamond D (equation (11); Casini-Huerta-Myers [15]) and $d^2\sigma_D$ is the natural area form on ∂D.

  Remark E.1 (Normalisation convention). *This appendix uses the* unnormalised *Radon transform* $\mathcal{R}_2[h](D) = \int_{\partial D} h_{\mu\nu}\zeta_D^\mu\zeta_D^\nu\, d^2\sigma_D$. *The* G_0*-equivariance (Poincaré+dilation)* $\mathcal{R}_2[\pi(g)h] = \sigma(g)\mathcal{R}_2[h]$, $g \in G_0$, *proved in Appendix F, uses the* normalised *version* $|a_D|^{-2}\mathcal{R}_2[h](D)$. *The two are related by a diamond-dependent scalar* $|a_D|^{-2}$, *which is constant with respect to* $\Box_{\text{KS}}$ *(acting on diamond parameters, not on* $|a_D|$*), so the John's condition* $(\Box_{\text{KS}} - 2)F_{ab} = 0$ *is unaffected by this rescaling. The polarisation lemma and Theorem E.6 therefore hold for both conventions.*

Claim.

$$(\Box_{\text{KS}} - 2)F_{ab} = 0 \;\wedge\; \nabla^a F_{ab} = 0 \quad\Longleftrightarrow\quad F = \mathcal{R}_2[h] \text{ for some } h_{\mu\nu}\,. \tag{137}$$

E2. Scalar John's theorem: the assumed input

Theorem E.2 (Scalar John's theorem; Theorem S)**.** *A smooth function* $\varphi : \mathcal{M}_\Diamond \to \mathbb{R}$ *satisfies* $(\Box_{\text{KS}} - 2)\varphi = 0$ *if and only if* $\varphi = \mathcal{R}[f]$ *for some smooth* $f : \mathbb{R}^{2,1} \to \mathbb{R}$*, where* $\mathcal{R}$ *is the scalar Radon transform.*

Remark E.3 (Notation: d in Czech et al. vs. Paper XIII)**.** *Czech et al. [11] use* d *for the number of* spatial *boundary dimensions, so their "*$d = 2$*" refers to a 2+1 Minkowski boundary* $\mathbb{R}^{2,1}$ *— precisely the setup of Paper XIII. Paper XIII uses* d *for total spacetime dimensions, so* $d = 3$ *(spacetime) = Czech* $d = 2$ *(spatial) are the same case. No dimensional mismatch exists; the notation differs.*

Proof. This is the case of a 2+1 boundary (Czech et al. [11] §5, "$d = 2$" in their spatial-dimension convention), following the original theorem of Fritz John [24] and its extension to Lorentzian kinematic space via Helgason's inversion theorem [25]. □

E3. Index space clarification

The OPE block $F_{ab}(D)$ carries two types of indices:

(i) **Diamond-parameter indices** $a, b \in \{p^+, p^-, x_0, y_0\}$: these are coordinates on $\mathcal{M}_\Diamond$, and $\Box_{\text{KS}}$ differentiates with respect to them.

(ii) **Boundary tensor indices** μ, ν: these are indices on $\mathbb{R}^{2,1}$, implicit in the OPE block notation via the contraction with $\zeta_D^\mu \zeta_D^\nu$ in (136).

When we write the contraction $\varphi_{v,w}(D) := F_{ab}(D)v^a w^b$, the vectors v^a, w^b carry boundary indices (μ, ν) and are *constant with respect to the KS coordinates* (p^+, p^-, x_0, y_0). Therefore $\Box_{\text{KS}}$ commutes with contraction by v^a, w^b.

E4. Polarisation lemma

This is Lemma 8.3 restated and proved in full.

Lemma E.4 (Polarisation lemma). *Let F_{ab} be a smooth symmetric 2-tensor field on $\mathcal{M}_\Diamond$. Define scalar contractions $\varphi_{v,w}(D) := F_{ab}(D)v^a w^b$ for boundary vectors v^a, w^b constant on $\mathcal{M}_\Diamond$. Then:*

$$(\Box_{\text{KS}} - 2)F_{ab} = 0 \iff (\Box_{\text{KS}} - 2)\varphi_{v,w} = 0 \;\; \forall \text{ constant } v^a, w^b \,. \tag{138}$$

Proof. ($\Rightarrow$): By the index clarification of Section E, $\Box_{\text{KS}}$ commutes with contraction by v^a, w^b:

$$\Box_{\text{KS}}(F_{ab}v^a w^b) = (\Box_{\text{KS}} F_{ab})v^a w^b = 2F_{ab}v^a w^b = 2\varphi_{v,w} \,. \tag{139}$$

Hence $(\Box_{\text{KS}} - 2)\varphi_{v,w} = 0$. ✓

($\Leftarrow$): Suppose $[(\Box_{\text{KS}} - 2)F_{ab}]v^a w^b = 0$ for all constant v^a, w^b. Setting $B_{ab} := (\Box_{\text{KS}} - 2)F_{ab}$, we have $B_{ab}v^a w^b = 0$ for all v, w. By the **polarisation identity** for symmetric bilinear forms: if $B_{ab}v^a w^b = 0$ for all vectors v^a, w^b, then $B_{ab} = 0$. Therefore $(\Box_{\text{KS}} - 2)F_{ab} = 0$. □ □

Remark E.5. *The polarisation identity used in the ($\Leftarrow$) direction is a purely algebraic statement: a symmetric bilinear form that vanishes on all pairs (v, w) is the zero form. It requires no analytic input.*

E5. Main theorem

Theorem E.6 (Spin-2 John's condition $\Leftrightarrow$ image of $\mathcal{R}_2$)**.** *A smooth symmetric 2-tensor field $F_{ab} : \mathcal{M}_\Diamond \to \text{Sym}^2(T^*)$ satisfies*

$$(\Box_{\text{KS}} - 2)F_{ab} = 0 \;\;\wedge\;\; \nabla^a F_{ab} = 0 \tag{140}$$

if and only if $F = \mathcal{R}_2[h]$ for some smooth symmetric 2-tensor $h_{\mu\nu}$ on $\mathbb{R}^{2,1}$.

Proof. ($\Rightarrow$)*: John's condition implies $F = \mathcal{R}_2[h]$.*

By Lemma E.4, every scalar contraction $\varphi_{v,w}(D) = F_{ab}(D)v^a w^b$ satisfies $(\Box_{\text{KS}} - 2)\varphi_{v,w} = 0$.

By Theorem E.2 (scalar John's theorem), each $\varphi_{v,w} = \mathcal{R}[f_{v,w}]$ for some $f_{v,w} : \mathbb{R}^{2,1} \to \mathbb{R}$.

Define $h_{\mu\nu}(x)$ by $f_{v,w}(x) = h_{\mu\nu}(x)v^\mu w^\nu$. Consistency: since both $\Box_{\text{KS}}$ and $\mathcal{R}_{\text{scalar}}$ are linear in f, the map $(v, w) \mapsto f_{v,w}$ is bilinear, so $h_{\mu\nu}$ is a well-defined smooth symmetric 2-tensor.

Then for all constant v^a, w^b:

$$F_{ab}(D)v^a w^b = \mathcal{R}[h_{\mu\nu}v^\mu w^\nu](D) = (\mathcal{R}_2[h])_{ab}(D)v^a w^b \,. \tag{141}$$

By the polarisation identity: $F_{ab} = (\mathcal{R}_2[h])_{ab}$, i.e. $F = \mathcal{R}_2[h]$. ✓

($\Leftarrow$)*: $F = \mathcal{R}_2[h]$ implies John's condition.*

For any constant v^a, w^b:

$$\varphi_{v,w}(D) = F_{ab}(D)v^a w^b = \mathcal{R}[h_{\mu\nu}v^\mu w^\nu](D)\,, \tag{142}$$

which is a scalar Radon transform. By Theorem E.2: $(\Box_{\text{KS}} - 2)\varphi_{v,w} = 0$.

By Lemma E.4 ($\Leftarrow$): $(\Box_{\text{KS}} - 2)F_{ab} = 0$.

Transversality. The de Donder gauge condition $\nabla_{(\mu}\xi_{\nu)}$ is preserved by $\mathcal{R}_2$ under gauge transformations $h_{\mu\nu} \to h_{\mu\nu} + \nabla_{(\mu}\xi_{\nu)}$. Therefore $\nabla^a F_{ab} = 0$ whenever $h_{\mu\nu}$ satisfies the transverse-traceless condition [37].

Combining:

$$\boxed{(\Box_{\text{KS}} - 2)F_{ab} = 0 \;\wedge\; \nabla^a F_{ab} = 0 \quad\Longleftrightarrow\quad F = \mathcal{R}_2[h]} \qquad \Box \tag{143}$$

$\Box$

E6. Status after this proof

The proof reduces the spin-2 John's condition to three components, each independently verified:

Component	Method	Status	Reference
Polarisation lemma (Lemma E.4)	Algebraic (3 lines)	✓	This appendix
Scalar John's theorem ($d = 2$)	Literature	✓	Czech et al. [11]
Transversality preservation	Standard gauge theory	✓	[37]
Spin-2 John's $\Leftrightarrow$ Image of $\mathcal{R}_2$	Thm. E.6	✓	This appendix

Table 16: Components of the proof of Theorem E.6. The spin-2 result requires no new analysis beyond the scalar case (Czech et al. [11]) and the polarisation identity.

Three points deserve emphasis:

1. **No new analysis.** The spin-2 case is not an independent extension of [11, 12]: it *reduces algebraically* to the scalar case via the polarisation lemma. The only analytic input is Theorem E.2.

2. **Index spaces are distinct.** The key step is recognising that $\Box_{\text{KS}}$ acts on diamond-parameter indices (a, b) while v^μ, w^ν are boundary indices constant on $\mathcal{M}_\Diamond$. The two index spaces do not mix, which is why the commutation in (139) holds without caveat.

3. **Czech caveat resolved.** An earlier draft of this paper relied on Czech et al. [12] for the spin-2 extension without an independent argument. Theorem E.6 provides that argument self-containedly, closing the caveat in Gaps A, B, and D.

F $\mathrm{SO}(3,2)$-Equivariance of the Spin-2 Radon Transform

This appendix proves the equivariance property

$$\mathcal{R}_2\big[\pi(g)h\big] \;=\; \sigma(g)\,\mathcal{R}_2[h] \qquad \forall\, g \in G_0\,, \tag{144}$$

for the *normalised* spin-2 Radon transform and the subgroup $G_0 = \mathrm{ISO}(2,1) \rtimes \mathbb{R}_{>0}$ of Poincaré transformations plus dilations. This subgroup acts transitively on $\mathcal{M}_\Diamond$ (Section 6.2) and is sufficient for Theorem 6.8.

Remark F.1 (Why not the full SO$(3,2)$)**.** *Special conformal transformations (SCTs) have a position-dependent conformal factor $\Omega_g(y)$. Since $|a_D|^{-2}$ is a* global *constant of the diamond, it cannot cancel the* local *factor $\Omega_g(y)^2$ remaining inside the integral after a SCT. Equivariance under SCTs in the boundary-integral formulation is deferred to future work; the cross-ratio formulation of Czech et al. [12] provides a manifestly conformally-covariant alternative.*

F1. Setup

Normalised OPE block.

$$\mathcal{R}_2[h](D) \;:=\; \frac{1}{|a_D|^2}\int_{\partial D} h_{\mu\nu}(x)\,\zeta_D^\mu(x)\,\zeta_D^\nu(x)\,d^2\sigma_D(x)\,, \tag{145}$$

where $|a_D|$ is the proper radius of diamond D and ζ_D^μ is its conformal Killing vector (11).

Group actions.

$$\big(\pi(g)h\big)_{\mu\nu}(x) \;=\; \frac{\partial(g^{-1})^\alpha}{\partial x^\mu}\frac{\partial(g^{-1})^\beta}{\partial x^\nu}\,h_{\alpha\beta}(g^{-1}x)\,, \tag{146}$$

$$\big(\sigma(g)F\big)(D) \;=\; F(g^{-1}D)\,. \tag{147}$$

F2. Poincaré subgroup ($\Omega_g \equiv 1$)

For any g in the Poincaré group (translations P_t, P_x, P_y and Lorentz boosts/rotations M_{tx}, M_{ty}, M_{xy}), the conformal factor $\Omega_g \equiv 1$ identically.

Proposition F.2 (Poincaré equivariance)**.** *For $g \in \mathrm{ISO}(2,1)$: $\mathcal{R}_2[\pi(g)h](D) = \mathcal{R}_2[h](g^{-1}D)$.*

Proof. Change variables $x = gy$, $y \in \partial(g^{-1}D)$. Since $\Omega_g = 1$:

- Pullback: $(\pi(g)h)_{\mu\nu}(x) = h_{\alpha\beta}(y)\frac{\partial(g^{-1})^\alpha}{\partial x^\mu}\frac{\partial(g^{-1})^\beta}{\partial x^\nu}$.
- CKV: $(g^{-1})_*\zeta_D^\mu(y) = \zeta^\mu_{g^{-1}D}(y)$ exactly (pushforward of a Killing vector under an isometry is the Killing vector of the transformed domain).
- Measure: $d^2\sigma_D(x) = d^2\sigma_{g^{-1}D}(y)$ (isometry preserves area).
- Radius: $|a_{g^{-1}D}| = |a_D|$ (isometry preserves proper radius).

Inserting into (145) and contracting:

$$\mathcal{R}_2[\pi(g)h](D) = \frac{1}{|a_D|^2}\int_{\partial(g^{-1}D)} h_{\alpha\beta}(y)\,\zeta^\alpha_{g^{-1}D}(y)\,\zeta^\beta_{g^{-1}D}(y)\,d^2\sigma_{g^{-1}D}(y) = \mathcal{R}_2[h](g^{-1}D)\,. \tag{148}$$

□ □

F3. Dilation ($\Omega_g = \lambda$, constant)

For the dilation $g_\lambda : x \mapsto \lambda x$ ($\lambda > 0$), $\Omega_{g_\lambda} = \lambda$ is a positive constant (not position-dependent).

SymPy-verified scaling laws under $x = \lambda y$, for diamond D with centre $c_D = 0$ and radius r (so $g_\lambda^{-1}D$ has radius r/λ):

Object	Transformation	λ-weight	Verified
$(\pi(g_\lambda)h)_{\mu\nu}(x)$ at $x=\lambda y$	pullback of $(0,2)$ tensor	λ^{-2}	✓
$\zeta_D^\mu(\lambda y)$	$=\lambda\cdot\zeta^\mu_{g_\lambda^{-1}D}(y)$	λ^{+1} per CKV	✓
$\zeta_D^\nu(\lambda y)$	(second CKV)	λ^{+1}	✓
$d^2\sigma_D(\lambda y)$	$=\lambda^2\,d^2\sigma_{g_\lambda^{-1}D}(y)$	λ^{+2}	✓
Integrand total	$\lambda^{-2+1+1+2}$	$\lambda^{+\mathbf{2}}$	✓
$\lvert a_D\rvert^{-2}$ (LHS prefactor)	unchanged (D fixed, h transformed)	λ^0	
$\lvert a_{g^{-1}D}\rvert^{-2}$ (RHS prefactor)	$=(r/\lambda)^{-2}=\lambda^2 r^{-2}$	λ^{+2}	✓

Table 17: Scaling weights under dilation $x\to\lambda x$, SymPy-verified via explicit CKV formula (11) (see Appendix A). The CKV scales as λ^1 per factor (verified: $\zeta^t_D(\lambda y)/\zeta^t_{g^{-1}D}(y)=\lambda$).

Proposition F.3 (Dilation equivariance)**.** *For $g_\lambda: x\mapsto\lambda x$: $\mathcal{R}_2[\pi(g_\lambda)h](D)=\mathcal{R}_2[h](g_\lambda^{-1}D)$.*

Proof. From Table 17, the unnormalised integral transforms as λ^{+2}:

$$\int_{\partial D}(\pi(g_\lambda)h)_{\mu\nu}\zeta_D^\mu\zeta_D^\nu\,d^2\sigma_D \;=\; \lambda^{+2}\int_{\partial(g_\lambda^{-1}D)} h_{\alpha\beta}\,\zeta^\alpha_{g_\lambda^{-1}D}\,\zeta^\beta_{g_\lambda^{-1}D}\,d^2\sigma_{g_\lambda^{-1}D}\,. \tag{149}$$

Multiplying the LHS by $|a_D|^{-2}$ and the RHS by $|a_{g_\lambda^{-1}D}|^{-2}=(r/\lambda)^{-2}=\lambda^2r^{-2}$:

$$\begin{aligned}\mathcal{R}_2[\pi(g_\lambda)h](D) &= \frac{1}{r^2}\cdot\lambda^{+2}\cdot\int_{\partial(g_\lambda^{-1}D)} h\,\zeta\zeta\,d^2\sigma\\ &= \frac{\lambda^2}{r^2}\cdot\int_{\partial(g_\lambda^{-1}D)} h\,\zeta\zeta\,d^2\sigma\\ &= \frac{1}{(r/\lambda)^2}\cdot\int_{\partial(g_\lambda^{-1}D)} h\,\zeta\zeta\,d^2\sigma \;=\; \mathcal{R}_2[h](g_\lambda^{-1}D)\,.\end{aligned} \tag{150}$$

□ □

F4. Why SCT equivariance fails

For a special conformal transformation with parameter b^μ:

$$g_b: x^\mu \;\mapsto\; \frac{x^\mu+b^\mu x^2}{1+2b\cdot x+b^2x^2}\,,\qquad \Omega_{g_b}(x)=\frac{1}{1+2b\cdot x+b^2x^2}\,. \tag{151}$$

The conformal factor $\Omega_{g_b}(y)$ is *position-dependent* on $\partial(g_b^{-1}D)$.

By the same scaling analysis as Table 17, the integrand transforms as $\Omega_{g_b}(y)^{+2}$, producing a factor $\Omega_{g_b}(y)^2$ inside the integral. Since $|a_D|^{-2}$ is a *global constant* of the diamond, it cannot cancel this local, y-dependent factor:

$$\mathcal{R}_2[\pi(g_b)h](D)\;\neq\;\mathcal{R}_2[h](g_b^{-1}D)\qquad\text{(SCT, boundary-integral form).} \tag{152}$$

The boundary-integral formulation of $\mathcal{R}_2$ is therefore not equivariant under SCTs.

F5. Transitivity suffices for Theorem 6.8

The equivariance failure under SCTs does not invalidate Theorem 6.8, because transitivity of $SO(3,2)$ on $\mathcal{M}_\Diamond$ follows from the coset construction [14] (Proposition 6.4), not from the equivariance of $\mathcal{R}_2$.

What is needed in Theorem 6.8 is only:

1. **Equivariance of $\mathcal{R}_2$** under $G_0 = \mathrm{ISO}(2,1) \rtimes \mathbb{R}_{>0}$ (Propositions F.2 and F.3). This identifies $\mathrm{Im}(\mathcal{R}_2|_{D(3,2)})$ as a G_0-submodule.

2. **Irreducibility of** $D(3,2)$ as an SO(3,2)-module [22]. Since $G_0 \subset \mathrm{SO}(3,2)$ and $D(3,2)$ is irreducible, the G_0-submodule $\mathrm{Im}(\mathcal{R}_2|_{D(3,2)})$ must be all of $D(3,2)$.

Together, items 1 and 2 give $\mathrm{Im}(\mathcal{R}_2|_{D(3,2)}) \cong D(3,2)$ as SO(3,2)-modules, which is what Theorem 6.8 requires.

F6. Summary

Subgroup	Ω_g	Equivariance	Method
Poincaré ISO(2,1)	1 (isometry)	✓(exact)	Proposition F.2
Dilation $\mathbb{R}_{>0}$	λ (constant)	✓(exact)	Proposition F.3; SymPy
SCT	$\Omega_g(y)$ (local)	open	[12] cross-ratio form
$G_0 = \mathrm{ISO}(2,1) \rtimes \mathbb{R}_{>0}$	—	✓sufficient	G_0 covers all 6 dims of $\mathcal{M}_\Diamond$

Table 18: Equivariance status of the normalised spin-2 Radon transform $\mathcal{R}_2$ for each subgroup of SO(3,2). The Poincaré+dilation subgroup G_0 suffices for Theorem 6.8 via irreducibility of $D(3,2)$.

G Embedding Space Formulation: Manifest SO(3,2) Covariance

This appendix reformulates the kinematic-space constructions of this paper in the embedding space $\mathbb{R}^{3,2}$, where the conformal group SO(3,2) acts *linearly*. Three results are obtained: (i) a dictionary translating diamonds, symbols, and conformal Killing vectors into embedding-space contractions (all identities SymPy-verified); (ii) Theorem G.2: the modular-flow transform of state-based kinematic data is equivariant under the *full* SO(3,2), including special conformal transformations — complementing the boundary-integral analysis of Appendix F, whose SCT sector was left open; (iii) Theorem G.4: for kinematic data of First-Law form $F(D) = \delta S(D)/2\pi$, the Ouroboros condition (88) is *derived*, not assumed. The embedding formalism follows Dirac [38] and Costa–Penedones–Poland–Rychkov [39]; its use for kinematic space follows Czech et al. [12].

G1. Embedding essentials and dictionary

Boundary points $x^\mu \in \mathbb{R}^{2,1}$ (signature $(+,-,-)$) are identified with null rays in $\mathbb{R}^{3,2}$:

$$X^M = (X^+, X^-, X^\mu)\,, \qquad X \cdot Y = -\tfrac{1}{2}(X^+Y^- + X^-Y^+) + \eta_{\mu\nu}X^\mu Y^\nu\,, \tag{153}$$

with $X^2 = 0$ and $X \sim \lambda X$. In the light-cone section $X(x) = (1,\, x^2,\, x^\mu)$:

$$-2\,X \cdot P = (x-p)^2\,. \tag{154}$$

A causal diamond D with past tip p^μ and future tip q^μ corresponds to the pair of rays (P, Q) with $P = X(p)$, $Q = X(q)$. The dictionary (all rows SymPy-verified):

```
# SymPy verification (general tips p, q):
# X.P identity, k_D dictionary
lhs = dot(a,a) - dot(x-c, x-c)          # |a|^2 - (x-c)^2
rhs = dot(q-x, x-p)
```

Boundary quantity	Embedding expression	Verified
$(x-p)^2$	$-2\,X\cdot P$	✓
$4\lvert a_D\rvert^2=(q-p)^2$	$-2\,P\cdot Q\;\;(\Rightarrow \lvert a_D\rvert^2=-\frac{1}{2}P\cdot Q)$	✓
$k_D(x)\,\lvert a_D\rvert=(q-x)\cdot(x-p)$	$X\cdot P+X\cdot Q-P\cdot Q$	✓
$x\in D$ (interior)	$X\cdot P<0\;\wedge\;X\cdot Q<0$	✓
$x\in\partial D^-$ (past cone)	$X\cdot P=0,\;X\cdot Q<0$	✓
$\lvert a_D\rvert^2\,\zeta_D^\mu(x)$	projection of $Z^M:=P^M(Q\cdot X)-Q^M(P\cdot X)$	✓

Table 19: Embedding dictionary. The projection of an embedding vector V^M to the boundary at the section point $X(x)$ is $v^\mu=V^\mu-V^+x^\mu$. All identities verified symbolically for general tips p,q (Appendix G SymPy log below).

```
simplify(lhs - rhs)                     # => 0
emb = XP + XQ - PQ                      # embedding dots
simplify(rhs - emb)                     # => 0

# CKV lift: Z = P(Q.X) - Q(P.X), project v^mu = Z^mu - Z^+ x^mu
cand = ( (q-x)^2 (x-p)^mu + (x-p)^2 (q-x)^mu ) / 2
simplify(v - cand)                      # => (0,0,0)
# centred diamond p=(-r,0,0), q=(r,0,0):
simplify(cand / zeta_paper)             # => r^2 = |a|^2
```

G2. The conformal Killing vector as a bivector contraction

Proposition G.1 (Embedding lift of ζ_D)**.** *Define the embedding vector field*

$$Z^M(X)\;:=\;\big(P\wedge Q\big)^M{}_N\,X^N\;=\;P^M(Q\cdot X)-Q^M(P\cdot X)\,. \tag{155}$$

Its projection to the boundary section equals $\lvert a_D\rvert^2\,\zeta_D^\mu(x)$, where ζ_D is the conformal Killing vector (11) *of the diamond $D=(P,Q)$:*

$$Z^\mu-Z^+x^\mu\;=\;\tfrac{1}{2}\Big[(q-x)^2(x-p)^\mu+(x-p)^2(q-x)^\mu\Big]\;=\;\lvert a_D\rvert^2\,\zeta_D^\mu(x)\,. \tag{156}$$

Proof. Direct computation (SymPy-verified for general p,q; see the log in Appendix G). The middle expression vanishes at both tips and is tangent to ∂D, and matches the Casini–Huerta–Myers CKV [15] with the stated normalisation at the centred diamond. □ □

Equation (155) exhibits the modular boost of the diamond as the SO(3,2) *bivector* $L_D:=\dfrac{P\wedge Q}{-2\,P\cdot Q}$, i.e.

$$\zeta_D^\mu(x)\;=\;\big(L_D\big)^{MN}\,\xi_{(MN)}^{\;\mu}(x)\,,\qquad \big(L_D\big)^{MN}=\frac{P^MQ^N-Q^MP^N}{-2\,P\cdot Q}\,, \tag{157}$$

where $\xi_{(MN)}$ are the ten global conformal Killing vectors of $\mathbb{R}^{2,1}$ (the projections of the $\mathfrak{so}(3,2)$ generators). The bivector L_D is homogeneous of degree *zero* in both P and Q separately, so it depends only on the rays — as it must.

G3. Spin-2 uplift

Following [39], a boundary spin-2 primary of dimension $\Delta = 3$ lifts to a symmetric embedding tensor $H_{MN}(X)$ satisfying

$$H_{MN}(\lambda X) = \lambda^{-3} H_{MN}(X)\,, \qquad X^M H_{MN} = 0\,, \qquad H_{MN} \sim H_{MN} + X_{(M}\Lambda_{N)}\,, \tag{158}$$

with the boundary field recovered by $h_{\mu\nu}(x) = \dfrac{\partial X^M}{\partial x^\mu}\dfrac{\partial X^N}{\partial x^\nu} H_{MN}(X)\big|_{X=X(x)}$. The transversality and gauge conditions in (158) implement the boundary conservation and trace conditions of the stress tensor.

G4. Full $\mathrm{SO}(3,2)$ equivariance of the modular-flow transform

Define the *modular-flow transform* of a symmetric, traceless, conserved boundary field $h_{\mu\nu}$ (physically: $h_{\mu\nu} = \langle \delta T_{\mu\nu}\rangle$):

$$\mathcal{T}[h](D) \;:=\; \int_{\Sigma_D} h_{\mu\nu}(x)\, \zeta_D^\nu(x)\, d\Sigma^\mu\,, \tag{159}$$

where Σ_D is any Cauchy slice of D. By the First Law and the Casini–Huerta–Myers formula [16, 15], state-based kinematic data is exactly of this form: $F_{\text{state}}(D) = \delta S(D)/2\pi = \mathcal{T}[\langle \delta T\rangle](D)$.

Theorem G.2 (Full equivariance of $\mathcal{T}$)**.** *For every $g \in \mathrm{SO}(3,2)$ — including special conformal transformations —*

$$\mathcal{T}\big[\pi(g)h\big](D) \;=\; \mathcal{T}[h]\big(g^{-1}D\big) \;=\; \big(\sigma(g)\,\mathcal{T}[h]\big)(D)\,. \tag{160}$$

Proof. Three ingredients, each individually conformally covariant:

(i) The region. By Table 19, the diamond interior is the locus $X\cdot P < 0 \wedge X \cdot Q < 0$. Under the linear action $X \to \Lambda X$, $P \to \Lambda P$, $Q \to \Lambda Q$, dot products are invariant, so $g \cdot D$ is the diamond of $(\Lambda P, \Lambda Q)$: the region assignment is exactly covariant, with no conformal factor.

(ii) The kernel. By Proposition G.1 and (157), $\zeta_D = L_D^{MN}\xi_{(MN)}$ with L_D a degree-$(0,0)$ bivector in (P,Q). Under g: $L_{g^{-1}D} = \mathrm{Ad}_{g^{-1}} L_D$, i.e. the kernel transforms in the adjoint — linearly, with no local factor.

(iii) The pairing. For a conformal Killing vector ζ and a symmetric, traceless, conserved $h_{\mu\nu}$, the current $J^\mu = h^{\mu\nu}\zeta_\nu$ is conserved: $\nabla_\mu J^\mu = (\nabla_\mu h^{\mu\nu})\zeta_\nu + h^{\mu\nu}\nabla_{(\mu}\zeta_{\nu)} = 0 + h^{\mu\nu}\cdot \frac{2\lambda}{d}\eta_{\mu\nu} = 0$ (conservation kills the first term; tracelessness kills the second, since $\nabla_{(\mu}\zeta_{\nu)} \propto \eta_{\mu\nu}$ for a CKV). The flux $\int_\Sigma J^\mu d\Sigma_\mu$ is therefore slice-independent, and for $\Delta = d = 3$ the conformal weights of h, ζ, and $d\Sigma$ balance exactly: this is the classical statement that fluxes of CKV-contracted conserved traceless currents are conformally invariant. No residual $\Omega_g(x)$ factor survives.

Combining (i)–(iii): every ingredient of $\mathcal{T}[h](D)$ maps covariantly under all of $\mathrm{SO}(3,2)$, giving (160). □ □

Remark G.3 (Relation to Appendix F)**.** *The obstruction found in Appendix F concerned the* double-contraction boundary integral $\int_{\partial D} h_{\mu\nu}\zeta^\mu\zeta^\nu d^2\sigma$*, whose integrand carries a residual local weight $\Omega_g(y)^2$ under SCTs. The modular-flow transform* (159) *contracts h with* one *CKV and one surface normal; the weight counting is then exactly balanced (step (iii) above), which is why full covariance holds here while the double-contraction form required the G_0 restriction. In embedding language the same fact appears as homogeneity counting: on the null boundary the double-contraction kernel carries net X-degree $+1$, whereas the kernel of $\mathcal{T}$ has degree 0.*

G5. Derivation of Ouroboros for state-based kinematic data

Theorem G.4 (Ouroboros from the First Law)**.** *Let $|\Psi\rangle$ be a CFT state with finite local energy density and let $F_{\text{state}}(D) := \delta S(D)/2\pi = \mathcal{T}[\langle \delta T\rangle](D)$ be the associated kinematic data. Then F_{state} satisfies the Ouroboros condition (88).*

Proof. By Theorem G.2, $\mathcal{T}$ is a fully $\mathrm{SO}(3,2)$-equivariant map from the conformal multiplet of the stress tensor ($\Delta = 3$, $s = 2$, twist $\tau = 1$) to functions on $\mathcal{M}_\Diamond$. By the OPE-block Casimir analysis of Czech et al. [12] (used as Assumption cited in Section 2.9), any such equivariant image of the stress-tensor multiplet is a C_2-eigenspace with $M^2_{\text{KS}} = \tau(\tau + d - 2) = 2$:

$$\big(\Box_{\text{KS}} - 2\big)F_{\text{state}} \;=\; 0\,. \tag{161}$$

By the triple equivalence (93) of Section 8, $(\Box_{\text{KS}} - 2)F = 0$ is equivalent to the Ouroboros condition. Hence F_{state} satisfies Ouroboros. □ □

Remark G.5 (Scope and the role of non-commutativity)**.** *Theorem G.4 derives Ouroboros for kinematic data of* First-Law form *— data arising from an actual CFT state via $\delta S/2\pi$. For* abstract *kinematic data (an arbitrary assignment $D \mapsto F(D)$ not presumed to come from a state), Ouroboros remains an independent axiom, as stated in Section 8. The modular non-commutativity $[\hat{K}_A, \hat{K}_B] \neq 0$ plays its role upstream: it guarantees that the modular data of distinct diamonds are genuinely independent probes of the state, so that F_{state} is a non-trivial function on $\mathcal{M}_\Diamond$ rather than a constant (cf. Step A of chain (35)).*

G6. The two kernels reconciled

Section F and the present appendix involve two different spin-2 transforms:

Transform	Null-boundary weight	Full covariance	Where
$\mathcal{T}[h](D) = \int_{\Sigma_D} h\,\zeta\,d\Sigma$	$g(\lambda)$	✓ (Thm. G.2)	this appendix
$\mathcal{R}_2[h](D) = \lvert a\rvert^{-2}\int_{\partial D} h\,\zeta\zeta\,d^2\sigma$	$g(\lambda)^2$	G_0 proved; SCT via [12]	App. F

Table 20: The two spin-2 transforms. On the past null cone of the diamond, $\zeta_D = g(\lambda)k$ with $g(\lambda) = \lambda(r - \lambda)/r$ (SymPy-verified), so the two kernels differ by one factor of $g(\lambda)$.

Both transforms map the stress-tensor multiplet equivariantly into functions on $\mathcal{M}_\Diamond$ with the same quantum numbers ($\Delta = 3$, $s = 2$, $C_2 = 6$, $M^2_{\text{KS}} = 2$). By irreducibility of $D(3,2)$ [22] — now legitimately applicable because Theorem G.2 provides full-group equivariance for $\mathcal{T}$, and the cross-ratio construction of [12] provides it for $\mathcal{R}_2$ — the two images coincide:

$$\mathrm{Im}\big(\mathcal{T}\big|_{D(3,2)}\big) \;=\; \mathrm{Im}\big(\mathcal{R}_2\big|_{D(3,2)}\big) \;\cong\; D(3,2)\,. \tag{162}$$

In particular, $F_{\text{state}} \in \mathrm{Im}(\mathcal{R}_2)$, so state-based data automatically admits the representation $F_{\text{state}} = \mathcal{R}_2[h]$ used throughout the main text.

G7. Summary and consequences for the main text

Two consequences for the main argument:

1. Step 2 of Theorem 6.8 may cite Theorem G.2 (full covariance of the modular-flow form) alongside Appendix F (G_0 covariance of the boundary-integral form) and the cross-ratio construction [12].

Item	Before this appendix	After
Equivariance of state-based transform	G_0 only (App. F)	full $\mathrm{SO}(3,2)$ (Thm. G.2)
Ouroboros for state-based data	axiom	derived (Thm. G.4)
Ouroboros for abstract data	axiom	axiom (unchanged)
$\mathrm{Im}(\mathcal{T})$ vs $\mathrm{Im}(\mathcal{R}_2)$	open (g vs g^2 kernels)	equal, $\cong D(3,2)$ (162)
SCT gap of App. F	open for $\zeta\zeta$ form	explained (Rem. G.3); open for $\zeta\zeta$ form onl

Table 21: What the embedding-space formulation establishes.

2. For the physically relevant case of kinematic data arising from a CFT state, the Ouroboros input of chain (35) is no longer an independent assumption: it follows from the First Law (Theorem G.4). The conditional structure "non-commutativity *and* Ouroboros" of Section 3 remains the honest statement for abstract kinematic data.

References

[1] P. Ninsook, "Time as Phase Flow: A Geometric Semiclassical Framework for Cosmological Anomalies," Zenodo, https://doi.org/10.5281/zenodo.18316215 (2026).

[2] P. Ninsook, "Time as Phase Flow II: Information-Induced Temporal Inertia and Cosmological Perturbations in Information-Geometric Spacetime," Zenodo, https://doi.org/10.5281/zenodo.18315946 (2026).

[3] P. Ninsook, "Time as Phase Flow III: Information-Geometric Backreaction and the Microscopic Origin of Temporal Inertia," Zenodo, https://doi.org/10.5281/zenodo.18316429 (2026).

[4] P. Ninsook, "Time as Phase Flow IV: Observational Signatures and Falsifiability in Late-Time Cosmology," Zenodo, https://doi.org/10.5281/zenodo.18358816 (2026).

[5] P. Ninsook, "Information-Geometric Spacetime: Actualization as the Mechanism for Spacetime Emergence from Quantum Information," Zenodo, https://doi.org/10.5281/zenodo.18396902 (2026).

[6] P. Ninsook, "Information-Geometric Spacetime II: Ouroboros Closure and Fixed-Point Stability in Actualization Dynamics," Zenodo, https://doi.org/10.5281/zenodo.18420042 (2026).

[7] P. Ninsook, "Information-Geometric Spacetime III: The Q_μ Field and and the Necessity of Universal Dynamics," Zenodo, https://doi.org/10.5281/zenodo.18517894 (2026).

[8] P. Ninsook, "Information-Geometric Spacetime IV: The Gravitational Sector and its Modular Reduction," Zenodo, https://doi.org/10.5281/zenodo.21196116 (2026).

[9] P. Ninsook, "IGPS I: Geometry and Spin Structure of the Single Oloid Manifold as the Origin of Leptonic Mass," Zenodo, https://doi.org/10.5281/zenodo.18617881 (2026).

[10] P. Ninsook, "IGPS II: Multi-Seam Configuration and the Topological Scaling of Baryonic Mass," Zenodo, https://doi.org/10.5281/zenodo.18618316 (2026).

[11] B. Czech, L. Lamprou, S. McCandlish, and J. Sully, "Integral Geometry and Holography," *JHEP* **10**, 175 (2015). *arXiv:1505.05515 [hep-th].*

[12] B. Czech, L. Lamprou, S. McCandlish, B. Mosk, and J. Sully, "A Stereoscopic Look into the Bulk," *JHEP* **07**, 129 (2016). *arXiv:1604.03110 [hep-th].*

[13] J. de Boer, F. M. Haehl, M. P. Heller, and R. C. Myers, "Entanglement, Holography and Causal Diamonds," *JHEP* **08**, 162 (2016). *arXiv:1606.03307 [hep-th].*

[14] B. Czech, L. Lamprou, and J. Sully, "Hyperbolic Space from the Entanglement Structure," *Phys. Rev. Lett.* **123**, 131301 (2019). *arXiv:1909.05847 [hep-th].*

[15] H. Casini, M. Huerta, and R. C. Myers, "Towards a Derivation of Holographic Entanglement Entropy," *JHEP* **05**, 036 (2011). *arXiv:1102.5016 [hep-th].*

[16] D. D. Blanco, H. Casini, L.-Y. Hung, and R. C. Myers, "Relative Entropy and Holography," *JHEP* **08**, 060 (2013). *arXiv:1305.3182 [hep-th].*

[17] J. J. Bisognano and E. H. Wichmann, "On the Duality Condition for a Hermitian Scalar Field," *J. Math. Phys.* **16**, 985 (1975).

[18] S. Ryu and T. Takayanagi, "Holographic Derivation of Entanglement Entropy from the AdS/CFT Correspondence," *Phys. Rev. Lett.* **96**, 181602 (2006). *hep-th/0603001.*

[19] T. Faulkner, A. Lewkowycz, and J. Maldacena, "Quantum Corrections to Holographic Entanglement Entropy," *JHEP* **11**, 074 (2013). *arXiv:1307.2892 [hep-th].*

[20] D. L. Jafferis, A. Lewkowycz, J. Maldacena, and S. J. Suh, "Relative Entropy Equals Bulk Relative Entropy," *JHEP* **06**, 004 (2016). *arXiv:1512.06431 [hep-th].*

[21] T. Faulkner, F. M. Haehl, E. Hijano, O. Parrikar, C. Rabideau, and M. Van Raamsdonk, "Nonlinear Gravity from Entanglement in Conformal Field Theories," *JHEP* **08**, 057 (2017). *arXiv:1705.03026 [hep-th].*

[22] M. Flato and C. Fronsdal, "On Dis and Racs," *Phys. Lett. B* **97**, 236 (1980).

[23] C. Fronsdal, "Massless Fields with Integer Spin," *Phys. Rev. D* **18**, 3624 (1978).

[24] F. John, "The Ultrahyperbolic Differential Equation with Four Independent Variables," *Duke Math. J.* **4**, 300 (1938).

[25] S. Helgason, *Integral Geometry and Radon Transforms*, Springer (2011).

[26] E. Witten, "2+1 Dimensional Gravity as an Exactly Soluble System," *Nucl. Phys. B* **311**, 46 (1988).

[27] S. Deser, R. Jackiw, and G. 't Hooft, "Three-Dimensional Einstein Gravity: Dynamics of Flat Space," *Ann. Phys.* **152**, 220 (1984).

[28] S. Deser, "Selfinteraction and Gauge Invariance," *Gen. Rel. Grav.* **1**, 9 (1970). *gr-qc/0411023.*

[29] R. M. Wald, "Spin-Two Fields and General Covariance," *Phys. Rev. D* **33**, 3613 (1986).

[30] T. Jacobson, "Thermodynamics of Spacetime: The Einstein Equation of State," *Phys. Rev. Lett.* **75**, 1260 (1995). *gr-qc/9504004.*

[31] L. McGough, M. Mezei, and H. Verlinde, "Moving the CFT into the Bulk with $T\bar{T}$," *JHEP* **04**, 010 (2018). *arXiv:1611.03470 [hep-th].*

[32] P. Kraus, J.-L. Liu, and D. Marolf, "Cutoff AdS_3 Versus the $T\bar{T}$ Deformation," *JHEP* **07**, 027 (2018). *arXiv:1801.02714 [hep-th].*

[33] O. Aharony and E. Silverstein, "Supercritical Stability, Transitions and (Pseudo)tachyons," *Phys. Rev. D* **75**, 046003 (2007). *hep-th/0608089.*

[34] V. Shyam, "Background Independent Holography and the $T\bar{T}$ Deformation," *Phys. Rev. D* **96**, 066016 (2017). *arXiv:1707.08118 [hep-th].*

[35] Q. Long, "Modular Hamiltonian and Entanglement Entropy for Disjoint Intervals in CFT_2," *Int. J. Mod. Phys. A* **34**, 1950172 (2019). *arXiv:1907.00646 [hep-th].*

[36] V. Iyer and R. M. Wald, "Some Properties of the Noether Charge and a Proposal for Dynamical Black Hole Entropy," *Phys. Rev. D* **50**, 846 (1994). *gr-qc/9403028.*

[37] R. M. Wald, *General Relativity*, University of Chicago Press (1984).

[38] P. A. M. Dirac, "Wave equations in conformal space," Ann. Math. **37** (1936) 429–442.

[39] M. S. Costa, J. Penedones, D. Poland and S. Rychkov, "Spinning Conformal Correlators," JHEP **11** (2011) 071, arXiv:1107.3554 [hep-th].